Anaerobic *O*-demethylation in *Acetobacterium dehalogenans*

Interactions mediated by *O*-demethylase components

Dissertation

zur Erlangung des akademischen Grades

doctor rerum naturalium (Dr. rer. nat.)

vorgelegt dem Rat der Biologisch-Pharmazeutischen Fakultät
der Friedrich-Schiller-Universität Jena

von
M. Sc. Hai Dang Nguyen

geboren am 22.09.1980 in Hanoi, Vietnam

1. Gutachter:	Prof. Dr. Gabriele Diekert
2. Gutachter:	Prof. Dr. Kirsten Küsel
3. Gutachter:	Prof. Dr. Volker Müller
Tag der öffentlichen Disputation:	13.08.2013

Contents

Abbreviations

3AT	3-amino-1,2,4-triazole
AE	Activating enzyme
AMP	Adenosine monophosphate
Amp	Ampicillin
APS	Ammonium persulfate
ATP	Adenosine triphosphate
B2H	Bacterial two-hybrid
BCIP	(5-bromo-4-chloro-1*H*-indol-3-yl) dihydrogen phosphate
BSA	Bovine serum albumin
CH_3-FH_4	Methyltetrahydrofolate
COG	Clusters of orthologous groups
CP	Corrinoid protein
DMSO	Dimethylsulfoxide
DNA	Deoxyribonucleic acid
dNTP	Deoxyribonucleotide triphosphate
DTT	Dithiothreitol
EDTA	Ethylene diamine tetra-acetic acid
FH_4	Tetrahydrofolate
FPLC	Fast protein liquid chromatography
gua	Guaiacol
HABA	2-(4′-hydroxy-benzeneazo) benzoic acid
HEPES	4-(2-hydroxyethyl)-1-piperazineethanesulfonic acid
IPTG	Isopropyl β-D-1-thiogalactopyranoside
Kan	Kanamycin
LB	Luria-Bertani
MT	Methyltransferase
NBT	Nitro blue tetrazolium chloride
OD	Optical density
ONPG	*ortho*-Nitrophenyl-β-galactoside
p	Plasmid
PAGE	Polyacrylamide gel electrophoresis

PBST	Phosphate Buffered Saline / Tween
PCR	Polymerase Chain Reaction
PEG 4000	Polyethylene glycol 4000
PMSF	Phenylmethylsulfonyl fluoride
PVDF	Polyvinylidene fluoride
rpm	Rounds per minute
SDS	Sodium dodecyl sulfate
SOB	Super optimal broth
syr	Syringate
TAE	Tris acetate EDTA
TB	Transformation buffer
TEMED	N,N,N',N'-Tetramethylethylenediamine
Ti(III)citrate	Titanium(III)citrate
Tris	Tris(hydroxymethyl)-aminomethane
UV/Vis	Ultraviolet-visible spectroscopy
v/v	Volume per volume
van	Vanillate
ver	Veratrol
w/v	Weight per volume
Y2H	Yeast two-hybrid

Summary

The gram positive bacterium *Acetobacterium dehalogenans* belongs to the group of acetogens. The anaerobe utilizes the methyl group of phenyl methyl ethers, which are products of the lignin degradation process, as a carbon and energy source. The *O*-demethylation reaction in which the methyl group of the substrate is transferred to tetrahydrofolate is mediated by the key enzymes, the *O*-demethylases, in the methylotrophic metabolism. The *O*-demethylase enzyme complex consists of four components: a methyltransferase I (MT I) transfers the methyl group of a phenyl methyl ether to a super-reduced corrinoid protein ([Co^{I}]-CP) to form methylcobalamin (CH_3-[Co^{III}]-CP). The second methyltransferase (MT II) mediates the methyl transfer from CH_3-[Co^{III}]-CP to tetrahydrofolate forming methyltetrahydrofolate. The inactive form of the corrinoid protein ([Co^{II}]-CP), which is occasionally generated by inadvertent oxidation, is reduced by the activating enzyme (AE) in an ATP dependent reaction. Four different *O*-demethylase enzyme systems were identified as guaiacol-, syringate-, vanillate-, and veratrol-*O*-demethylase.

In the work presented here, the interactions of the *O*-demethylase components were studied using two-hybrid assays, gel shift experiments and far-Western blot analyses. Emphasis was laid on studies on the interaction of AE and CP. With the exception of the yeast two-hybrid assay (Y2H), an interaction between AE and CP was always observed. In gel shift experiments, the presence of the corrinoid cofactor was a prerequisite for the interaction of the two components. On native PAGE, AE appeared as dimer. The Y2H experiments pointed to an involvement of the *N*-terminal fragment of AE (AE 1-133) in the oligomerization of the protein. Interaction studies in the presence of the other *O*-demethylase components revealed interactions of CP and the two MTs which is in accordance to the proposed reaction mechanism of the *O*-demethylases.

The reductive activation of CP catalyzed by AE in an ATP dependent reaction was also studied. It was shown that AE is able to reduce the corrinoid cofactor of different CPs and therefore, AE seems to be an universal reductive activator of corrinoid enzymes of *A. dehalogenans*. The physiological electron donor for the corrinoid reduction is unknown so far. In this study two genes of *A. dehalogenans* encoding putative ferredoxins (Fds) were cloned and heterologously expressed in *Escherichia coli*. The reconstituted Fds I and II showed typical UV/Vis spectra for the presence of iron-sulfur clusters. The amino acid sequence analyses and iron determinations indicated that Fd I contains 4 [4Fe-4S] clusters while Fd II harbors two of these. However, the involvement of the two ferredoxins in corrinoid activation could not be demonstrated by the biochemical assays used.

Zusammenfassung

Der gram-positive Mikroorganismus *Acetobacterium dehalogenans* gehört zur Gruppe der acetogenen Bakterien. Er verwendet die Methylgruppe von Phenylmethylethern, Abbauprodukten des Lignins, als Kohlenstoff- und Energiequelle. Die Methylgruppe der Substrate wird durch *O*-Demethylasen, die Schlüsselenzyme des methylotrophen Stoffwechsels, auf Tetrahydrofolat übertragen. *O*-Demethylasen sind Enzymkomplexe und bestehen aus vier Proteinen: die Methyltransferase I (MT I) überträgt die Methylgruppe vom Phenylmethylether auf das super-reduzierte Corrinoidprotein ([Co^{I}]-CP) unter Bildung von Methylcobalamin (CH_3-[Co^{III}]-CP). Die Methyltransferase II (MT II) katalysiert den Methylgruppentransfer von CH_3-[Co^{III}]-CP auf Tetrahydrofolat. Methyltetrahydrofolat wird gebildet. Die inaktive Form des Corrinoidproteins ([Co^{II}]-CP), die aufgrund von Autoxidation entsteht, wird in einer ATP-abhängigen Reaktion durch das Aktivierende Enzym (AE) reduziert. Vier verschiedene *O*-Demethylase-Systeme – die Guaiacol-, die Syringat-, die Vanillat- und die Veratrol-*O*-Demethylase – wurden bisher in *A. dehalogenans* identifiziert.

In der vorliegenden Arbeit wurde die Interaktion der *O*-Demethylasekomponenten unter Verwendung von Two-Hybrid-Systemen, Gel-Shift- sowie Far-Western Blot-Experimenten untersucht. Schwerpunkt war hierbei die Interaktion von AE und CP, die mit Ausnahme des Yeast Two-Hybrid-Systems (Y2H) für alle Methoden nachgewiesen werden konnte. In Gel-Shift-Experimenten war das Vorhandensein des Corrinoid-Cofaktors Voraussetzung für die Interaktion dieser beiden Proteinkomponenten. Auf nativen Gelen wurde AE als Dimer detektiert. Y2H-Analysen zeigten, dass für die Oligomerisierung wahrscheinlich ein *N*-terminales AE-Fragment verantwortlich ist. Interaktionsstudien in Anwesenweit weiterer *O*-Demethylasekomponenten führten zum Nachweis der Interaktion von CP mit beiden MT-Proteinen. Dieses Ergebnis stimmt mit dem postulierten Reaktionsmechanismus überein.

Die Reduktion von inaktivem CP, die durch AE in einer ATP-abhängigen Reaktion katalysiert wird, war ebenfalls Bestandteil der hier durchgeführten Untersuchungen. Es wurde gezeigt, dass AE verschiedene Corrinoidproteine reduzieren kann. Somit scheint AE in *A. dehalogenans* als universeller reduktiver Aktivitator von Corrinoidproteinen zu fungieren. Der physiologische Elektronendonor dieses Prozesses ist bisher nicht bekannt. Es wurden zwei mutmaßliche Ferredoxingene von *A. dehalogenans* heterolog in *Escherichia coli* exprimiert. Die rekombinanten Ferredoxine (Fd) I und II wiesen nach Rekonstituion typische UV/Vis-Spektren für Eisen/Schwefel-Cluster-enthaltende Proteine auf. Sequenzanalysen sowie die Bestimmung von Eisen zeigten, dass Fd I vier und Fd II zwei [4Fe-4S]-Cluster enthält. Eine Beteiligung der Ferredoxine bei der Corrinoidaktivierung konnte bisher jedoch nicht gezeigt werden.

1. Introduction

1.1. Phenyl methyl ether metabolism of acetogens

Lignin is the most abundant polymer containing aromatic compounds in the biosphere; it constitutes about 25% of the earth's biomass (Bugg *et al.*, 2011b). It is a component of wood, of secondary cell walls of plants and of algae. Lignin is a heterogeneous polymer consisting of hydroxylated and methoxylated phenylpropanoids linked by different types of covalent bonds such as C-C or C-O-C (Heldt & Heldt, 2005; Masai *et al.*, 2007). The composition of lignin varies greatly between plants species. The complex and non-repeating heterogeneous structure makes plant tissues difficult to digest. Only a few bacteria and fungi are able to degrade lignin. In nature, degradation of lignin is achieved by specific enzyme systems such as lignin peroxidase, manganese peroxidase, and laccase secreted by fungi (brown rot, soft rot, or white rot fungi) (Bugg *et al.*, 2011a), and bacteria (Zimmermann, 1990). The depolymerization process generates monomeric methoxylated aromatic compounds (phenyl methyl ethers) that can be further degraded by aerobic and anaerobic bacteria. The acetogens are strictly anaerobic bacteria which are able to catalyze the reduction of 2 mol of CO_2 to acetate in their energy metabolism (Diekert & Wohlfarth, 1994). The involvement of acetogens in the anaerobic degradation of phenyl methyl ethers was discovered in the early 1980s (Bache & Pfennig, 1981). The key reactions in phenyl methyl ether degradation are the cleavage of substrate ether bond in an *O*-demethylation reaction and the transfer of the methyl group to tetrahydrofolate (Kaufmann *et al.*, 1997).

1.1.1. O-*demethylase systems of acetogens*

Several acetogenic bacteria comprising *Acetobacterium dehalogenans* (Kaufmann *et al.*, 1997), *A. woodii* (Bache & Pfennig, 1981), *Moorella thermoacetica* (formerly *Clostridium thermoaceticum*) (Daniel *et al.*, 1991), *M. thermoautotrophica* (formerly *C. thermoautotrophicum*) (Daniel et al., 1988), *Sporomusa ovata* (Stupperich & Konle, 1993), and an acidobacterium *Holophaga foetida* (Kreft & Schink, 1997; Anderson *et al.*, 2012) can use phenyl methyl ethers (e.g. syringate or vanillate) as energy sources. Upon cleavage of the substrate ether bond in an *O*-demethylation reaction, the corresponding hydroxylated compound is formed. The aromatic ring is usually not metabolized further whereas the *O*-

methyl group is used as an one carbon growth substrate (Bache & Pfennig, 1981). The methyl group is transferred to tetrahydrofolate (FH_4) forming methyltetrahydrofolate (CH_3-FH_4). In the energy metabolism, 25% of the methyl group of CH_3-FH_4 is subsequently oxidized to CO_2. The reducing equivalents generated in this process are utilized for the reduction of CO_2 to enzyme-bound carbon monoxide by the bifunctional carbon monoxide dehydrogenase/acetyl-CoA synthase (CODH/ACS) (for reviews on the acetogenic catabolism, see Diekert & Wohlfarth, 1994; Müller, 2003). The remaining part of the CH_3-FH_4 serves as methyl donor during synthesis of acetyl-CoA. To gain energy, acetyl-CoA is further converted to acetate (Wood, 1991; Ragsdale, 2008). The methylotrophic metabolism of acetogens is summarized in Figure 1.1.

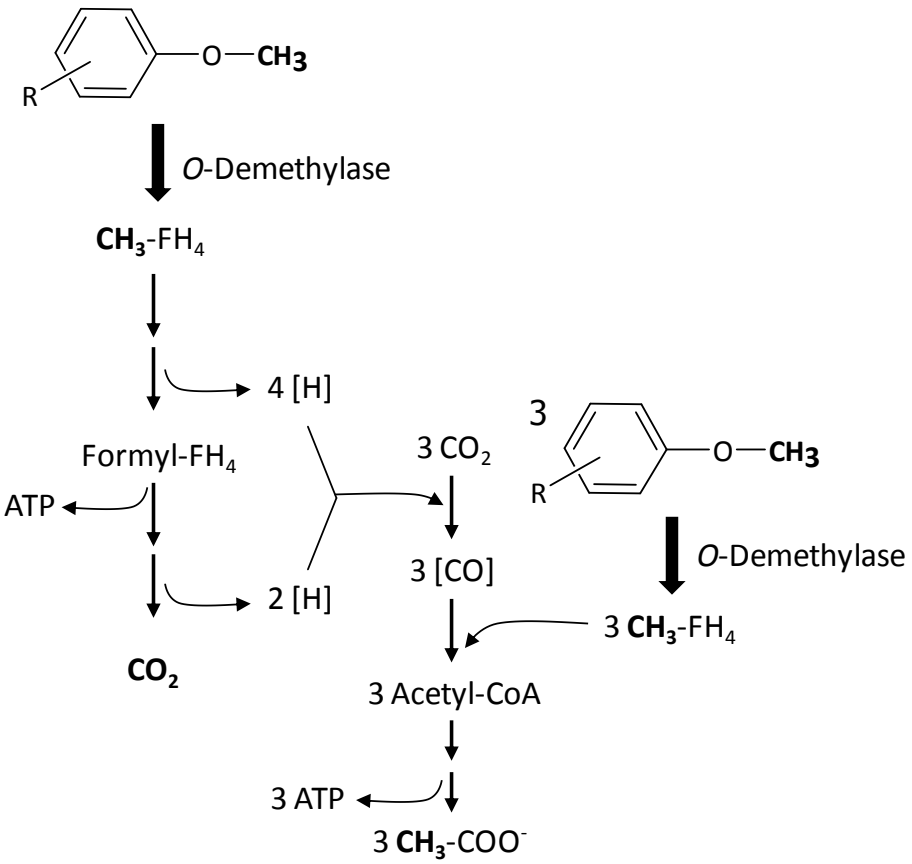

Fig. 1.1. Methylotrophic metabolism of acetogens. FH_4: tetrahydrofolate; [H]: reducing equivalents. The thick black arrows indicate where the methyl compounds enter the pathway (Diekert & Wohlfarth, 1994).

The *O*-demethylation reaction is mediated by the key enzymes, the inducible *O*-demethylases (Messmer *et al.*, 1993). Depending on the growth substrate, different *O*-demethylases are

induced. Investigations on the specificity of the *O*-demethylating activity of *M. thermoacetica* revealed that the bacterium can metabolize at least twenty out of forty-two methoxylated aromatics tested (Daniel *et al.*, 1991). *A. woodii* can grow on at least 11 methoxylated aromatic compounds (Frazer, 1995). *O*-demethylase systems were purified and characterized from *A. dehalogenans* (Kaufmann *et al.*, 1997) and *M. thermoacetica* (Naidu & Ragsdale, 2001). The characterization of an *O*-demethylase enzyme system of the non-acetogenic bacterium *Desulfitobacterium hafniense* DCB-2 was recently reported (Studenik *et al.*, 2012).

The enzyme systems characterized so far consist of three or four different components. In *M. thermoacetica*, three components of the vanillate-*O*-demethylase were isolated (Naidu & Ragsdale, 2001). MtvB catalyzes the transfer of the methyl group from a phenyl methyl ether to MtvC, a corrinoid protein. A second methyltransferase MtvA mediates the transfer of the methyl group from MtvC to tetrahydrofolate, producing CH_3-FH_4. The vanillate-*O*-demethylase of *A. dehalogenans* was the first *O*-demethylating enzyme system purified (Kaufmann *et al.*, 1997) followed by the isolation of another *O*-demethylase system, the veratrol-*O*-demethylase, from the same organism (Engelmann *et al.*, 2001). Recently, two more enzyme systems, the syringate-*O*-demethylase and the guaiacol-*O*-demethylase, were identified (Lange, 2009; Frenkel, 2010). The enzyme systems of *A. dehalogenans* are composed of four components: a methyltransferase I (MT I), a methyltransferase II (MT II), a corrinoid protein (CP) and an activating enzyme (AE). The methyl group is transferred from the phenyl methyl ether to the super-reduced corrinoid protein by MT I. The methylated corrinoid protein is subsequently demethylated and the methyl group is transferred to tetrahydrofolate by MT II. The inactive form of the corrinoid protein, the cob(II)alamin form, which is occasionally generated by inadvertent oxidation, is reduced by the activating enzyme in an ATP dependent reaction; hence, AE exerts a repair function. The reaction mechanism is shown in Figure 1.2.

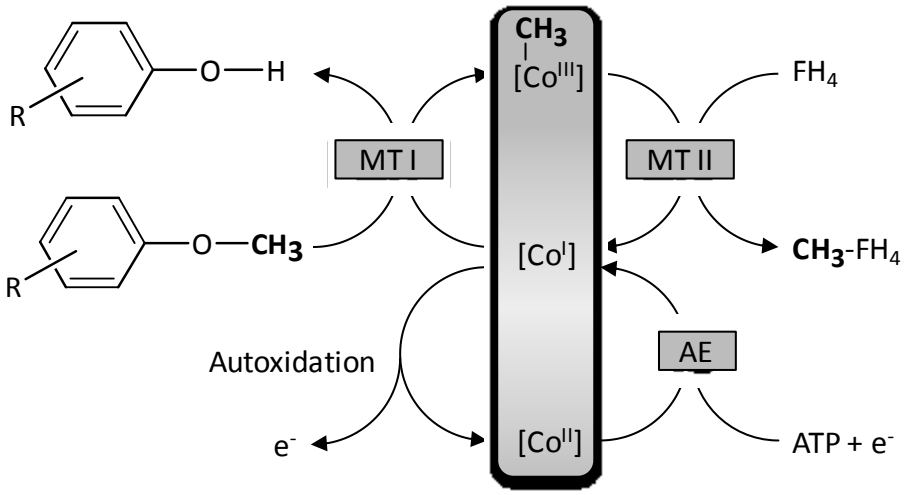

Fig. 1.2. Scheme of the *O*-demethylase reaction catalyzing the methyl group transfer from a phenyl methyl ether to tetrahydrofolate in *A. dehalogenans*. FH_4: Tetrahydrofolate. AE: activating enzyme, MT I: methyltransferase I; MT II: methyltransferase II; [Co^I], [Co^{II}], [Co^{III}]: corrinoid protein with cobalt in the given redox states.

1.1.2. Characteristics of the O-*demethylase components of* Acetobacterium dehalogenans

A. dehalogenans is able to grow on phenyl methyl ethers or on methyl chloride as energy source (Traunecker *et al.*, 1991). Studies on the *O*-demethylation revealed that it contains more than one *O*-demethylase system which enables the growth on different substrates. Methyltransferase I of the vanillate-*O*-demethylase (MT I_{van}) was purified from *A. dehalogenans* together with three other components in the study of Kaufmann *et al.* (1997). Upon the observation that *A. dehalogenans* can grow with methoxylated aromatic compounds which were not demethylated by the vanillate-*O*-demethylase, the second methyltransferase I was isolated and characterized as a single component of the veratrol-*O*-demethylase system (MT I_{ver}). Both MTs I share the same functions: they cleave the ether bond of a phenyl methyl ether and transfer the methyl group to the corrinoid protein of the enzyme system. These enzymes are similar to methanogenic methyltransferases (Daas *et al*., 1996a; Sauer & Thauer, 1997; Matthews *et al*, 2008). MT I_{van} is a monomer with an apparent molecular mass of 36 kDa. The enzyme is colorless and exhibits the UV/Vis spectrum of a protein lacking a visible prosthetic group. In the presence of AE, titanium(III)citrate, ATP, and the corrinoid protein (CP_{van}), MT I_{van} converted vanillate to 3,4-dihydroxybenzoate and transferred the methyl group to the reduced corrinoid (Kaufmann *et al.*, 1998a). MT I_{ver} was purified to apparent

homogeneity. It was a monomer with an apparent molecular mass of 32 kDa (Engelmann *et al.*, 2001). Like MT I_{van}, MT I_{ver} is colorless and shows a typical UV/Vis spectrum of a protein without any additional visible cofactors. The two proteins exhibit different substrate spectra. While MT I_{van} usually cleaves the ether bond of phenyl methyl ethers with a hydroxyl group in *ortho*-position to the methoxy group, MT I_{ver} can catalyze the demethylation of phenyl methyl ethers independent from the presence or absence of the *ortho*-hydroxyl group (Engelmann *et al.*, 2001). It should be mentioned that the enzymes are named according to the substrate yielding the highest activity of MT I. As an example, MT I_{ver} showed the highest activity with veratrol in an *in vitro* assay, however, it was isolated from cells cultivated on 3-hydroxyanisole as growth substrate and veratrol was not a growth substrate for the bacterium. For the syringate- and guaiacol-*O*-demethylases, the specific growth substrates inducing these proteins are not yet known. The substrate spectra of MT I_{van} and MT I_{ver} partially overlap as illustrated in Figure 1.3.

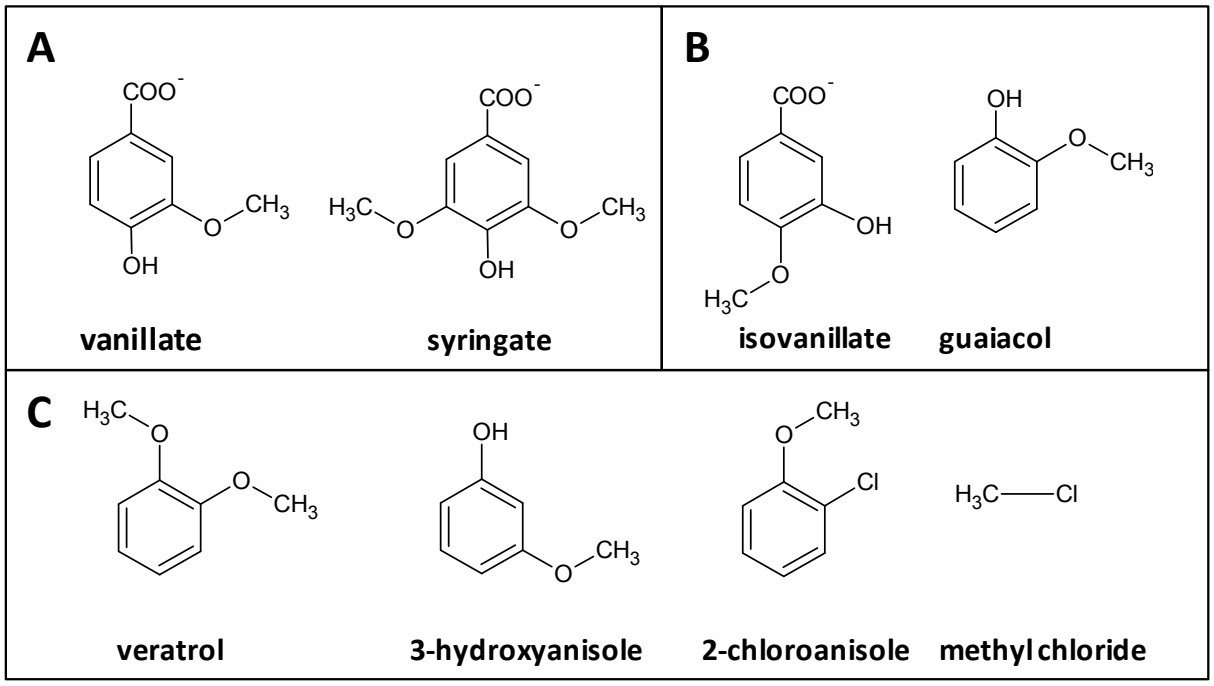

Fig. 1.3. Several substrates for the methyltransferases I of the vanillate- and veratrol-*O*-demethylases (MT I_{van} and MT I_{ver}). (**A**) Substrates of MT I_{van}; (**B**) Substrates of both enzymes; (**C**) Substrates of MT I_{ver}.

Amino acid sequence analyses revealed that the two proteins show only 22% of sequence identity and do not share any conserved regions (Kreher *et al.*, 2010). Both proteins were heterologously produced in *Escherichia coli*. They were found to contain zinc (Schilhabel *et*

al., 2009). Unique zinc binding motifs were identified by site directed mutagenesis, namely **E**-X_{14}-**E**-X_{20}-**H** for MT I_{van} and **D**-X_{27}-**C**-X_{39}-**C** for MT I_{ver} (Studenik *et al.*, 2011). Different from all other characterized corrinoid-dependent methyltransferases, cysteine is apparently not involved in zinc binding in MT I_{van} (Studenik *et al.*, 2011). Zinc was found to be located in the TIM-barrel structure of the *C*-terminal part of MT I which is in accordance to the proposed catalytic function of this domain, whereas the *N*-terminal part of MT I is responsible for the substrate specificity of the enzymes (Kreher *et al.*, 2010).

The corrinoid protein was purified as a monomer. The apparent molecular mass determined by SDS-PAGE and gel filtration was 25 kDa and 26 kDa, respectively. The reddish-brown as-isolated protein had an UV/Vis spectrum typical for the presence of a cob(II)alamin corrinoid cofactor with a major peak at 475 nm (Kaufmann *et al.*, 1997). In the *O*-demethylase system, it functions as a methyl group acceptor in the reaction catalyzed by MT I and as a methyl donor for MT II. Hence, CP is a substrate for MT I in its super-reduced, non-methylated form and for MT II in its methylated form. Usually, the genes encoding the methyltransferases and the corrinoid protein are located on one operon. The gene encoding the corrinoid protein of the vanillate-*O*-demethylase (*odmA*) was cloned, sequenced and expressed in *E. coli*. Sequence analyses revealed the presence of the conserved vitamin B_{12} binding motif [**D**X**H**XX**G**-41-**S**X**L**-(26/28)-**GG**] in the gene product of CP_{van} (OdmA) (Kaufmann *et al.*, 1998b). The OdmA sequence shows high similarity to that of the cobalamin-binding region of the cobalamin-dependent methionine synthase of *E. coli* (Banerjee *et al.*, 1989), to the corrinoid protein of the monomethylamine:coenzyme M methyltransferase of *Methanosarcina barkeri* (Burke *et al.*, 1998) and to the corrinoid-binding subunit of the methanol:coenzyme M methyltransferase of the same methanogen (Sauer & Thauer, 1997). The prosthetic group of the corrinoid protein of *A. dehalogenans* is apparently base- or his-on as in the methanol:coenzyme M methyltransferase of *M. barkeri* (Sauer & Thauer, 1999). Recombinant CP_{van} was produced in *E. coli* as cofactor-free protein. The reconstitution with hydroxocobalamin recovered its function as methyl group acceptor.

The methyltransferase II was found as dimeric protein with an apparent molecular mass of 30 kDa for the monomer. It does not contain any prosthetic group that was detectable by UV/Vis spectroscopy. MT II catalyzes the tetrahydrofolate-dependent demethylation reaction of the methylated corrinoid protein. MT II has the similar function as MtvA and the methylcobalamin dependent methyltransferase (AcsE) of *M. thermoacetica* (Doukov *et al.*,

2000; Naidu & Ragsdale, 2001). The *N*-terminal sequence of MT II exhibits a high similarity to tetrahydrofolate:corrinoid protein methyltransferases of *M. thermoacetica* and *S. ovata* (Kaufmann *et al.*, 1998a) indicating the functional relationship between these proteins.

The fourth component of the *O*-demethylase system, AE, was purified as homotrimeric protein with an apparent molecular mass of 67 kDa for a single subunit. The function of the protein was described as "reductive activator for corrinoid enzymes" (RACE) which reactivates and reduces CP-bound cob(II)alamin to cob(I)alamin in an ATP dependent reaction (Schilhabel *et al.*, 2009). Enzymes with a similar function are the reductive activator (RamA) of the methylamine:CoM methyltransferase of the methanogenic archaeon *M. barkeri* (Ferguson *et al.*, 2009) and an ATP-dependent reductive activator (RACo) of the corrinoid/iron-sulfur protein of *Carboxydothermus hydrogenoformans* (Hennig *et al.*, 2012; Meister *et al.*, 2012). AE was heterologously produced in *E. coli*. Sequence analyses showed that this enzyme is a member of the COG3894 protein family which seems to be involved in the protein-bound corrinoid activation and reduction (Schilhabel *et al.*, 2009). Structural analyses revealed that the RACE proteins belong to the ASKHA-type (acetate and sugar kinases, Hsp70, and actin) ATPases (Hennig *et al.*, 2012). The gene product of AE (OdmC) exhibits 30% identity to a gene encoding an AE-like protein in *M. thermoacetica*, however, it shows very low sequence identities to other members of the ASKHA family (Schilhabel *et al.*, 2009; Hennig *et al.*, 2012). OdmC contains one [2Fe-2S] cluster binding motif (**C**-X_5-**C**-X_2-**C**-X_n-**C**) at the *N*-terminus. A similar observation was reported for RACo of *C. hydrogenoformans*. Recombinant AE of *A. dehalogenans* was isolated by affinity chromatography and was reconstituted to its active form by incubation with iron and sulfur. The reconstituted protein exhibited the presence of a [2Fe-2S] cluster in the UV/Vis spectrum. Iron sulfur cluster containing activators were also found in methanogenic archaea, however, the latter enzymes harbor two [4Fe-4S] cluster binding motifs close to the C-terminus (Ferguson *et al.*, 2009). Until now, only a single AE was purified from *A. dehalogenans*.

1.1.3. Reactions mediated by O*-demethylase components*

The *O*-demethylase reaction of *A. dehalogenans* is illustrated in Figure 1.2. As mentioned above, the four components of the vanillate-*O*-demethylase of *A. dehalogenans* mediate the

methyl group transfer of a phenyl methyl ether to FH_4. The MTs I and II are members of the corrinoid dependent methyltransferases which can be found in methanogenic archaea, anaerobic bacteria, and in humans and other mammals (Matthews *et al.*, 2008). The mammalian methyltransferases seem to be the only corrinoid dependent methyltransferases known in Eukarya. In Archaea and Prokarya, these enzyme systems play essential roles in metabolism, particularly in anaerobic microorganisms which use a wide range of methyl substrates (methanol, methylamines, methyl thiols and phenyl methyl ethers) (Banerjee & Ragsdale, 2003).

The methyl group of the phenyl methyl ether is transferred to the cobalt of the corrinoid cofactor to form the organometallic methyl-cob(III)alamin intermediate by MT I. The key step of *O*-demethylation and also *N*-demethylation is to activate the methyl groups of the substrates since the methyl bond strength such as C-O or C-N is quite large. Therefore, the powerful nucleophile cob(I)alamin is required (Schrauzer & Deutsch, 1969). Studies on the crystal structure of the CH_3-FH_4 dependent methyltransferase (MeTr) from *M. thermoacetica* (Doukov *et al.*, 2000), the CH_3-FH_4 binding domain of the cobalamin-dependent methionine synthase of *E. coli* (Evans *et al.*, 2004), and the methanol-cobalamin methyltransferase complex of *M. barkeri* (Hagemeier *et al.*, 2006) revealed a similar mechanism of methyl group activation. These enzymes seem to activate the methyl moiety by donating a positive charge to the heteroatom (O, N, or S) attached to the methyl group. The enzymes bind the methyl substituent within an α/ß TIM barrel structure. The presence of zinc in MT I also plays a role in catalyzing the methyl transfer reaction (Matthews & Goulding, 1997). Recently, the crystal structures of the corrinoid iron sulfur protein/methyltransferase (CFeSP/MeTr) complex in the presence and absence of the methyl donor, CH_3-FH_4, have been solved (Kung *et al.*, 2012). Studies on this complex unveiled the mechanism of the methyl transfer. Before methyl group binding occurs, cobalamin (B_{12}) is capped in the small subunit of CFeSP designated as the resting state. Upon the presence of substrate, the B_{12} domain becomes loosened and moves toward the access site. Binding of CH_3-FH_4 to the MeTr shifts the conformational equilibrium of the B_{12} domain in such a way that CH_3-FH_4 is accessible to the B_{12} and the nucleophilic attack. After methyl transfer, B_{12} returns to its resting state (Kung *et al.*, 2012). Like the methyl transfer of methylamines in *M. barkeri*, the methylation of cob(I)alamin in *A. dehalogenans* was found to be irreversible (Kaufmann *et al.*, 1998b), whereas the methyl transfer of methanol in *M. barkeri* and of CH_3-FH_4 in the cobalamin-

dependent methionine synthase of *E. coli* are reversible (Matthews, 2001). In *A. dehalogenans*, the methyl group of the methylated corrinoid protein is transferred to tetrahydrofolate by MT II. Unlike the methyltransferase II of *H. foetida*, the MT II of *A. dehalogenans* cannot catalyze the demethylation of free methylcobalamin (Kreft & Schink, 1994; Liesack *et al.*, 1994; Kaufmann *et al.*, 1998a). The reaction was also found to be irreversible (Kaufmann *et al.*, 1998a).

The interaction between components of the methyltransferases is necessary for the methyl transfer reaction. In *C. hydrogenoformans*, the methyl group transfer from CH_3-FH_4 to acetyl-CoA synthase (ACS) by the cobalamin-dependent methyltransferase system CFeSP/MeTr is believed to depend on the conformational change of the corrinoid protein CFeSP (Svetlitchnaia *et al.*, 2006). The *C*-terminal domain of the large subunit of CFeSP is flexible and allows the interaction between the acetyl-CoA synthase and the methylcobalamin cofactor to facilitate the methyl transfer. In *M. barkeri*, the formation of a complex composed of three components (MtaABC) seems to be essential for the methyl transfer by the methanol-cobalamin dependent methyltransferase (Hagemeier *et al.*, 2006). The cobalamin-dependent methionine synthase (MetH) of *E. coli* catalyzes the reaction of transferring the methyl group from CH_3-FH_4 to *L*-homocysteine to form methionine. Four modules of the enzyme show functional interactions which are essential for the catalytic reaction. The *N*-terminal module binds and activates methyltetrahydrofolate and presents it to the cobalamin which is bound to the corrinoid binding module. The methyl acceptor module binds homocysteine and presents it to methylcobalamin for methyl transfer. The *C*-terminal module binds *S*-adenosylmethionine (AdoMet) for reductive activation/methylation of the protein (Matthews, 2009).

Three redox states are known for the corrinoid cofactor. The super-reduced cob(I)alamin acts as a methyl acceptor, methyl-cob(III)alamin acts as a methyl donor and the inactive form in methyl transfer reactions is cob(II)alamin. During the *O*-demethylase reaction, the cobalt center cycles between the Cob(I) and methylated Cob(III) states. The standard midpoint redox potential of the Cob(II)/Cob(I) couple is usually very low which depends on the corrinoid type and environment. In *A. dehalogenans*, the midpoint potential of Cob(II)/Cob(I) was estimated to be lower than -550 mV. Therefore, it is very likely that the Cob(I) occasionally undergo inadvertent oxidative inactivation to Cob(II) during the catalytic cycles. Reentry into the cycle requires the reductive activation by a low potential electron donor. In methionine

synthase of human, the reduction is achieved by methionine synthase reductase, a protein with homology to flavodoxin oxidoreductase (Leclerc *et al.*, 1998). In *E. coli*, the enzyme requires flavodoxin as electron donor (Bandarian & Matthews, 2004); after reduction the corrinoid is methylated by AdoMet which prevents the re-oxidation. In the CH_3-FH_4/CFeSP methyltransferase systems of *M. thermoacetica*, the reactivation occurs by the transfer of one electron from the [4Fe-4S] cluster to the Co center of CFeSP (Menon & Ragsdale, 1998). In *A. dehalogenans* and some other anaerobes, the reductive activation was shown to require an activator. For *A. dehalogenans* it was shown that in the presence of ATP, the activating enzyme shifts the redox potential of the cob(II)/cob(I)alamin couple in CP from <-550 mV to about -300 mV, which facitlitates reduction of the corrinoid cofactor (Siebert *et al*., 2005). In methanol and methylamine methyltransferase systems of methanogens, the methyltransferase activation protein (MAP) was shown to be involved in the ATP dependent reductive activation of the Cob(II) species (Daas *et al.*, 1996a; Daas *et al.*, 1996b). However, no prosthetic group was detected in MAP by UV/Vis spectroscopy. The RACE systems which are represented by AE of *A. dehalogenans*, RamA of *M. barkeri*, and RACo of *C. hydrogenoformans*, catalyze the reduction of the Cob(II) to the Cob(I) state in an ATP dependent reaction. All these enzymes contain [Fe-S] clusters. *In vitro*, AE of *A. dehalogenans* reduces cob(II)- to cob(I)alamin of CP in the presence of ATP under anoxic conditions. Titanium(III)citrate serves as artificial electron donor. The physiological electron donor is unknown so far.

1.2. Aims of the study

Although recent studies have unveiled a part of the mechanisms of the *O*-demethylase reactions, still a number of questions remained open. One of these questions is how AE can shift the very low redox potential of Cob(II)/Cob(I) couple (≤-550 mV). The midpoint potential of the $[2Fe\text{-}2S]^{2+/1+}$ redox couple of AE (-330 mV) is more positive than that of the cob(II)/cob(I)alamin couple, which makes the electron transfer to the non-activated CP thermodynamically unfavorable ((Siebert *et al*., 2005; Schilhabel *et al.*, 2009). It is feasible that the hydrolysis of ATP provides the energy for a conformational change of the corrinoid protein bound to AE in such a way that the redox potential of the cob(II)/cob(I)alamin couple is shifted to a more positive value (Kaufmann *et al.*, 1997). It is assumed that the electrons for

the corrinoid reduction are supplied by the Fe-S cluster of AE. The physiological electron donor for the reduction of AE is not yet known. A preliminary study indicated that *O*-demethylation is mediated by crude extracts of *A. dehalogenans* in the presence of ATP, hydrogen, hydrogenase, and methyl viologen instead of Ti(III)citrate (Kaufmann *et al.*, 1998a). Methyl viologen could be replaced by enriched ferredoxin (the redox potential is usually between -350 and -550 mV) of *A. dehalogenans*.

Since a protein's role is reflected in its interactions with others, much of the function can be predicted from identifying its interacting partners. Interaction between proteins may result in a change of the kinetic properties of enzymes, in signaling for a start of a reaction, in allowing for substrate channeling, or in creating a new binding site (Phizicky & Fields, 1995; Berggard *et al.*, 2007). Hence, studies on the interaction between the *O*-demethylase components may provide insight into the structural properties and the reaction mechanism of these enzymes such as the native form of proteins (monomer of multimer), the stoichiometry of two interacting partners, the binding affinity of proteins, the conformation of proteins, and interaction sites or domains. As mentioned above, protein interaction between methyltransferase and corrinoid protein was studied so far in methanogenic archaea, where the corrinoid protein appears to be a subunit of the methyltransferase rather than a separate protein. There is, however, little information about the interaction of these components in *O*-demethylase systems of acetogens such as *A. dehalogenans*, where the corrinoid protein is a distinct and separate protein. Recently, the interaction between AE and CP of *A. dehalogenans* was shown by gel shift experiments. The interaction appears to require the presence of the corrinoid cofactor (Schilhabel *et al.*, 2009). However, further experiments are required to confirm this observation.

The aims of the study are:

- To study the interactions between the *O*-demethylase components to gain more information on the reaction mechanism of the enzyme system.
- To search for the physiological electron donors for the ATP dependent reductive activation of corrinoid proteins catalyzed by the activating enzyme.

2. Materials and Methods

All chemicals and reagents used in the experiments, if not stated otherwise, were of the highest available purity and were purchased from Aldrich (Steinheim, Germany), AppliChem GmbH (Darmstadt, Germany), Fluka (Neu-Ulm, Germany), Merck (Darmstadt, Germany), Sigma (Deisenhofen, Germany), and VWR (Darmstadt, Germany).

2.1. Cultivation of microorganisms

2.1.1. Cultivation of Acetobacterium dehalogenans

A. dehalogenans was cultivated anaerobically on the substrates fructose, syringate or vanillate as described earlier (Traunecker *et al.*, 1991). One liter of basal medium contained 0.1% (w/v) NH_4Cl, 3 ml 1 M potassium phosphate buffer, pH 7.5, 40 ml 0.5 M sodium phosphate buffer, pH 7.25, 0.01% (w/v) $MgSO_4$ and 0.0005 % (w/v) resazurin, 1 ml vitamin solution, 2 ml trace element solution (Table 2.1), and 0.2% (w/v) yeast extract. The anaerobisation of the medium was achieved by repeated degassing and flushing with nitrogen for at least 25 cycles (3 min each). The nitrogen and carbon dioxide were then added to the gas phase of the medium at a ratio of 25% N_2/ 75% CO_2 and 0.5 bar. After autoclaving, 10 ml 5% (w/v) cysteine-HCl and 25 ml 10% (w/v) potassium carbonate were added to one liter of the medium. To cultivate the bacteria, 20 mM (final concentration) of the substrate (fructose, syringate, or vanillate) was added to the autoclaved medium. 10 to 15 % of the final volume of the culture was used for inoculation. The culture was allowed to grow anaerobically at 28 °C on a shaker at 120 rpm for 3 days.

2.1.2. Cultivation of Escherichia coli

E. coli was cultivated in Luria-Bertani broth (LB) medium. Appropriate antibiotic(s) with the plasmid used in the *E. coli* strain was added to the culture before inoculation with the preculture. A defined amount of IPTG was added when an optical density of 0.6 was reached.

Table 2.1. Trace element solution and vitamin solution of *A. dehalogenans*.

Trace element solution (500fold)		Vitamin solution (1,000fold)	
Nitrilotriacetic acid	5 g/l	Biotin	2 mg/l
0.5 M NaOH	100 ml/l	Folic acid	2 mg/l
$MgSO_4$ x 7 H_2O	62 g/l	Pyridoxal-HCl	10 mg/l
$MnSO_4$ x H_2O	5 g/l	Thiamine-HCl	5 mg/l
NaCl	10 g/l	Riboflavin	5 mg/l
$FeSO_4$ x 7 H_2O	1 g/l	Nicotinic acid	5 mg/l
$CoCl_2$ x 6 H_2O	1.7 g/l	Calcium pantothenate	5 mg/l
$CaCl_2$ x 2 H_2O	1.3 g/l	Vitamin B_{12}	2 mg/l
$CuSO_4$ x 5 H_2O	0.5 g/l	4-Aminobenzoic acid	5 mg/l
$ZnSO_4$ x 7 H_2O	1.8 g/l	Lipoic acid	5 mg/l
$AlCl_3$ x 3 H_2O	0.1 g/l		
Na_2MoO_4 x 2 H_2O	0.11 g/l		
$NiCl_2$	0.2 g/l		
Na_2SeO_3 x 5 H_2O	21 mg/l		

2.1.3. Cell harvest and storage

The cells were harvested under aerobic conditions in the late exponential growth phase by centrifugation at 10,000 xg and 10 °C for 10 min. Cell pellets were resuspended in 50 mM Tris HCl pH 7.5 and were stored at -20 °C until use.

2.2. Molecular biology methods

2.2.1. DNA agarose gel electrophoresis

The gel was prepared by heating 0.7% (w/v) agarose in TAE buffer (40 mM Tris, 20 mM acetic acid, 1 mM EDTA) in a microwave oven for 5 min. 0.5 µg/ml ethidiumbromide was added to the melted agarose solution and the mixture was poured directly into a Mini Sub®Cell GT gel casting tray (Biorad, Munich, Germany). The gel was cooled down and solidified at room temperature for 30 min. Samples were mixed with the 6x DNA loading dye (Fermentas, St. Leon-Rot, Germany) with a ratio of five volumes of sample to one volume of buffer. After loading the samples to the wells of the agarose gel, the lid and power leads were

placed on the apparatus, and the electrophoresis was started with a voltage of 90 V for one hour. The DNA fragments were visualized by using the Gel Doc 2000 (Bio-Rad Laboratories GmbH, Munich, Germany).

2.2.2. Amplification of A. dehalogenans *genes*

The PCR was performed in the Primus Thermal Cycler (MWG Biotech, Ebersberg, Germany) according to Mullis (1994). Amplification of DNA fragments from the genomic DNA of *A. dehalogenans* as template was achieved by adding 100 ng DNA template, 25 pmol of each primer, 0.2 mM dNTPs, 1.5 mM $MgCl_2$, 10 mM Tris HCl pH 8.0, 50 mM KCl, and 2.5 units of *Taq*-polymerase in a final volume of 25 µl. The mixture was initially denatured for 2 min at 95 °C and was subjected to 35 cycles of denaturation (95 °C, 2 min), annealing (55 °C, 45 s), and elongation (72 °C, 2 min). The PCR product was applied onto an agarose gel for analyzing the efficiency of PCR.

2.2.3. Ligation

The PCR product was extracted from the gel using a gel DNA recovery kit (Zymoclean, Epigenetics, USA). The isolated DNA fragments were mixed with a molar ratio of insert to vector of 10:1. The mixture was preincubated at 45 °C for 5 min and was put on ice. The final reaction volume was adjusted to 20 µl. The reaction started with the addition of T4-ligase. The mixture was incubated at 22 °C for 1 hour. The ligation reaction was stopped by incubating at 65 °C for 15 min.

2.2.4. Preparation of chemically competent E. coli *cells*

A stock culture of an isolated colony of *E. coli* strain (either XL1-blue or BL21(DE3)) was inoculated into 5 ml LB medium for making competent cells. The culture was grown overnight at 28 °C. 10% of the final volume of the culture were used for inoculation to 100 ml SOB medium (2% (w/v) tryptone, 0.5% (w/v) yeast extract, 10 mM NaCl, 2.5 mM KCl, 10 mM $MgCl_2$, 10 mM $MgSO_4$). The culture was then cultivated at 28 °C until the $OD_{578\ nm}$ reached 0.6. It was then incubated on ice for 10 min and centrifuged at 4 °C and 2,500 xg for 10 min. The supernatant was removed and 40 ml of TB buffer (10 mM HEPES, 15 mM $CaCl_2$, 250 mM KCl, 55 mM $MnCl_2$, pH 6.7) were added to resuspend the cells. After 10 min incubation on ice, the cells were centrifuged again using the same conditions. The cells were

resuspended in 10 ml of TB buffer followed by the drop-wise addition of 0.75 ml DMSO. The cell suspension was incubated for 10 min on ice before transferring 250 µl to 1.5 ml tubes that were then stored at -80 °C.

2.2.5. Transformation of E. coli

For transformation of *E. coli*, 5 µl of vector was mixed with 250 µl of competent cells of *E. coli* in a 1.5 ml tube and was incubated on ice for 30 min. The mixture was then placed in a heat block for 45 seconds at 42 °C and immediately cooled down on ice. 750 µl of LB medium was added to the tube. The culture was grown for one hour at 37 °C on a mixing block (Biozym Scientific, Oldendorf, Germany) at 1,000 rpm. The cells were spread on a LB-agar plate containing the antibiotic and were incubated at 37 °C for 18 - 24h.

2.2.6. Isolation of plasmid DNA

Isolation of the plasmid DNA was achieved by either using GeneJet plasmid miniprep kit (Fermentas, St. Leon-Rot, Germany) or by the method according to Birnboim & Doly (1979). The cells containing the plasmid were cultivated and harvested as described above. The cell pellets were resuspended in a 1.5 ml tube containing 300 µl 25 mM Tris, 10 mM EDTA solution. Afterward, 300 µl of 0.2 M NaOH, 1% (w/v) SDS was added to the cell suspension. After inverting for 3-4 times, 300 µl of 3 M sodium acetate pH 5.2 was added and the sample was mixed thoroughly. The sample was incubated on ice for 10 min and was centrifuged at top speed for 10 min. The supernatant was transferred to a new tube and 750 µl of isopropyl alcohol was added and mixed thoroughly. The sample was again incubated on ice for 10 min and centrifuged for 20 min. The supernatant was discarded. 500 µl of 70% (v/v) ethanol was used to wash the plasmid DNA. The ethanol was then removed by centrifugation and the plasmid was dried at 50 °C for 20 min. 50 µl of sterile water containing 0.01% (w/v) RNase was used for resuspending the sample.

2.3. Cloning and expression of putative ferredoxin genes

Isolation of genomic DNA from *A. dehalogenans* was performed as described previously (Schilhabel *et al.*, 2009). Via PCR, *A3KS_00044* was initially amplified from the genomic DNA of *A. dehalogenans* by using primer probes Awo_c25230_Fw and Awo_c25230_Rv1

which are degenerated oligonucleotides derived from the *Awo_c23230* gene of *Acetobacterium woodii*. After successfully amplifying the DNA fragment, a set of specific primers was designed using the genomic DNA from *A. dehalogenans* as template. A DNA fragment containing *A3KS_00044* was amplified (primers Amp_A3KS_00044_Fw and Amp_A3KS_00044_Rv). The amplified fragment was subsequently used as a template for the second PCR using primers A3KS_00044_NdeI_Fw and A3KS_00044_Strep_Rv introducing *Nde*I and a part of the *Strep*-tag sequence. The third PCR was performed to complete the *Strep*-tag sequence (IBA, Goettingen, Germany) and insert the restriction site *Bam*HI at the 3' end of *A3KS_00044* by using primers A3KS_00044_NdeI_Fw and Strep_BamHI_Rv (Table 2.2).

The DNA fragment containing *A3KS_02576* was amplified by PCR using primers Amp_ A3KS_02576_Fw and Amp_ A3KS_02576_Rv. The amplified fragment was used as a template for secondary PCR using primers A3KS_02576_NdeI_Fw and A3KS_02576_Strep_Rv introducing *Nde*I and a part of the *Strep*-tag sequence. The third PCR was performed to complete the *Strep*-tag sequence (IBA, Goettingen, Germany) and insert the restriction site *Bam*HI at the 3' end of *A3KS_02576* by using primers A3KS_02576_NdeI_Fw and Strep_BamHI_Rv. List of the primers used for cloning of *A3KS_00044* was shown in Table 2.2.

Table 2.2. Oligonucleotides used for the amplification of the genes encoding the two putative ferredoxins.

Primer	Sequence	PCR Step
Awo_c25230_Fw	GCATAATGAAAAAA(G)TTA(G)GTTGTC(T)	
Awo_c25230_Rv1	ATCTTAAGATTCTTTAATTGC	
Amp_A3KS_00044_Fw	TACCCATCGCTGAAGTAGTTGC	1st
Amp_A3KS_00044_Rv	CAGTAGGAAGCTCATAATCAGCGTAG	1st
A3KS_00044_NdeI_Fw	CGCGTTCATATGATGAAAAAAGTAGTCG	2nd
A3KS_00044_Strep_Rv	CTGCGGGTGGCTCCAAGCGCTGGATTCTTTAAT	2nd
A3KS_00044_NdeI_Fw	CGCGTTCATATGATGAAAAAAGTAGTCG	3rd
Strep_BamHI_Rv	CAGCCGGATCCTTATTTTTCGAACTGCGGGTGGC	3rd
Amp_ A3KS_02576_Fw	TGCGGTCGAACGACC	1st
Amp_ A3KS_02576_Rv	GAGCTAAAGCTCTTTTTTGGC	1st
A3KS_02576_NdeI_Fw	CGCGTTCATATGGCTTATAAAA	2nd
A3KS_02576_Strep_Rv	CTGCGGGTGGCTCCAAGCGCTGTCCTGAAC	2nd
Amp_ A3KS_02576_Fw	TGCGGTCGAACGACC	3rd
Strep_BamHI_Rv	CAGCCGGATCCTTATTTTTCGAACTGCGGGTGGC	3rd

The amplified *A3KS_00044* fragment was digested with *Nde*I and *Bam*HI and was ligated into pET11a (Stratagene, Heidelberg, Germany), yielding pET11a_A3KS_00044. The *A3KS_02576* fragment was digested with *Nde*I and *Bam*HI and ligated into pET11a, generating pET11a_A3KS_02576. The resulting plasmids were transformed into *E. coli* XL1-blue and were grown in the LB medium containing 100 µg/ml ampicillin. The plasmids were isolated from the cell extracts and the sequences were verified by DNA sequence analyses. The pET11a_A3KS_00044 and pET11a_A3KS_02576 were aerobically expressed in *E. coli* BL21(DE3) (Stratagene, Heidelberg, Germany) after induction with 0.5 mM and 0.25 mM IPTG, respectively. At OD_{578} of 1.5 (after overnight induction), cells were collected by centrifugation for 10 min at 10,000 xg.

2.4. Polyacrylamide gel electrophoresis

2.4.1. SDS-PAGE

Separation of denatured proteins can be achieved by SDS-PAGE (Laemmli, 1970). The electrophoresis was performed on the Mini Gel Twin apparatus (Biometra, Goettingen, Germany). The mixture of the resolving gel contained 410 mM Tris-HCl pH 8.8, 0.1% (w/v) SDS, 12-15% (v/v) acrylamide (Rotiphorese® Gel 30; Roth, Karlsruhe), 0.1% (w/v) APS, and 0.04% (w/v) TEMED. The resolving gel should polymerize in 30 min. After the polymerization process was finished, the stacking gel was prepared on top of the resolving gel. The mixture of the stacking gel contained 58 mM Tris-HCl pH 6.8, 0.05% (w/v) SDS, 5% (v/v) acrylamide (Rotiphorese® Gel 30), 0.1% (w/v) APS and 0.1% (w/v) TEMED. The comb was inserted and the mixture was polymerized for 20-30 min. Samples were prepared by mixing one to one with the loading buffer (125 mM Tris-HCl pH 6.8, 4% (w/v) SDS, 20% (v/v) glycerol, 10% (v/v) mercaptoethanol and 0.01% (w/v) bromophenol blue) and heating at 95 °C for 5 min. The samples were loaded into the wells of the stacking gel. The running buffer containing 25 mM Tris, 100 mM glycerol and 0.1% (w/v) SDS was filled in the upper and lower reservoir of the apparatus. The electrophoresis was started with a current of 13 mA and increased to 25 mA when the samples entered the stacking gel. The electrophoresis was continued until the blue dye reached the bottom of the gel. The gel was then fixed with the fixing solution containing 25% (v/v) isopropyl alcohol and 10% (v/v) acetic acid for 15 min

and stained with staining solution (0.025% (w/v) Coomassie Brilliant Blue G250 in 10% (v/v) acetic acid) for 20-30 min. The background was destained by incubating the gel in 10% (v/v) acetic acid on a shaker until the background color was washed out.

2.4.2. Tricine SDS PAGE

Tricine SDS PAGE was performed according to Schägger (2006). Samples were run on a 4% stacking gel and 12% resolving gel. The resolving gel was composed of 1 M Tris HCl pH 8.4, 0.1% (w/v) SDS, 0.4% (w/v) APS, 0.04% (w/v) TEMED. The stacking gel contained 0.75 M Tris HCl pH 8.4, 0.075% (w/v) SDS, 0.125% (w/v) APS, 0.0125% (w/v) TEMED. The upper reservoir of the apparatus was filled up with the cathode buffer containing 0.1 M Tris tricine, 0.1% (w/v) SDS, pH 8.25. The lower reservoir was filled up with the anode buffer (0.1 M Tris HCl pH 8.9). A voltage of 30 V was applied to the system and gradually increased (10 V in every 20 min) up to 100 V during the electrophoresis. The gel was stained with Coomassie Brilliant Blue and destained as described above.

2.4.3. Gel shift experiment

The experiment was performed with anoxic buffers under the room conditions. Two recombinant proteins of interest were incubated in different ratios (30 pmol:10 pmol, 10 pmol:10 pmol, 10 pmol:30 pmol) for two hours at 4 °C under anoxic conditions. The mixtures were then mixed one to one with non-denaturing loading buffer (125 mM Tris-HCl pH 6.8, 20% (v/v) glycerol, 10% (v/v) mercaptoethanol and 0.01% (w/v) bromophenol blue) and were applied to a native polyacrylamide gel. The samples were run on a stacking gel composed of 58 mM Tris-HCl pH 6.8, 5% acrylamide, 0.1% (w/v) APS and 0.1% (w/v) TEMED and a resolving gel containing 410 mM Tris-HCl pH 8.8, 8.5% acrylamide, 0.1% (w/v) APS, and 0.04% (w/v) TEMED. The running buffer was 25 mM Tris, 100 mM glycerol. The separated bands were visualized by silver stain (Switzer *et al.*, 1979). After the electrophoresis was finished, the gel was incubated in the fixing solution. The gel was washed twice with water and was then incubated with 0.005% (w/v) sodium thiosulfate for 15 min. The gel was incubated with 0.1% (w/v) silver nitrate for 15-30 min. After washing with water for few seconds, the gel was developed in 0.036% (v/v) formaldehyde, 2% (w/v) sodium carbonate for 1 - 2 min. The reaction was stopped by incubating the gel in 50 mM EDTA for 15-60 min.

For the mixtures that contained methylcobalamin, all manipulation steps were performed in the dark.

2.5. Purification of recombinant AE , CP, MT I and MT II

The proteins were produced in *E. coli* according to Schilhabel *et al.* (2009). The plasmids used are summarized in Table 2.3. The cells were disrupted by French Press procedure. The recombinant proteins except for MT I were purified by pH shift using a 1ml HiTrap Streptavidin HP column (GE Healthcare, Freiburg, Germany). The column was pre-equilibrated with ten bed volumes of washing buffer (67 mM sodium phosphate buffer pH 8.5 containing 150 mM NaCl and 1 mM PMSF). One ml of cell extract was loaded to the column by using a syringe. Purification of the recombinant proteins was carried out according to manufacturer's protocol. Twenty column volumes of washing buffer were passed through the column before eluting with 67 mM sodium phosphate buffer pH 5.0 containing 150 mM NaCl and 1 mM PMSF. The column could be reused after equilibrating with ten column volumes of the washing buffer.

Table 2.3. Plasmids used for production of *O*-demethylase components.

Plasmid	Relevant characteristics	Source
pAEvanStrep	Gene of AE *odmC* in pASK IBA3+	Schilhabel *et al*. (2009)
pCPguaStrep	Gene of CP_{gua} *gdmA* in pET11a	Frenkel (2010)
pCPsyrStrep	Gene of CP_{syr} *sdmA* in pET11a	Lange (2009)
pCPvanStrep	Gene of CP_{van} *odmA* in pET11a	Schilhabel *et al*. (2009)
pCPverStrep	Gene of CP_{ver} *vdmA* in pET11a	Schilhabel *et al*. (2009)
pMTIvanStrep	Gene of MT I *odmB* in pET11a	Schilhabel *et al*. (2009)
pMTIIvanStrep	Gene of MT II *odmD* in pET11a	Schilhabel *et al*. (2009)

Purification of MT I was achieved by applying the MT I-cell extract on a pre-equilibrated 1 ml *Strep*-Tactin Superflow affinity column. Unbound protein was washed out with twenty column volumes of the buffer and MT I protein was then eluted with 2 mM desthiobiotin in the washing buffer. To regenerate the column desthiobiotin was displaced by 1 mM of HABA in the washing buffer. After removal of HABA by ten column volumes of washing buffer, the column could be re-used. The purified proteins were enriched using a Vivaspin 10 kDa

MWCO concentrator (Vivascience AG, Hannover, Germany) by centrifugation at 6,000 xg and at 4 °C for 30 min. An appropriate volume of c*O*mplete EDTA-free Protease Inhibitor Cocktail solution (Roche Diagnostics, Mannheim, Germany) was added to the purified proteins. All isolated proteins were stored at 10 °C until use. Protein determination was performed by using the Bradford method (Bradford, 1976) with BSA as a standard protein.

2.6. Isolation and reconstitution of recombinant corrinoid proteins by FPLC

Recombinant corrinoid proteins (CP_{gua}, CP_{syr}, CP_{van}, CP_{ver}) were produced as *Strep*-tag fusion in *E. coli*. The cells were harvested by the procedure described above. Cell pellets was resuspended in 3 volumes (w/v) of 50 mM Tris HCl pH 7.5 and were disrupted with French Press (2,000 kPa). The cell extracts were ultra-centrifuged at 133,000 xg (36,000 rpm) and 10 °C for 45 min. The supernatants were diluted by the addition of an equal volume of 50 mM Tris HCl pH 7.5 anoxic buffer containing 0.5 mM dithiothreitol (DTT) (buffer A) and 1 mM PMSF before applying to the ÄKTA FPLC system (GE Healthcare, Freiburg, Germany). All chromatographic steps were carried out in an anoxic chamber with N_2/H_2 (95%/5%) as gas phase. The isolation procedure was identical for all four different CPs. The crude extracts were separately applied onto a Q-Sepharose HP column (1 x 10 cm) pre-equilibrated with buffer A. Components were eluted from the column with an increasing gradient from 0 to 0.25 M KCl in buffer A (5 column volumes), then from 0.25 to 1 M KCl in buffer A (5 column volumes). The column was washed with 3 column volumes of 1 M KCl in buffer A. The CP containing fractions were eluted between approximately 0.25 - 0.3 M KCl. The fractions were combined and 3.6 M ammonium sulfate in buffer A was added to the pool to adjust to a final concentration of 1.2 M ammonium sulfate. After filtration, the solution was loaded onto a phenyl superose HR column (1 x 10 cm) pre-equilibrated with 1.2 M ammonium sulfate in buffer A. The samples were eluted with a decreasing gradient from 1.2 to 0 M of ammonium sulfate in buffer A. The CP containing fractions were collected and evaluated by SDS-PAGE. One c*O*mplete EDTA-free protease inhibitor cocktail tablet and 25 mM DTT were added to the pooled fractions (from approximately 0.2 to 0.3 M $(NH_4)_2SO_4$). Protein determination was carried out by using the Bradford method as described above.

Reconstitution of proteins was performed under strictly anoxic conditions. 6 M betaine was step-wise added to the pool of each apo-protein. The mixtures were stirred until the compound was completely dissolved. A five-fold molar excess of hydroxocobalamin or methylcobalamin (in case of CP_{van}) was added and dissolved. The solutions were incubated for at least 48 h at 10 °C. The mixtures were then diluted 1:60 by drop-wise addition of buffer A with 1 mM PMSF at 4 °C. If methylcobalamin was used for reconstitution, the samples were protected from light during all manipulations. The samples were then filtrated and oxygen was removed by repeated degassing and flushing with N_2 before applying to the MonoQ HR (1 x 10 cm) column pre-equilibrated with buffer A. The samples were eluted with an increasing gradient from 0 - 0.4 M KCl in buffer A (5 column volumes), then from 0.4 to 1 M KCl in buffer A (2.5 column volumes). The column was washed with 1 column volume of 1 M KCl in buffer A. The reconstituted corrinoid proteins were eluted at approximately 0.3 M KCl. Purity of proteins was determined by SDS-PAGE. The fractions containing purified proteins were used for the corrinoid reduction assay.

2.7. Purification and reconstitution of putative ferredoxins

The cells harboring putative ferredoxins Fd I and Fd II, which were encoded by *A3KS_00044* and *A3KS_02576*, respectively, were disrupted by French Press. Therefore, the cell sediment was suspended with an equal volume of 67 mM sodium phosphate buffer containing 150 mM NaCl, pH 8.8 (washing buffer) with 1 mg DNase and 1 mM phenylmethyl sulfonyl fluoride (PMSF). The cells were disrupted in a French pressure cell (G. Heinemann, Schwäbisch Gmünd, Germany) at 14 MPa. The cell extracts were centrifuged at 10,000 xg and 10 °C for 10 min and then the cell debris was removed. The supernatants were mixed with an equal volume of washing buffer containing 1 mM PMSF and were ready for protein purification. For purification, the samples were diluted 1:1 (v/v) with the washing buffer and 2 ml were applied to a pre-equilibrated 1 ml Strep-Tactin Superflow affinity column (IBA, Goettingen, Germany). After washing with 20 column volumes of buffer, the putative ferredoxins were eluted with 2 mM desthiobiotin in the washing buffer. The column was regenerated with 1 mM of HABA in the washing buffer before re-applying samples. The fractions which contained Fd I or Fd II were pooled and concentrated on a Vivaspin 3 kDa MWCO

concentrator (Vivascience AG, Hannover, Germany) by centrifugation at 6,000 xg to a final volume of about 1 ml. The purity of proteins was checked by SDS PAGE.

Insertion of the Fe-S clusters into apo-Fd I and apo-Fd II was performed as follows. The pooled fractions of Fd I and Fd II were purged by nitrogen for 10 min at room temperature. DTT (2 mM) was added followed by addition of 5 fold molar excess (in respect to the theoretical values of iron in the proteins) of ammonium iron(III)citrate. After incubation on ice for 30 min, a 5 fold molar excess (in respect to the theoretical values of sulfur in the proteins) of lithium sulfide was added. The solution was incubated for 16 hours at 10 °C under anoxic conditions. The unbound iron and sulfide were removed by passing the sample through a 5 ml HiTrap Desalting column (GE Healthcare, Freiburg, Germany) pre-equilibrated with 50 mM Tris HCl pH 7.5 containing 0.5 mM DTT. The pooled fractions with Fd I and Fd II were collected and used for determination of iron (Fish, 1988).

2.8. Enzyme assays

2.8.1. Corrinoid reduction assay

The test was performed in anoxic rubber-stopper closed quartz cuvettes purged with nitrogen. Cob(II)alamin is converted to cob(I)alamin in the presence of activating enzyme, ATP and an artificial electron donor Ti(III)citrate and is quantified photometrically. An appropriate amount of a CP containing sample was added to the cuvette. 2 mM of ATP and 5 µl of Ti(III)citrate were subsequently added to the solution. The reaction started by adding 5 µl of AE crude extract. The reduction was recorded by the increasing absorption at 386 nm and decreasing absorption at 475 nm.

2.8.2. Hydrogenase activity assay

The hydrogenase activity was measured in crude extracts and fractions of *A. dehalogenans* in a photometric assay. The assay was carried out in an anoxic quartz cuvette with methyl viologen as artificial electron acceptor. 100 µl assay solutions contained 5 mM methyl viologen in 100 mM Tris HCl (pH 8.0) saturated with H_2. Ti(III)citrate was added prior to the conduction of the assay until a slightly blue color of the buffer was observed. Absorbance increase was measured at 578 nm after addition of crude extract of *A. dehalogenans*. The

assay was monitored for 2 - 3 min at room temperature. Slopes were converted into activity using Beer's Law with an extinction coefficient of 9.7 mM^{-1} x cm^{-1}. 1 mol MV reduced corresponds to 0.5 mol H_2 oxidized.

2.8.3. Formate dehydrogenase activity assay

Formate dehydrogenase activity was measured using a methyl viologen-coupled colorimetric assay in an anoxic quartz cuvette. 100 µl assay solutions contained 5 mM methyl viologen in 100 mM Tris HCl (pH 8.0) and 5 mM formate. Ti(III)citrate was added prior to the start of assay until a slightly blue color of the buffer was observed. Absorbance was measured at 578 nm after addition of the crude extract of *A. dehalogenans.* The assay was monitored for 2 - 3 min at room temperature. Slopes were converted into activity using Beer's Law with an extinction coefficient of 9.7 mM^{-1} x cm^{-1}. 1 mol MV reduced corresponds to 0.5 mol formate oxidized.

2.9. Dot far-Western blot

For far-western blotting, one protein of the *O*-demethylase system was used as a prey and the other components were used as baits. Different amounts of prey proteins (30, 15, 5, and 1 pmol) were spotted as dots on a PVDF membrane (Roche Diagnostics, Mannheim, Germany). The membranes were dried at room temperature. Prey protein-containing strips were incubated with the bait proteins (0.1 mg/ml) in PBST buffer (140 mM NaCl, 1 mM KCl, 6.4 mM Na_2HPO_4, 2 mM KH_2PO_4 and 0.05% (v/v) Tween 20) overnight at 18 °C. The strips were then washed three times (10 min each) with PBST buffer. Bait proteins which bound to the prey proteins in case of protein-protein interaction were detected by incubating with bait-protein-specific 1st antibodies for at least 3 hours at room temperature. The primary antibodies were rabbit polyclonal antisera against AE, MT I or MT II and guinea pig polyclonal antiserum against CP (Sigma, Deisenhofen, Germany). Negative control for each interaction pair was the prey protein blotted on the membrane and incubated with specific antibodies against bait proteins without incubation with the bait proteins. After incubation with the 1st antibody, the membranes were washed again three times with PBST (10 min each) and were incubated with alkaline-phosphatase labeled secondary antibodies against either rabbit or guinea pig for one hour (Sigma, Deisenhofen, Germany). After washing, signals on the

membranes were visualized in the NBT/BCIP reaction. The strips were pre-equilibrated with the substrate buffer (100 mM Tris-HCl pH 9.5, 100 mM NaCl, 50 mM $MgCl_2$) for 2 min. Ten ml buffer containing 0.34 mg NBT and 0.175 mg BCIP were subsequently applied to the membranes. Signals were allowed to develop for several minutes. The staining reaction was stopped by addition of 10 mM Tris-HCl pH 7.4 and 1 mM EDTA.

2.10. Bacterial two-hybrid system

2.10.1. Plasmid construction

For the generation of the pKNT25, pKT25, pUT18 and pUT18C-derived plasmids (Euromedex, Souffelweyersheim, France), AE, CP, MT I, and MT II genes were amplified from *A. dehalogenans* genomic DNA by PCR as described above. A list of the primer pairs used is shown in Table 2.4.

Table 2.4. Oligonucleotides for the amplification of the genes encoding the *O*-demethylase components used in the B2H system.

Primer	Sequence	Vectors
AE_Fw_HindIII	ATCCAAGCTTGATGTCATCTTTGAATAC	pKNT25, pUT18
AE_Rv_BamHI	GCATGGATCCTCTTTCATTTCATTTTG	pKNT25, pUT18
CP_Fw_HindIII	ATCCAAGCTTGATGTCAAAAATTGAAG	pKNT25, pUT18
CP_Rv_BamHI	GCATGGATCCTCCGCTGTTGCCAG	pKNT25, pUT18
MT1_Fw_HindIII	ATTGAAGCTTGATGTTAACAAAAAGACAG	pKNT25, pUT18
MT1_Rv_BamHI	GCATGGATCCTCGAACAATTTCTCTG	pKNT25, pUT18
MT2_Fw_HindIII	ATCCAAGCTTGATGATTATTATCGGAG	pKNT25, pUT18
MT2_Rv_BamHI	GCATGGATCCTCTTTCTTCTGACCG	pKNT25, pUT18
AE_Fw_BamHI	ATCTGGATCCCATGTCATCTTTGAATAC	pKT25, pUT18C
AE_EcoRI_Rv	GCATGAATTCTTATTTCATTTCATTTTGACC	pKT25, pUT18C
CP_Fw_BamHI	ATCCGGATCCCATGTCAAAAATTGAAG	pKT25, pUT18C
CP_EcoRI_Rv	ACTAGAATTCTTACGCTGTTGCCAGTTC	pKT25, pUT18C
MT1_Fw_BamHI	ATTGGGATCCCATGTTAACAAAAAGACAG	pKT25, pUT18C
MT1_KpnI_Rv	GCTTGGTACCTTAGAACAATTTCTCTGACATC	pKT25, pUT18C
MT2_Fw_BamHI	ATCCGGATCCCATGATTATTATCGGAG	pKT25, pUT18C
MT2_EcoRI_Rv	GCTAGAATTCTTATTTCTTCTGACCGAAAATCC	pKT25, pUT18C

The PCR products were ligated into pKNT25 and pUT18 vectors using the *Bam*HI/*Hind*III restriction sites and into pKT25 and pUT18C vectors using *Bam*HI/*Eco*RI restriction sites. As an exception, *Bam*HI/*Kpn*I restriction sites were used for the ligation of MT I and pKT25/pUT18C. Positive controls, pT25-zip/pT18-zip, which contain the sequence of a 35 amino acid leucine zipper motif of GCN4, a yeast transcriptional activator (Blondel & Bedouelle, 1991), were cloned into pKNT25 and pUT18 and were provided in the kit. As negative controls the empty vectors pKNT25 and pUT18 were used. The insert sequence of positive clones was checked by DNA sequence analyses. The resulting plasmids were used for the screening (Table 2.5).

Table 2.5. Plasmids used for the bacterial two-hybrid screen.

Plasmid	Relevant characteristics	Source
pKNT25	Cloning vector for creating in frame fusions at the *N*-terminal end of T25 fragment of *CyaA* , Kan^r	Karimova *et al*. (1998a)
pKNT25-AE	*odmC* in pKNT25	This study
pKNT25-CP	*odmA* in pKNT25	This study
pKNT25-MT1	*odmB* in pKNT25	This study
pKNT25-MT2	*odmD* in pKNT25	This study
pKT25	Cloning vector for creating in frame fusions at the *C*-terminal end of T25 fragment of *CyaA*, Kan^r	Karimova *et al*. (1998a)
pKT25-AE	*odmC* in pKT25	This study
pKT25-CP	*odmA* in pKT25	This study
pKT25-MT1	*odmB* in pKT25	This study
pKT25-MT2	*odmD* in pKT25	This study
pUT18	Cloning vector for creating in frame fusions at the *N*-terminal end of T18 fragment of *CyaA*, Amp^r	Karimova *et al*. (1998a)
pUT18-AE	*odmC* in pUT18	This study
pUT18-CP	*odmA* in pUT18	This study
pUT18-MT1	*odmB* in pUT18	This study
pUT18-MT2	*odmD* in pUT18	This study
pUT18C	Cloning vector for creating in frame fusions at the *C*-terminal end of T18 fragment of *CyaA*, Amp^r	Karimova *et al*. (1998a)
pUT18C-AE	*odmC* in pUT18C	This study
pUT18C-CP	*odmA* in pUT18C	This study
pUT18C-MT1	*odmB* in pUT18C	This study
pUT18C-MT2	*odmD* in pUT18C	This study
pT18-zip	Gene of the leucine zipper of GCN4 in pUT18	Karimova *et al*. (1998a)
pT25-zip	Gene of the leucine zipper of GCN4 in pUTKT25	Karimova *et al*. (1998a)

2.10.2. Screening procedure

Bacterial two-hybrid assays were performed as described in Karimova *et al.* (1998). All combinations of the recombinant plasmids were co-transformed into the reporter strains *E. coli cya* DHM1 or *cya* BTH101 (Euromedex, Souffelweyersheim, France) by heat-shock (Sambrook *et al.*, 2006). Transformants were plated on selective LB-plates containing 25 µg/ml kanamycin and 50 µg/ml ampicillin. Six randomly chosen cotransformants were inoculated into 5 ml of LB-medium containing 50 µg/ml ampicillin, 25 µg/ml kanamycin and 0.5 mM isopropyl β-D-1-thiogalactopyranoside (IPTG) and were grown at 28 °C to an $OD_{600\ nm}$ of 0.6 - 1. The clones were then spotted on LB/X-Gal (LB medium including 40 µg/ml β-X-gal) and MacConkey (56 g/l MacConkey (AppliChem, Darmstadt, Germany), 1% (w/v) maltose) plates containing 100 µg/ml ampicillin, 50 µg/ml kanamycin and 0.5 mM IPTG. The plates were incubated at 28 °C for 2 - 4 days.

The efficiency of the complementation of the interaction pairs could be quantified by measuring the β-galactosidase activity for test clones grown overnight in LB medium under the conditions described above. The assay was performed as described by Miller (1972) with some modifications. The optical density of each culture was recorded at 600 nm. Afterwards, 800 µl of assay buffer (70 mM Na_2HPO_4, 30 mM NaH_2PO_4, 1 mM $MgSO_4$, 0.2 mM $MnSO_4$, and 100 mM β-mercaptoethanol) were added to 200 µl of each culture. Permeabilization solution containing 30 µl 10% (w/v) SDS and 60 µl chloroform was subsequently added to each sample. After incubation at 30 °C for 10 min, 0.25 µl 0.4% (w/v) ONPG was added to the mixtures and the color development started. When the samples turned yellow, the reaction was stopped by adding 500 µl 1 M Na_2CO_3. The mixtures were then centrifuged and the top layer was taken to measure the absorption at 420 nm. The activity in Miller units was calculated by following equation:

$$1{,}000 \times (A_{420\ nm}) / (A_{600\ nm} \times \text{assay volume (ml)} \times \text{reaction time (min)})$$

2.10.3. Confirmation of the protein production by Western blot

The Western blotting was carried out to confirm the correct production of the fusion proteins (Towbin *et al.*, 1979). Cells containing fusion proteins were disrupted by direct lysis in Laemmli buffer. Fusion proteins of B2H assay were separated by Tris glycine SDS-PAGE (13.5%). The PVDF membrane and the gel after PAGE were incubated in blotting buffer (25

mM Tris, 100 mM glycerol, 20% (v/v) methanol) for 15 min. The proteins were transferred to the membranes by using a semi-dry blot apparatus (Biorad, Munich, Germany) at a voltage of 15 V for 1 h. To prevent unspecific binding on the remaining surface, the membrane was then incubated in the blocking solution containing 3% (w/v) nonfat dried milk in PBST buffer. The membrane was washed three times with PBST buffer (10 min each) and was incubated with 1st antibody overnight at 18 °C. The primary antibodies were rabbit polyclonal antisera against AE, MT I or MT II and guinea pig polyclonal antiserum against CP. After repeating the washing step, the membrane was incubated in the solution containing secondary antibodies against either rabbit or guinea pig labeled with alkaline phosphatase. Signals were visualized as described above (see 2.9).

2.11. Yeast two-hybrid system

2.11.1. Plasmid construction

The DNA fragments encoding CP, MT I and MT II were amplified by PCR and fused in frame into the yeast two-hybrid vectors pGADT7 and pGBKT7 (CLONTECH, Saint-Germain-en-Laye, France) using the *Nde*I/*Bam*HI restriction sites. The DNA fragment encoding AE was amplified by PCR and were cloned in frame into pGADT7 and pGBKT7 using the *Nde*I/*Eco*RI and *Nco*I/*Bam*HI restriction sites, respectively. Similarly, the DNA fragments encoding test fragments CP 1-78, CP 79-209, MT I 1-87, MT I 88-326 were amplified by PCR and were cloned in frame into pGADT7 or pGBKT7 using the *Nde*I/*Bam*HI restriction sites. The coding regions of AE 1-133 and AE 134-598 were cloned in frame into pGADT7 and pGBKT7 using the *Nde*I/*Eco*RI and *Nco*I/*Bam*HI restriction sites, respectively. The DNA fragments encoding AE 101-176 were amplified by PCR and were cloned in frame into pGADT7 or pGBKT7 using the *EcoR*I/*Bam*HI restriction sites. List of the primers used for the test is indicated in Table 2.6. As positive control the plasmids pGBKT7-AMTR-AG and pGADT7-LITU-AGL2 were used. These DNA fragments were kindly provided by the Department of Genetics of the Friedrich-Schiller-University Jena, Germany (Härter, 2011). The insert sequences of positive clones were checked by DNA sequence analyses. The resulting plasmids were used for the screening (Table 2.7).

Table 2.6. Oligonucleotides used for the amplification of the genes and gene fragments encoding the *O*-demethylase components used in the Y2H system.

Primer	Sequence	Vectors
AEvan_FspBI_FW01	CGCGTTCTAGCATGTCATCTTTGAATAC	pGADT7
AEvan_EcoRI_RV	ATGAATTCTTATTTCATTTCATTTTGACC	pGADT7
AEvan_PciI_FW	GATATAACATGTCATCTTTGAATACTATTCGCG	pGBKT7
AEvan_BamHI_RV	ATGGATCCTTATTTCATTTCATTTTGACCAAGGG	pGBKT7
CPvan_NdeI_FW	GGAGATATACATATGTCAAAAATTGAAGAAG	pGADT7, pGBKT7
CPvan_BamHI_RV1	ATGGATCCTTACGCTGTTGCCAGTTCTTTAGC	pGADT7, pGBKT7
MTIvan_NdeI_FW	GGAGATATACATATGTTAACAAAAAGACAG	pGADT7, pGBKT7
MTIvan_BamHI_RV1	ATGGATCCTTAGAACAATTTCTCTGACATCTTGT	pGADT7, pGBKT7
MTIIvan_NdeI_FW	GGAGATATACATATGATTATTATCGGAG	pGADT7, pGBKT7
MTIIvan_BamHI_RV	ATGGATCCCTTTCTTCTGACCGAAAATCC	pGADT7, pGBKT7
AEvan_FspBI_FW01	CGCGTTCTAGCATGTCATCTTTGAATAC	pGADT7
AEvan_aa01-133_Stop_EcoRI_RV	TGATGAATTCTAACTTAACTGGCATTTCAAGG	pGADT7
AEvan_aa134-598_FspBI_FW	CGCGTTCTAGCATGTCTTCTATTAAAGTATTAC	pGADT7
AEvan_EcoRI_RV	ATGAATTCTTATTTCATTTCATTTTGACC	pGADT7
AEvan_PciI_FW	GATATAACATGTCATCTTTGAATACTATTCGCG	pGBKT7
AEvan_aa01-133_Stop_BamHI_RV	TGATGGATCCCTTACTTAACTGGCATTTC	pGBKT7
AEvan_aa134-598_PciI_FW	GATATAACATGTCTTCTATTAAAGTATTAC	pGBKT7
AEvan_BamHI_RV	ATGGATCCTTATTTCATTTCATTTTGACCAAGGG	pGBKT7
AEvan_aa101-176_EcoRI_FW	GCATAGAATTCATGAAAACCAGAGTGGTA	pGADT7, pGBKT7
AEvan_aa101-176_BamHI_RV	TGATGGATCCCATTGAGCTCTTT	pGADT7, pGBKT7
CPvan_NdeI_FW	GGAGATATACATATGTCAAAAATTGAAGAAG	pGADT7, pGBKT7
CPvan_aa01-78_Stop_BamHI_RV	TGATGGATCCCTTACAGTGGTTTTAAAAC	pGADT7, pGBKT7
CPvan_aa79-209_NdeI_FW_Y2H	AGATATACATATGGCTGGCGACGG	pGADT7, pGBKT7
CPvan_BamHI_RV1	ATGGATCCTTACGCTGTTGCCAGTTCTTTAGC	pGADT7, pGBKT7
MTIvan_NdeI_FW	GGAGATATACATATGTTAACAAAAAGACAG	pGADT7, pGBKT7
MTIvan_aa01-87_Stop_BamHI_RV	TGATGGATCCCTTAGGGAGCTTTAACATAATC	pGADT7, pGBKT7
MTIvan_aa88-326_NdeI_FW_Y2H	GGAGATATACATATGAATCTTGATTATCCTG	pGADT7, pGBKT7
MTIvan_BamHI_RV1	ATGGATCCTTAGAACAATTTCTCTGACATCTTGT	pGADT7, pGBKT7

Table 2.7. Plasmids used for the yeast two-hybrid assay.

Plasmid	Relevant characteristics	Source
pGADT7	Cloning vector for creating in frame fusion with the GAL4 activation domain (AD; amino acids 768–881)	Louvet *et al*. (1997)
pGADT7-AE	*odmC* in pGADT7	This study
pGADT7-AE 1-133	Derivative of pGADT7-AE, *odmC* 1-133[a]	This study
pGADT7-AE 101-176	Derivative of pGADT7-AE, *odmC* 101-176[a]	This study
pGADT7-AE 134-598	Derivative of pGADT7-AE, *odmC* 134-598[a]	This study
pGADT7-CP	*odmA* in pGADT7	This study
pGADT7-CP 1-78	Derivative of pGADT7-CP, *odmA* 1-78[a]	This study
pGADT7-CP 79-209	Derivative of pGADT7-CP, *odmA* 79-209[a]	This study
pGADT7-MT I	*odmB* in pGADT7	This study
pGADT7-MT I 1-87	Derivative of pGADT7-MT I, *odmB* 1-87[a]	This study
pGADT7-MT I 88-326	Derivative of pGADT7-MT I, *odmB* 88-326[a]	This study
pGADT7-MT II	*odmD* in pGADT7	This study
pGBKT7	Cloning vector for creating in frame fusion with the GAL4 binding domain (DNA-BD; amino acids 1-147)	Louvet *et al.* (1997)
pGBKT7-AE	*odmC* in pGBKT7	This study
pGBKT7-AE 1-133	Derivative of pGBKT7-AE, *odmC* 1-133[a]	This study
pGBKT7-AE 101-176	Derivative of pGBKT7-AE, *odmC* 101-176[a]	This study
pGBKT7-AE 134-598	Derivative of pGBKT7-AE, *odmC* 134-598[a]	This study
pGBKT7-CP	*odmA* in pGBKT7	This study
pGBKT7-CP 1-78	Derivative of pGBKT7-CP, *odmA* 1-78[a]	This study
pGBKT7-CP 79-209	Derivative of pGBKT7-CP, *odmA* 79-209[a]	This study
pGBKT7-MT I	*odmB* in pGBKT7	This study
pGBKT7-MT I 1-87	Derivative of pGBKT7-MT I, *odmB* 1-87[a]	This study
pGBKT7-MT I 88-326	Derivative of pGBKT7-MT I, *odmB* 88-326[a]	This study
pGBKT7-MT II	*odmD* in pGBKT7	This study
pGADT7-LITU-AGL2	LITU-AGL2 in pGADT7	Härter (2011)
pGBKT7-AMTR-AG	AMTR-AG in pGADT7	Härter (2011)

[a] Numbers correspond to the amino acid position.

2.11.2. Transformation of Yeast

According to manufacturer's protocol the constructs of pGADT7 and pGBKT7 were subsequently transformed into the yeast strains Y187 and AH109 (CLONTECH, Saint-Germain-en-Laye, France), respectively. A tube containing 1% (w/v) carrier DNA was heated at 95 °C for 10 min and then was chilled on ice. A blob of yeast from YPAD plate was picked up and suspended in 1 ml sterile water. The suspension was centrifuged for 1 min and the transformation mix (120 µl PEG 4000 50% (v/v), 0.1 M lithium acetate, 5 µl boiled carrier DNA, 1 µg plasmid DNA in sterile water, final volume 180 µl) was transferred to the pellet.

The cells were resuspended by mixing vigorously. The mixture was incubated at 42 °C for 1 - 3 hours. The transformants were then recovered by centrifugation of the mixture for 2 min. The pellets were resuspended in 200 µl sterile water and were spread on a selection plate, SD-Leu for Y187 clones and SD-Trp for AH109 clones. The transformants were grown at 30 °C for 3-4 days in the selective media (Gietz & Schiestl, 2007a; Gietz & Schiestl, 2007b).

2.11.3. Screening procedure

The clones grown on selection plates were used for yeast mating. Single colonies from a-type (AH109) and α-type (Y187) were mated and grown on YPAD plates for one day and were then transferred to a selective plate, SD-Leu-Trp (+His). After 2 - 3 days of incubation, the colonies were selected and used for testing. To screen the colonies, the diploid yeast cells were spotted on the SD-Leu-Trp (+His) as control plate, and on SD-Leu-Trp-His and SD-Leu-Trp-His with 0.5 mM of 3-aminotriazole (3AT) as test plates and were incubated at 28 °C for 3-4 days (Miller & Stagljar, 2004). Positive and negative controls were included on each test plate. The positive control was the diploid yeast of pGBKT7-AMTR and pGADT7-LITU. The negative controls were the diploid cells of either two empty vectors or of one empty vector and a test protein. The clones grown on the test plates were considered to be putative positive interaction pairs. The presence of *HIS3* inhibitor, 3AT, reduces the background and may eliminate the unspecific activation. β-galactosidase assay was performed directly on the colonies grown on the SD-Leu-Trp-His plates as described in the Matchmaker^{TM} Library construction and screening kits protocol (CLONTECH, Saint-Germain-en-Laye, France). The composition of media used in the screen was also described in the protocol.

3. Results

3.1. Interactions of the activating enzyme and the corrinoid protein

This study is devoted to analyze the interaction of the *O*-demethylase components of *Acetobacterium dehalogenans.* In this section, the interaction of AE and CP and the role of the corrinoid cofactor of CP are investigated. Efforts to identify specific residues that are important for the oligomerization of the two proteins are also described.

3.1.1. Sequence analysis of genes encoding for the activating enzyme and corrinoid proteins of different O-*demethylases of* A. dehalogenans

Recent studies indicated that there are several *O*-demethylase enzyme systems present in the anaerobe *A. dehalogenans*. The isolation and characterization of two *O*-demethylating systems vanillate- (*Odm*) and veratrol-*O*-demethylase (*Vdm*) were published (Kaufmann *et al.*, 1997; Engelmann *et al.*, 2001). Two others have been recently identified as syringate- (*Sdm*) and guaiacol-*O*-demethylase (*Gdm*) based on their substrate preferences (unpublished data). The genes of the four different *O*-demethylase systems were found in separate operons. However, they all contain the genes encoding for the three major components of the system: MT I, MT II, and CP. For *Odm*, the gene of MT II is missing. While the genes encoding for CP, MT I and MT II are usually present in the same operon, the gene encoding for AE (*odmC*) is located separately. This is the first and only AE that was identified and characterized from *A. dehalogenans* so far. The *odmC* gene was found approximately 3 kb upstream of the syringate-*O*-demethylase operon (Schilhabel *et al.*, 2009). The gene product consists of 598 amino acids and contains a [2Fe-2S] cluster binding motif in the *N*-terminal part. The recombinant enzyme shared the same characteristics of the purified one from *A. dehalogenans*. Recently, the four different CP genes encoding CP_{gua}, CP_{syr}, CP_{van}, CP_{ver} were heterologously expressed as *Strep*-tag fusions in *Escherichia coli*. Amino acid sequence analyses showed a high similarity between the four CPs (from 80 to 90%). They consist of 208 to 209 amino acids, corresponding to the molecular masses of approximately 21-22 kDa. They all contain the consensus sequence for vitamin B_{12} binding [DXHXXG-41-SXL-(26-28)-GG] (Kaufmann *et al.*, 1998a) (Fig. 3.1). Since a high similarity between the four corrinoid proteins was observed and only one AE has been known so far, it was assumed that

the *O*-demethylases may utilize one AE for the reactivation of different corrinoid proteins. In order to confirm this hypothesis, several approaches were employed. The first attempt was to study the interaction of AE and different CP by gel shift experiments.

```
CPvan  MSKIEEVKAK VEVGKSKLVP GLVQEALDEG SAPGEILQAM VDSMGVVGEK FSSGEIFVPE  60
CPsyr  MSKIQEVKEK VEIGKTKLVP GLVQEALDEG SSAADILQAM VDSMGVVGEK FSSGEIFVPE  60
CPver  MSKITEVKQL VEAGKSKKIG PAVQEALNAG GQPVEILQPM VDSMSVVGDK FSAGEIFVPE  60
CPgua  MSKIEEVKAK VEIGKTKLIP GLVQEALDEG NAPGEILQAM VDSMSVVGEK FSSGEIFVPE  60

CPvan  MLIAAKAMSK GVEVLKPLMA GDGSASLGTC VIGTVAGDLH DIGKNLVSMM IESAGFDMVD  120
CPsyr  MLIAAKAMAK GVDVLRPLLA GDTSNSLGTR IIGTVAGDLH DIGKNLVSMM IESAGFTMVD  120
CPver  MLIAAKAMSK GVDVLRPLMA GDNAASLGTC VIGTVAGDLH DIGKNLVSMM IESAGFTMVD  120
CPgua  MLIAAKAMSK GVDVLRPLMA GDTSASLGTC IIGTVAGDLH DIGKNLVSMM IESAGFTMVD  120

CPvan  LGVDVPADTF VQAVKDNTNV KLVACSGLLT TTMPALKEAV QTIKAAYP-D MKVIVGGAPV  179
CPsyr  LGVDVPAERF VEAIKENKNV TLVACSGLLT TTMPALKEAV QTIKASGL-D VKVIVGGAPV  179
CPver  LGVDVPAEKF VAAARENDNV TLIACSGLLT TTMPALKEAV ATIKASGLAG CKVIVGGAPV  180
CPgua  LGVDVPAERF VEAVKENENV TLVACSGLLT TTMPALKEAV QTIKASGL-D CKVIVGGAPV  179

CPvan  TPEYAAEVGA DGYAPDAGSA AVKARELATA  209
CPsyr  TPEYAAEIGA DGFAPDAGSA AVKAKEMVA-  208
CPver  TSEFAAEIGA DGYAADAGSA AVKAKDLVK-  209
CPgua  TPEYAAEIGA DGFAPDAGSA AVKAKELVA-  208
```

Fig. 3.1. Sequence alignment of the corrinoid proteins of vanillate-*O*-demethylase (CP_{van}), syringate-*O*-demethylase (CP_{syr}), veratrol-*O*-demethylase (CP_{ver}), and guaiacol-*O*-demethylase (CP_{gua}) of *A. dehalogenans*. Amino acid residues in boxes were shown to participate in cobalamin binding of methionine synthase (MetH) of *E. coli*. The vitamin B_{12} binding region of MetH was determined from the X-ray structure (Drennan *et al.*, 1994).

3.1.2. Studies on the interactions of AE and CP by gel shift experiments

The interaction of AE and CP_{van} using gel mobility assay was already investigated by Schilhabel *et al.* (2009). In this study, AE appeared as dimer in the native gel whereas CP_{van} possessed a monomeric form. For the interaction, the presence of the corrinoid cofactor was essentially required. The stoichiometry of the dimeric complex of AE and CP_{van} was determined to be one to one. In order to prove the reproducibility of the method, the experiment was repeated before performing any further investigations. The result obtained was in good agreement with the previous observations (Fig. 3.2, CP_{van}). For that reason the interaction of AE with different CPs of *A. dehalogenans* was further investigated. The four different CPs were purified by column chromatography and were reconstituted with hydroxocobalamin. AE and cofactor-free CP were obtained by affinity chromatography using

1 ml HiTrap Streptavidin HP columns (see Materials and Methods). AE and CP were pre-incubated in different molar ratios in buffer containing 2 mM DTT and were separated by native PAGE. Protein bands were visualized by silver staining. For CP_{gua} a ladder of bands running from 21 kDa to 67 kDa was observed. CP_{syr} and CP_{van} were present as monomeric proteins in the gel shift experiment as shown by single bands at around 21 kDa. Interestingly, CP_{ver} appeared to migrate and form one major band at 42 kDa suggesting the formation of a dimer. The bands corresponding to the complex of 2AE/2CP appeared clearly at around 180 kDa for all interaction pairs (Fig 3.2). At the molar ratio of 1:1, only protein complex bands were observed, the bands of both interacting partners (AE and CP) almost disappeared. When incubating the mixtures with excess amounts of either AE or CP (molar ratios of 3:1 and 1:3, Fig. 3.2), the band corresponding to the protein with higher molar ratio was still present. Taken together, AE showed its ability to interact with all four different CPs. The dimeric complexes of AE and CPs have 1:1 stoichiometries.

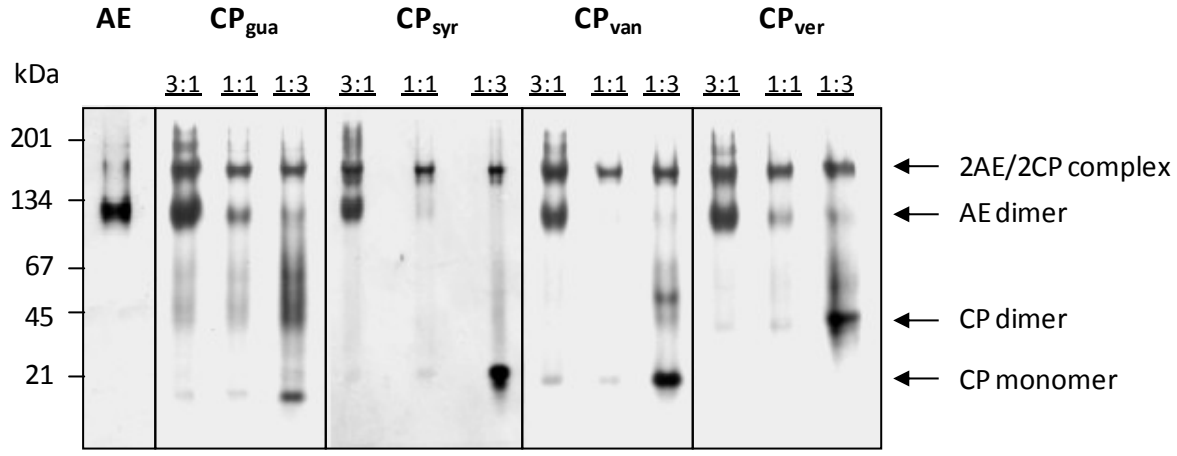

Fig. 3.2. Gel shift experiment to investigate the interaction of AE and reconstituted corrinoid proteins of different *O*-demethylase systems. Protein mixtures containing different molar ratios of AE and CP (30:10, 10:10, 10:30; pmol:pmol) were incubated under anoxic conditions for 2 hours at 10 °C before applying to the native PAGE (8.5%). Each interaction pair of AE and CP is shown in different boxes. The signals were developed by silver stain. The molecular masses of the marker proteins are shown on the left.

When incubating the AE:CP mixtures in the absence of the corrinoid cofactor, almost no signal of the 180 kDa band was observed (Fig. 3.3), whereas in the presence of the cofactor, the 180 kDa band of the 2AE/2CP complex were detected (Fig. 3.3). The observation that the

complex formation was obtained only in the presence of the corrinoid cofactor hydroxocobalamin appears to be valid for all interaction pairs.

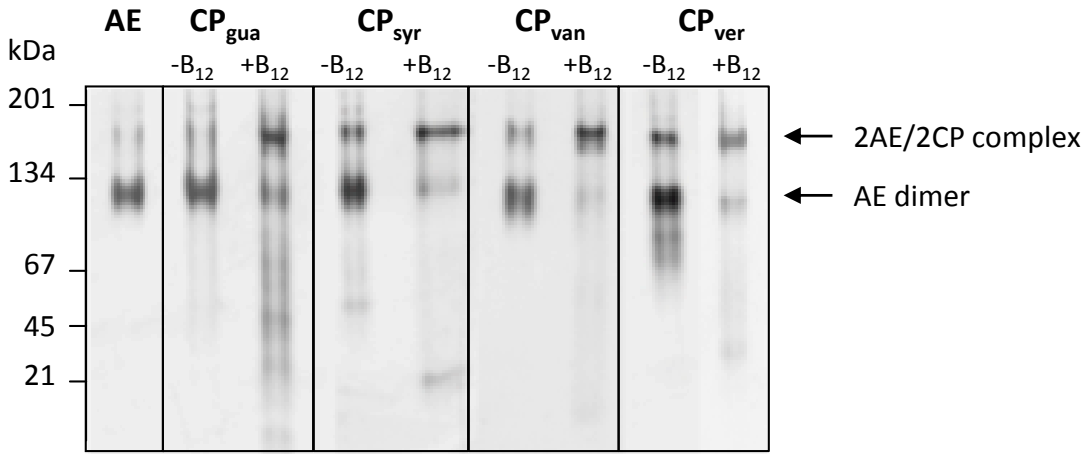

Fig. 3.3. Gel shift experiments to demonstrate the interaction of AE and CP in the absence and presence of the corrinoid cofactor hydroxocobalamin. AE:CP mixtures with a molar ratio of 1:1 without ($-B_{12}$) and with ($+B_{12}$) hydroxocobalamin as corrinoid cofactor were separated by native PAGE (8.5 %) after pre-incubation at 10 °C for 2 hours. Each interaction pair of AE and CP is shown in separate boxes. The molecular masses of the marker proteins are shown on the left.

In gel shift experiments of AE and cofactor-free CP, almost no AE/CP complex was formed. The main protein band detected was the AE dimer. This is also indicated in Figure 3.3 where no defined band of the CPs was found in the lanes of the AE/CP mixtures without the presence of the corrinoid cofactor. For that reason the behavior of both CP forms ($-B_{12}$/$+B_{12}$) on native PAGE was checked. Our experimental data indicated that the cofactor-free CPs showed no defined band on the native gel (Fig. 3.4.A). The presence of hydroxocobalamin has a significant effect on the conformation of CP in gel shift experiments. All four reconstituted CPs showed better shapes and clear major bands in comparison to those of the non-reconstituted ones.

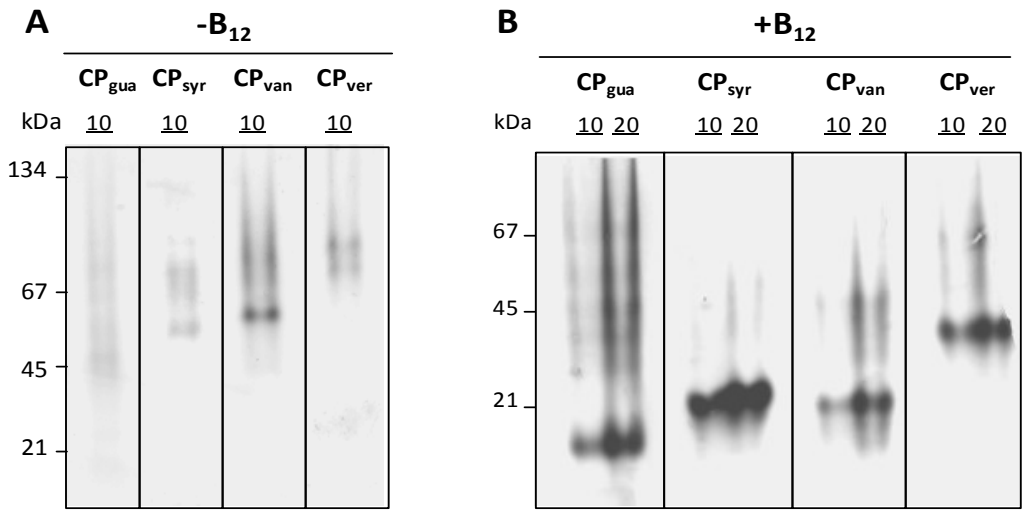

Fig. 3.4. Native PAGE of different corrinoid proteins without (A) and with (B) the corrinoid cofactor hydroxocobalamin. (**A**) Native gel of different CPs without corrinoid cofactor (-B_{12}) after silver stain (10 pmol each). (**B**) Native gel of different CPs after reconstitution with the corrinoid cofactor hydroxocobalamin (+B_{12}) after silver stain (10 and 20 pmol).

3.1.3. Specific activities of AE in the presence of different CPs

To compare the specificity of reductive activation of AE for different CPs, a corrinoid reduction assay was performed. The redox state of CP was monitored by continuous recording of the characteristic UV/Vis spectrum of the bound corrinoid cofactor. In the presence of ATP and Ti(III)citrate as artificial electron donor, the purified AE was able to reduce all four different corrinoid proteins. During the reduction, the absorbance at 475 nm decreased due to conversion of the cob(II)alamin species of CP coupled to an increase in absorbance at 386 nm due to the formation of cob(I)alamin (Fig. 3.5). The difference in absorption at 386 and 475 nm was used for determination of the specific corrinoid reduction activity of AE. As shown in Table 3.1, the enzyme activity was highest with CP_{syr} and CP_{van}, whereas in the presence of CP_{gua} and CP_{ver} the specific activity was lowered to 70% and 50%, respectively.

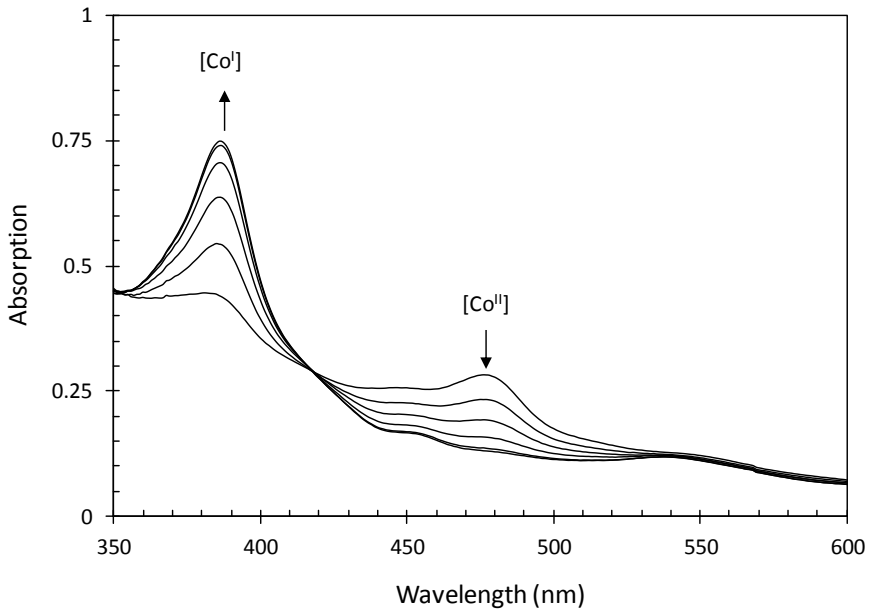

Fig. 3.5. Reduction of cob(II)alamin to cob(I)alamin in the presence of AE, ATP and Ti(III)citrate. The reaction was performed at room temperature under anaerobic conditions as described in the Materials and Methods section. Spectral changes occurring during the reduction of cob(II)alamin (475 nm) to cob(I)alamin (386 nm) were recorded every 1 min.

Table 3.1. Specific activities of AE with corrinoid proteins of different *O*-demethylases.
The activity was measured in triplicate for two different CP concentrations. Ti(III)citrate served as artificial electron donor. For details, see Materials and Methods.

Corrinoid protein	CP (μM)	Enzyme activity (nkat/mg)
CP_{gua}	40	3.37
CP_{gua}	15	1.97
CP_{syr}	40	6.70
CP_{syr}	15	4.16
CP_{van}	40	6.39
CP_{van}	15	3.82
CP_{ver}	40	4.79
CP_{ver}	15	2.66

The results of the corrinoid reduction assay were in accordance to those obtained in gel shift experiments. The shifted bands (dimeric AE/CP complex) were fully observed only in the mixtures of AE:CP_{syr} and AE:CP_{van} at a molar ratio of 1:1 (see Fig. 3.2). For mixtures containing CP_{gua} or CP_{ver}, there were still trace amounts of AE and CP left. However, these minor differences in the gel shift were not significant so that no conclusion can be drawn from

this observation. A relationship between the specific activity of AE and the sequence identities between the four CPs is not detectable. Although CP_{ver} shows the lowest sequence identity compared to the other three CPs, the corrinoid reduction activity is higher than for CP_{gua}.

For further investigation, several attempts were performed to create fragments of AE and CP. However, all attempts have not been successful so far. The fragments of either AE or CP seem to be unstable or were produced only in tiny amounts close to or below the detection limit.

3.1.4. Studies on the interactions of AE and CP by yeast two-hybrid screens

In order to verify the interaction of the two components, different methods including yeast and bacterial two-hybrid systems were employed. The first attempt was to use the yeast two-hybrid (Y2H) system which is based on the direct transcriptional activation of GAL4 domain. In the yeast two-hybrid assay, two proteins, either AE or CP_{van} were fused in frame to two domains, one is a GAL4 transcriptional activation domain (found on plasmid pGADT7) and the other is a DNA binding domain (found on plasmid pGBKT7). If two proteins interact, a functional reconstitution of the GAL4 transcription factor occurs and the expression of the reporter genes is activated (Fig. 3.6). The activation is shown as cell growth on medium without histidine. It is known that the yeast two-hybrid assay may generate a significant number of false positives which probably represents a random generation of histidine-positive colonies (Causier & Davies, 2002). To minimize the unspecific activation, 3-amino-1,2,4-triazole (3AT) was included in the test plates. 3AT is the competitive inhibitor of *HIS3* production, therefore only colonies with a strong activation of *HIS3* (as a result of the interaction) will produce histidine and can grow on the test plates. The positive control was the combination of pGADT7-LITU/pGBKT7-AMTR. Combinations of fusion proteins and empty vectors (pGADT7, pGBKT7) were used as negative control. If any clone of these combinations grows on the test plate, all interactions observed with the fusion protein in this clone will be considered to be false positive. In order to control the growth of the colonies, selection plates with histidine were used (Fig. 3.7A). The screening procedure was described in the Materials and Methods section.

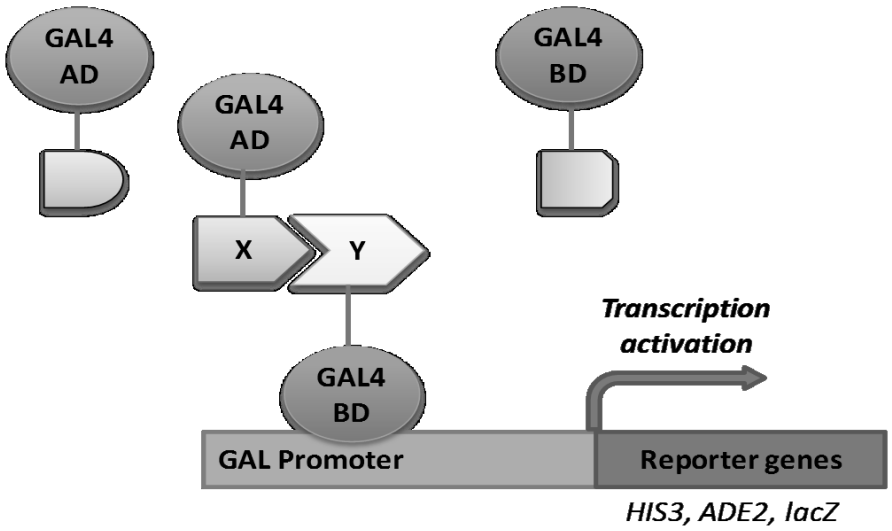

Fig. 3.6. Overview of the mechanism of the Matchmaker yeast two-hybrid system (Takara Bio Europe/Clontech, Saint-Germain-en-Laye, France). One protein of interest (X) is fused in frame to the GAL4 transcriptional activation domain (GAL4-AD), the other protein (Y) is fused in frame to the DNA binding domain (GAL4-BD). The two fusion proteins are transformed into the appropriate yeast strain. The yeast strains are mated and the diploid cells are used for the test. The interaction between proteins X and Y leads to the reconstitution of a transcription factor (GAL4) in such a way that the reporter genes (*HIS3, ADE2, lacZ*) are expressed (Coates & Hall, 2003).

Using this assay, no interaction between AE and CP was observed since no growth of colonies comprising AE-CP pairs in both directions (pGADT7-AE/pGBKT7-CP and pGADT7-CP/pGBKT7-AE) occurred (Fig. 3.7B). It should be mentioned that there is no cobalamin biosynthesis in yeast. In gel shift experiments, the presence of the corrinoid cofactor was a prerequisite for an interaction of AE and CP. This is probably also true for the yeast two-hybrid screen. Interestingly, a positive interaction was observed for the AE-AE pair (Fig. 3.7B).

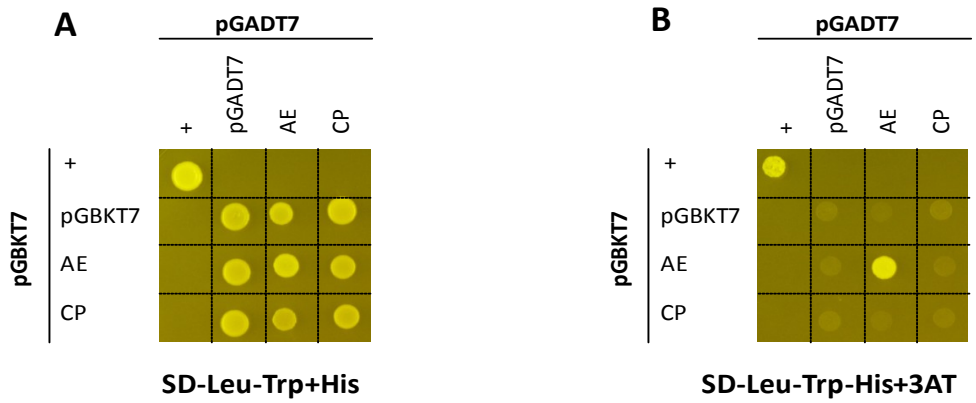

Fig. 3.7. Screening for interaction of AE and CP by Y2H assay. The genes of AE and CP were fused in frame to GAL4 BD (pGBKT7 plasmid) or GAL4 AD (pGADT7 plasmid). The constructs were transformed into the appropriate yeast strain of opposite mating type (a and α) and were grown on selection disks. After mating, both constructs were present in the diploid yeast. The diploid cells were cultivated for 72 h at 30 °C on the control plate with histidine (**A**), and on test plates lacking histidine but with the addition of 3AT (**B**). As positive control cells bearing the pGADT7-LITU/pGBKT7-AMTR pair were used. The combination of two empty vectors or one empty vector and one test protein represented the negative controls.

To have a closer look into the self-interaction of the AE molecule, two fragments of AE were prepared. *In silico* analyses of the structure indicated an [Fe-S] cluster binding motif at the *N*-terminus of the protein which comprises amino acids 1 to 133. As stated in the Introduction section, AE was shown to contain a [2Fe-2S] cluster which is involved in the activation and/or reduction of corrinoid proteins (Schilhabel *et al.*, 2009). The other part of the protein contains several functional domains where nucleotide binding and hydrolysis may occur. To specify the site of interaction, two fragments of AE, one at the *N*-terminus of the protein (residues 1-133, AE1-133) and the other at the *C*-terminal part of AE (residues 134-598, AE134-598) were prepared. The interaction of AE domains was assayed on the control and test plates (Fig. 3.8) as described above. The AE134-598 fragment was able to interact neither with itself nor with the parental AE. Interestingly, the fragment AE1-133 interacted with each other and also with full length AE. This result was observed in both directions, when AE1-133 was fused to either the activation or the binding domain of GAL4.

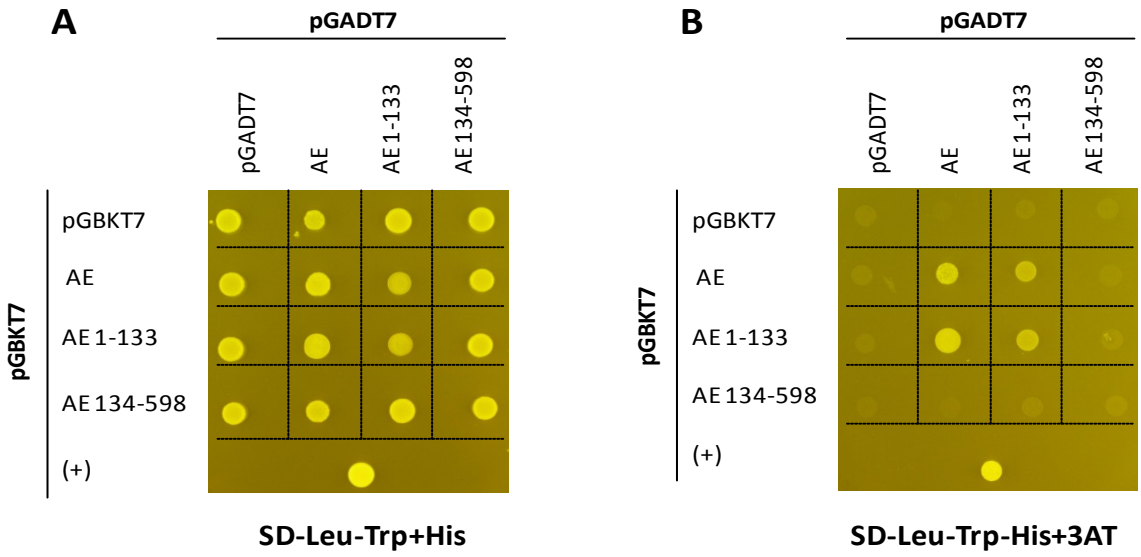

Fig. 3.8. Investigation of fragments involved in the oligomerization of AE by Y2H assay. The two AE fragments AE 1-133 and AE 134-598 were fused in frame to pGADT7 and pGBKT7 and were tested for the interaction by Y2H screen. The growth of the clones was monitored on the control plate (**A**). Positive interactions are shown as growth of clones on the test plate (**B**).

In the course of these investigations, a study was published indicating the site responsible for the dimerization of an AE-like protein (Hennig *et al.*, 2012). In this study, the crystal structure of the ATP-dependent reductive activator of the corrinoid iron/sulfur protein (CFeSP) of *Carboxydothermus hydrogenoformans* was solved. The structure of the activator (RACo) can be divided into four domains: the *N*-terminal domain (residues 3-94) with the [2Fe-2S] cluster, the linker domain (residues 95-125) which connects the *N*-terminal domain to the middle domain (residues 126-206) and the large *C*-terminal domain (residues 207-630). The middle domain was shown to be involved in the dimerization of RACo. On the basis of this structure a reliable computational model of AE of *A. dehalogenans* was predicted (Sperfeld, 2012). In this model the middle domain of AE was detected for residues 101-176. Therefore, new AE fragments (AE101-176 in pGADT7 and pGBKT7) for the further investigation of the interaction were prepared. The full-length AE-AE pair served as the positive control of the test. No interaction was detected between AE101-176 and full-length AE or AE101-176 itself (Fig. 3.9).

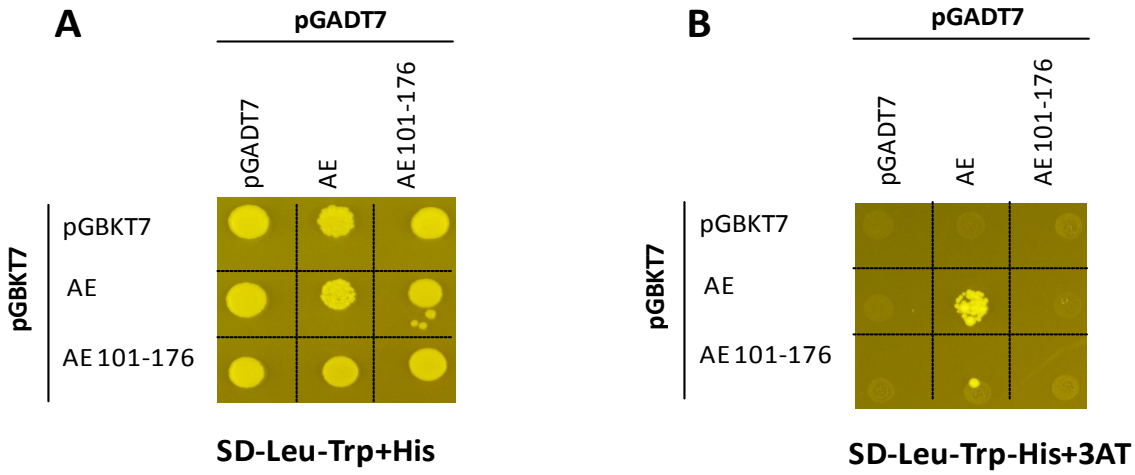

Fig. 3.9. Investigation of the interaction of the AE101-176 fragment with itself and with full length AE by the Y2H assay. The AE-AE pair served as the positive control in this assay. The growth of the clones was monitored on the control plate (**A**). Positive interaction is shown as growth of clones on the test plate (**B**).

3.1.5. Studies on the interactions of AE and CP by bacterial two-hybrid system

Because unspecific activation occasionally happens in yeast and there is a possibility that some interactions are not detected, we used another two-hybrid system which based on indirect activation – the bacterial two-hybrid (B2H) assay (Karimova *et al.*, 1998; Karimova *et al.*, 2000a). In the B2H system, one protein of interest is fused to the T25 fragment and the other is fused to the T18 fragment of the catalytic domain of *Bordetella pertussis* adenylate cyclase. The fused genes encoding the hybrid proteins were coexpressed in an *E. coli* strain deficient in its endogenous adenylate cyclase production. Upon interaction of the hybrid proteins, the T25 and T18 fragments are brought to proximity which results in the functional complementation of the two fragments, leading to cAMP synthesis and in turn to transcriptional activation of catabolic operons (Fig. 3.10).

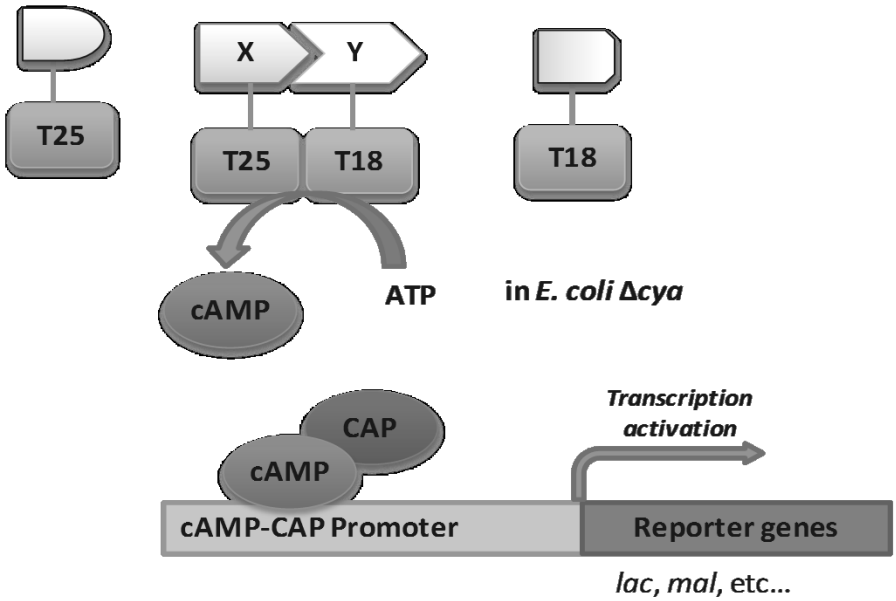

Fig. 3.10. Overview of the mechanism of the bacterial two-hybrid system (EUROMEDEX, Souffelweyersheim, France). Two proteins of interest (X and Y) were genetically fused to the complementary fragments T25 and T18 from the catalytic domain of *B. pertussis* and co-expressed in *E. coli Δcya* cells. Interaction between two-hybrid proteins resulted in functional complementation between the T25 and the T18 fragments leading to cAMP synthesis. Cyclic AMP produced by the reconstituted chimeric enzyme binds to the catabolite activator protein, CAP and activates catabolic operons of *E. coli*. The activation turns on the transcriptional process of reporter genes such as *lacZ* and *mal* giving rise to the selectable phenotypes (Karimova *et al*., 2000b).

An advantage of the B2H over Y2H is that the proteins of interest can be fused either to the *N*- or *C*-terminal end of the T25 or T18 fragment which provides an extended range of combinations to study protein-protein interactions. The pKNT25 and pUT18 allow the expression of the selected genes encoding proteins fused to the *N*-terminal ends of the T25 and T18 domains of the adenylate cyclase, respectively. The pKT25 and pUT18C allow the expression of the selected genes encoding proteins fused to the *C*-terminal ends of T25 and T18 domains of adenylate cyclase, respectively. The leucine zipper of the yeast GCN4 transcription factor served as a positive control (Karimova *et al.*, 2000b). As negative control the empty vectors pKNT25 and pUT18 were used. Full-length AE and CP were fused to T25 and T18 using all four possible fusion types (at either *C*- or *N*-terminus of the two fragments) and were co-transformed into the *cyaA* deficient BTH101 strain generating 16 interaction pairs. For each interaction pair, three clones were used for the screening. A positive interaction will create a functioning adenylate cyclase, which will then synthesize cAMP and subsequently turn on catabolic reporter genes such as *lacZ* or *mal* in *E. coli* (Fig. 3.10). The

clones which are capable of producing β-galactosidase or using maltose as unique carbon source can be discriminated by selectable phenotypes. The differences can be seen when clones grew on the LB/X-gal or MacConkey plates. On MacConkey plates, clones having positive protein-protein interaction will turn red because of acidic production as a result of the *mal* reporter gene activation. On LB/X-gal plates, clones showing positive interaction will turn blue because of the activation of the *lacZ* reporter gene resulting in the production of β-galactosidase. This enzyme degrades the X-gal on plate leading to the formation of blue color (Karimova *et al.*, 2000b).

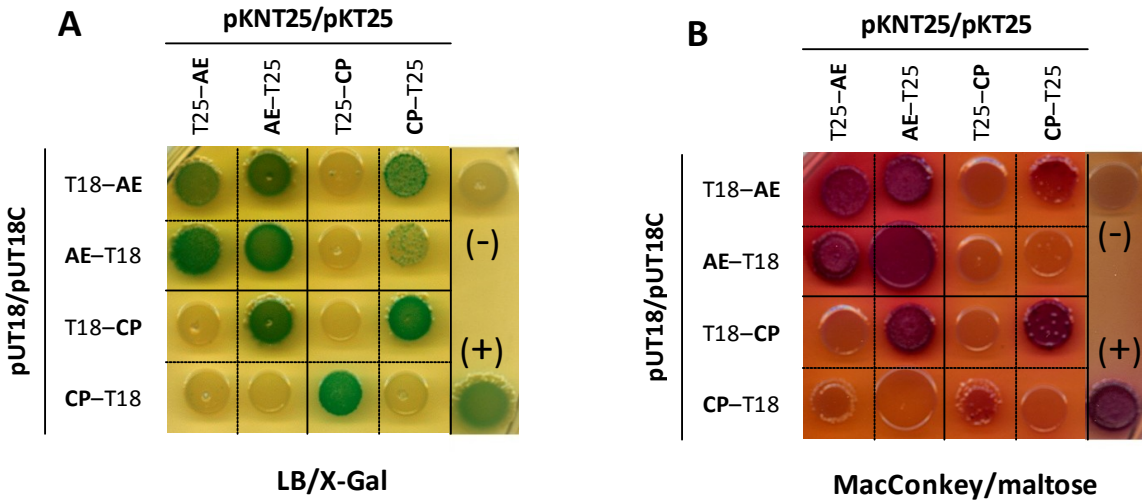

Fig. 3.11. Screening for interaction of AE and CP by B2H assay. AE and CP were fused to the *C*-terminus of the T25 and T18 fragment of *B. pertussis* adenylate cyclase by using plasmids pKT25 and pUT18C, respectively and to *N*-terminus of the T25 and T18 fragment by using plasmids pKNT25 and pUT18, respectively. Two constructs of each pair were co-transformed into *E. coli Δcya* and cells were dropped on the specific test plates. (**A**) Clones were cultivated on the LB/X-Gal plate. Positive interaction resulted in a blue color of colonies. (**B**) Clones were cultivated on the MacConkey plate. A positive interaction resulted in a red color of colonies. As positive control the leucine zipper of GCN4 transcription factor was used. Negative control was the combination of two blank vectors (pKNT25/pUT18).

Figure 3.11 depicts the results of the B2H assay with the selected clones after screening procedure. The two assays on LB/X-Gal and MacConkey plates gave conformable results. AE showed a strong self-interaction which was detected for all fusion types. Interestingly, the self-interaction of CP_{van} which was not found in Y2H system was observed in B2H. The interaction seems to be not as significant as that of AE. Notably, an interaction of AE and CP was also observed using this assay. To our knowledge the *E. coli* strain used for the test is not

able to produce cobalamin itself. Therefore, like in Y2H system, the interaction between AE and CP was not expected. It should be noted that the interaction was only observed when one protein was fused to *N*-terminal end of T25 and the other was fused to the *C*-terminus of T18 (AE-T25 / T18-CP or CP-T25 / T18-AE).

The reproducibility of the system was checked by carrying out the experiment in triplicate. The second test was in good agreement with the first one. The third test which was performed one month later showed different results. Most of the strong interactions obtained in the first experiment changed to either faint or moderate ones. Although discrimination between the positive and negative ones was still possible, the differences were not as significant as those obtained from the previous results. We carried out a number of tests in order to improve the reproducibility of method. As indicated in the manufacture's protocol, in BTH101 an unstability of the plasmids may appear. Therefore, the tests were repeated in the more stable DHM1 strain. However, similar observations were made. Several trials were performed to change the growth conditions, i.e. changing the concentration of antibiotics, IPTG, lowering the temperature, using new clones of BTH101. Unfortunately, all trials were not successful.

In order to interact, proteins must be accumulated in the host cells. The Western blot method was performed to investigate the protein expression and accumulation during the B2H assay. Cell extracts carrying the plasmids expressing the fusion pairs were tested for accumulation using specific antibodies against either AE or CP. The results obtained were not unambiguous. In most cases proteins of the fusion pairs did not accumulate but in some others they did. This observation can be even found in the cells showing positive interactions in the test plates. Figure 3.12 showed one example in which the Western blots were carried out for all pairs harboring the fusion protein of T25 and AE or T18 and CP. Using AE antibodies, only the accumulation of AE-T25 in the AE-T25/T18-CP pair, which showed significant interaction on both LB/X-gal and MacConkey plates, was detected. The others did not show any level of accumulation of T25-AE or AE-T25. In contrast, no accumulation of T18-CP of the AE-T25/T18-CP pair by using CP antibody occurred (Fig 3.12B). In this test, the pair AE-T25/CP-T18 appeared to accumulate CP-T18. As shown in Figure 3.11 this pair exhibited no interaction via plate assay. This pointed to the possibility that the constructs were not accumulated thus they could not be detected by Western blot. This was also the case for both BTH101 and DMH1 strains (data not shown). Similar observations were also obtained by

using anti-*Bordetella pertussis* CyaA (Santa Cruz Biotechnologies, CA, USA) antibodies to detect the accumulation of proteins by Western blot.

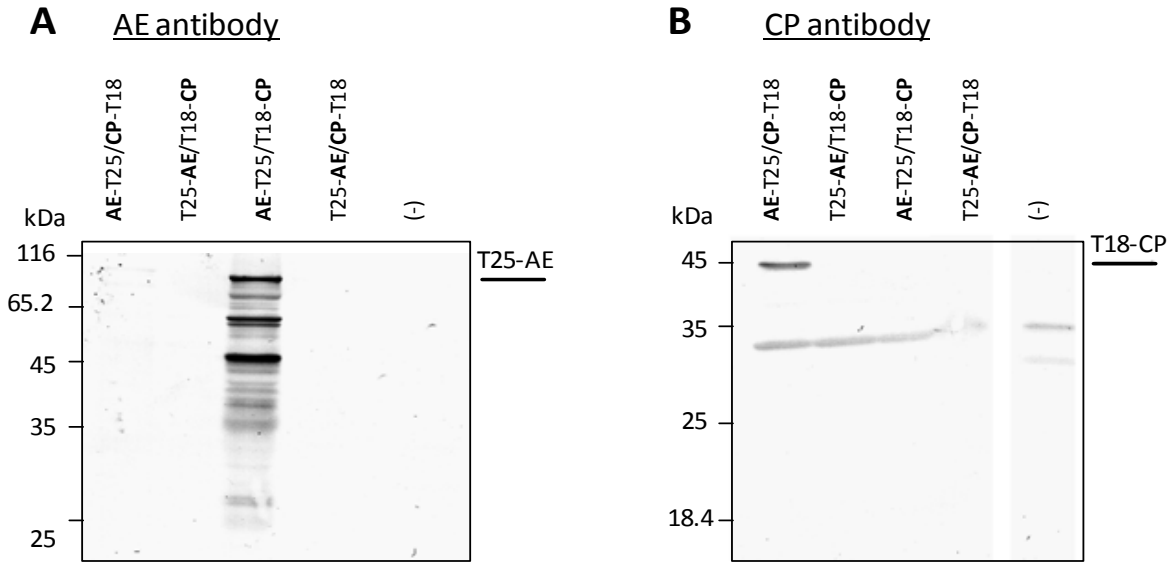

Fig. 3.12. Western blot to verify the presence of the recombinant proteins in *E. coli Δ*cya. The cell extracts were tested for the accumulation of the fusion proteins by Western blot using AE (**A**) or CP (**B**) antibodies. The negative control (-) applied to the last lane was the crude extract containing the empty vectors pKNT25/pUT18. The solid line on the right side of each blot was the expected band of the respective fusion protein. The molecular mass of the protein markers is indicated on the left.

3.1.6. Interaction between AE and CP studied by far-Western blot

Interestingly, the absence of the corrinoid cofactor did not have any effect on the interaction between AE and CP in B2H assay. To verify this observation, a second *in vitro* approach via far-Western blot was employed. The test was performed on a PVDF membrane. Another membrane material, nitrocellulose, was also used for the test but didn't show good results in comparison to those with PVDF membranes (data not shown). In far-Western blots, the test protein (prey protein) was spotted directly onto the membrane in different concentrations and was incubated with the interacting partner (bait protein). The mixture was then incubated with the first antibody against the bait protein, then with the secondary antibody labeled with alkaline phosphatase for visualizing the signals. A negative control was included to control the unspecific binding between the bait protein antibodies and the prey protein. The negative control was prepared as the test samples but without incubation of the membrane with the bait

protein. The intensity of signals detected in relation to that of the negative control was used to estimate the binding affinity of the proteins. A weak background staining occurred on almost all test strips as a result of incubating with an excess amount of bait protein. This phenomenon was not observed on the negative control strips.

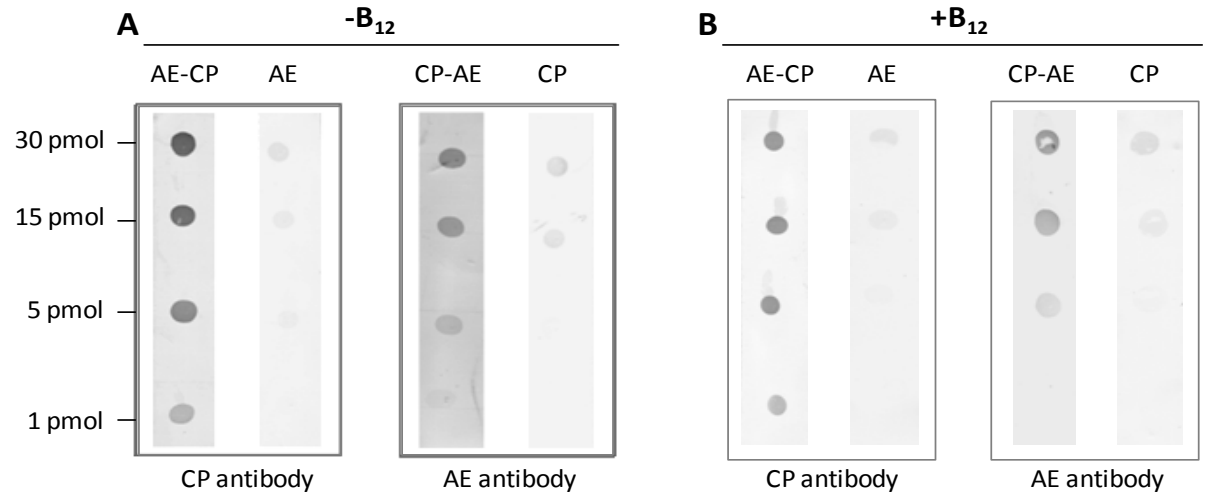

Fig. 3.13. Dot far-Western blot to study the interaction between AE and CP in the absence (A) and presence (B) of the corrinoid cofactor hydroxocobalamin. Proteins in different concentrations were directly spotted on a PVDF membrane and allowed to absorb as dots (as prey protein). The protein amount is indicated on the left. After blocking, the membrane was incubated with the interacting partner (bait protein in solution, 0.1 mg/ml) and afterwards with the first antibody against the bait. Signals were visualized in the NBT/BCIP reaction using alkaline-phosphatase labeled secondary antibodies. Two strips per interaction pair are shown – on the left: the interaction pair tested, on the right: the control without bait.

To continue in the same line of previous experiments, CP_{van} was used for testing the interaction with AE. As shown in Figure 3.13A, strong signals for the interaction of AE and CP were observed. The interaction of this pair can be detected in both directions when AE is on the membranes and CP in the solution or *vice versa*. Remarkably, the interaction occurred regardless of the absence or presence of the corrinoid cofactor hydroxocobalamin as the result obtained showed no difference between the two assays (Fig. 3.13).

3.2. Interactions of the other *O*-demethylase components

Beside the interactions of AE and CP, which were one target of the work presented here, the interactions of the other *O*-demethylase components were studied in more detail using the

methods described above. We used the same approaches to further investigate the additional interactions between the *O*-demethylase components.

3.2.1. Gel shift experiments

To analyze the interactions in which the methyltransferases I and II (MT I, MT II) and/or AE and CP are involved, all recombinant proteins were produced in *E. coli* as *C*-terminal *Strep*-tag fusions and were purified by one step purification using *Strep*-tactin columns as described above (see Materials and Methods). The purity of proteins was confirmed by SDS PAGE. Schilhabel *et al*. (2009) mixed AE, CP, MT I and MT II at a molar ratio of 1:1:1:1. After pre-incubation, the sample was subjected to native PAGE. Only the shifted band at 180 kDa which corresponds to a dimeric AE/CP complex (see also Fig. 3.2) was observed. No other interaction was found. Using the same approach, the interaction was studied for mixtures of only two components. The pair consisting of AE and reconstituted CP_{van} served as positive control. The CP used for the test was the one reconstituted with hydroxocobalamin. The four recombinant proteins were combined yielding six pairs: AE-CP, AE-MT I, AE-MTII, CP-MT I, CP-MT II and MT I-MT II. For each pair, three molar ratios (30:10, 10:10, and 10:30; in pmol) were used. The mixtures were incubated in the presence of 2 mM DTT for two hours at 10 °C. The results were obtained by native PAGE and silver stain.

Figure 3.14A showed the results of the test for the interaction of the activating enzyme and the two methyltransferases. MT I appeared as a single band in the gel at around 21 kDa. The apparent molecular mass is different from the predicted one (36 kDa). In native PAGE, protein mobility is determined by a complex combination of factors, e. g. the shape of the protein molecule. Under certain conditions, proteins may move in unpredictable ways. Moreover, since native charge is preserved, proteins can migrate towards either electrode, depending on their charge. Therefore, molecular mass determination by this method does not yield reliable results. For MT II a diffuse band at approximately 40 kDa was detected. The predicted molecular mass is 30 kDa. For both combinations (AE-MT I, AE-MT II), no shifted bands were observed (Fig. 3.14A). AE runs as dimer or trimer, MT I or MT II bands were visible. However, there was no decrease or increase in the intensity of the signals of the proteins in the three different molar ratios compared to the single protein bands suggesting that the quantities of the mixture components were not changed. For the pair CP-MT I (Fig.

3.14B) the CP and MT I bands overlap. No shifted band was visible. Similar results were obtained for the CP-MT II and MT I-MT II pairs. (Fig. 3.14B and C). Taken together, it seems that no further interaction was found except for AE and CP by using gel shift experiments.

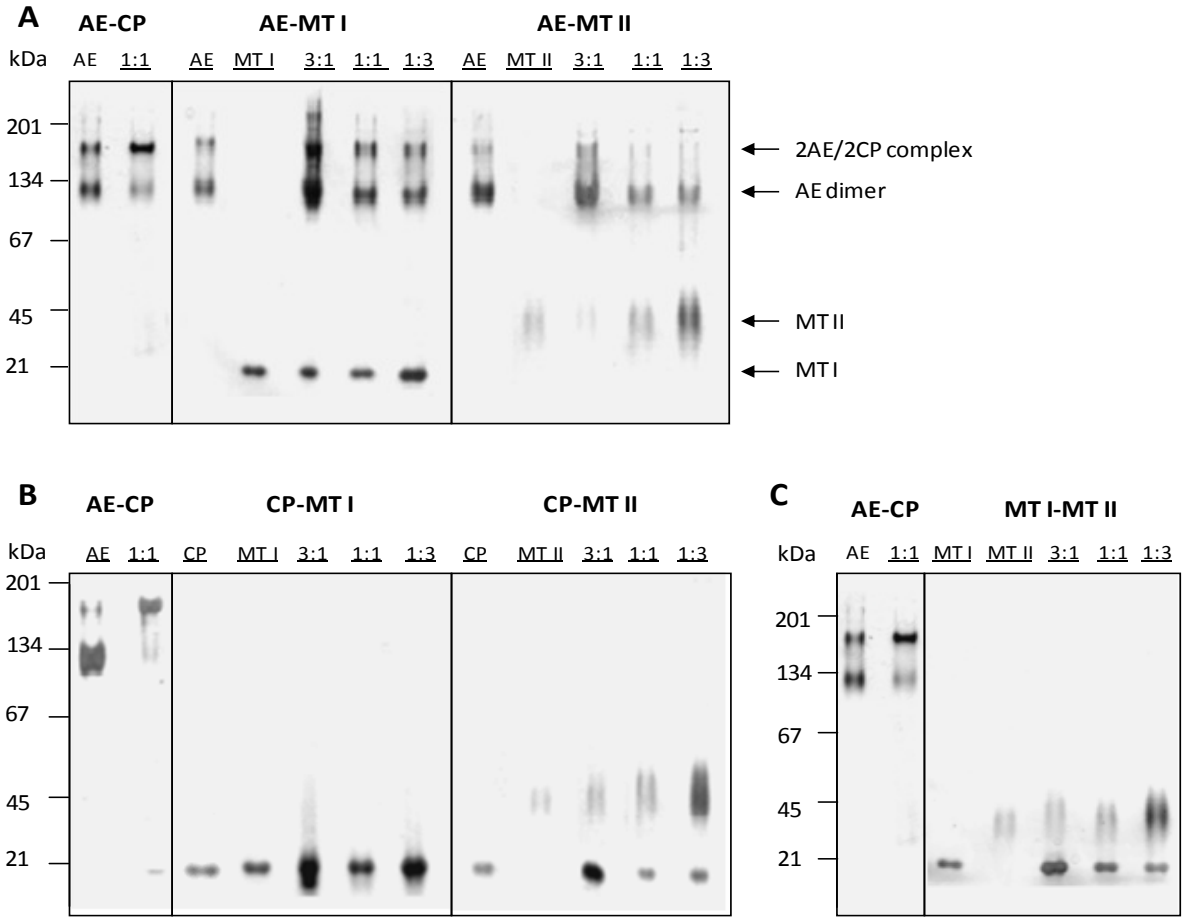

Fig. 3.14. Interaction of *O*-demethylase components investigated by gel shift experiments. The interaction pairs are separated in boxes. (**A**) Interaction between AE and MT I or MT II. (**B**) Interaction between CP and MT I or MT II. (**C**) Interaction between MT I and MT II. The AE-CP pair served as positive control. In each box, the first two lanes show the purified proteins (10 pmol, each). In the other three lanes the test mixtures in three molar ratios (30:10, 10:10, 10:30; pmol:pmol) were applied. The molecular masses of marker proteins are indicated on the left.

For the interaction of CP-MT II, it is possible that the oxidized form of CP may create a conformation which is not optimal for the MT II binding. According to the reaction mechanism of *O*-demethylases, methylcolabamin bound to CP (CH_3-[Co^{III}]-CP) may ensure a conformation of CP to allow the access of MT II. Therefore, the methylated form of CP was

prepared and the interaction of the CH_3-[Co^{III}]-CP and MT II was studied. Since the methylcobalamin is light sensitive, the entire test was performed in the dark. The mixture of CH_3-[Co^{III}]-CP and MT II was incubated for 2 hours at 10 °C and was separated on the native PAGE to check for the interaction. Similar to the results of the hydroxocobalamin harboring CP, no interaction of CH_3-[Co^{III}]-CP and MT II was observed (data not shown). We cannot exclude the possibility that the methylated form of CP was unstable under the experimental conditions. We continued with the two-hybrid screens to study the interactions in which both methyltransferases and/or AE and CP are involved.

3.2.2. Yeast two-hybrid assay

Interactions of the full length proteins of the *O*-demethylase components were evaluated using the Y2H screen. The genes encoding AE, CP, MT I, and MT II were cloned as fusions of the GAL4 DNA binding or activation domain into AH109 and Y187 strains, respectively. The clones were then mated in all possible 26 combinations. The negative controls were the combination of one protein and a blank vector (either pGADT7 or pGBKT7), or a combination of the two blank vectors. The positive control used is mentioned in the section 3.1.4.

The diploid cells were plated onto the medium lacking leucine and tryptophan (SD-Leu-Trp) to control the growth (Fig. 3.15A), and onto the medium lacking leucine, tryptophan, and histidine (SD-Leu-Trp-His) for primary selection of clones capable of activating the reporter genes like *ADE2* and *HIS3*. Clones which showed growth on the latter plate were used for the β-galactosidase assay. The presence of the *lacZ* gene encoding β-galactosidase in yeast served as an additional reporter gene which is activated as a result of interaction (Fields, 2001). The clones which were able to activate the *lacZ* gene will turn blue. To minimize the false positive signals, the diploid cells were also plated on the test plate which contains 3AT (SD-Leu-Trp-His+3AT).

As shown in Figure 3.15B, four combinations were found to grow on the test plate. The interactions of the positive control and of the AE-AE pair were already described in the section above. Interestingly, an additional interaction observed was CP-MT I. It has to be noted that the interaction of CP-MT I was only detected in a non-reciprocal way, i. e. when

CP was fused to the activation domain of GAL4 and MT I to the binding domain and not vice versa (pGADT7-CP/pGBKT7-MT I). The signal of the clone harboring the pGADT7-CP/pGBKT7 pair growing on the SD-Leu-Trp-His plate could be referred as false positive, which resulted from an unspecific activation in Y2H. This was confirmed by the β-galactosidase assay (Fig. 3.15C). On the β-galactosidase assay plate, only three clones turned blue as a result of activation of the *lacZ* reporter gene. The clone harboring the combination of CP and pGBKT7 remained white. This observation was further supported by the results of the test plate containing 3AT (Fig. 3.15D). Here, only three clones grew, the false positive one failed to show any growth on this plate.

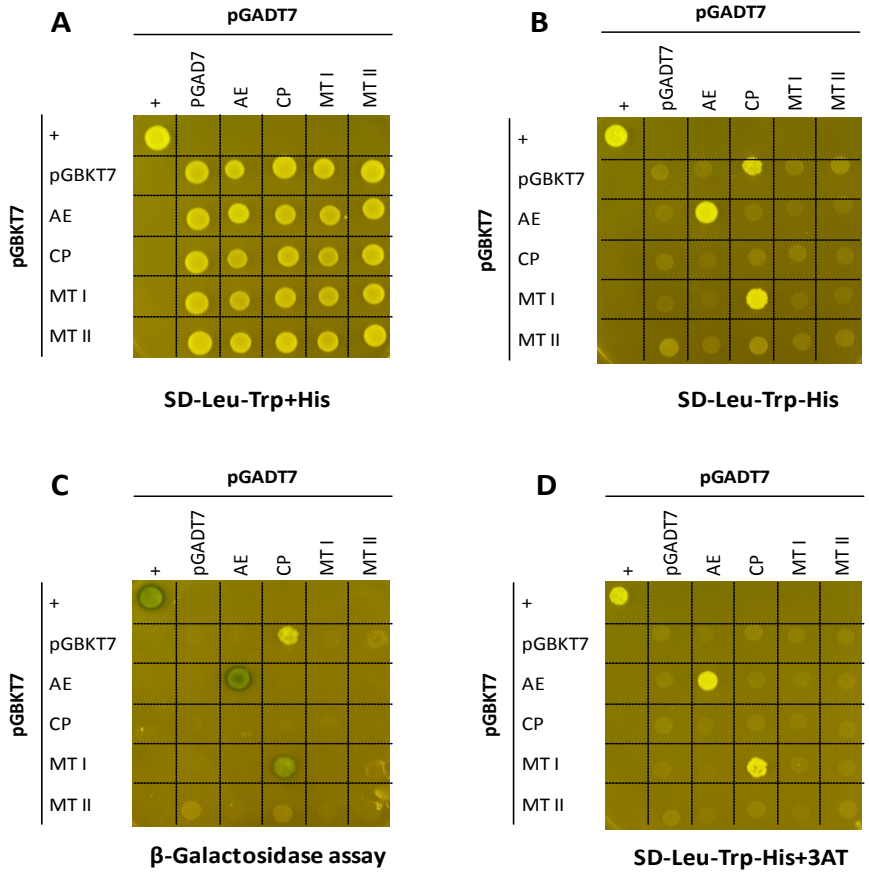

Fig. 3.15. Screening of the interaction of all *O*-demethylase components by Y2H assay. The genes of the four components were fused in frame with GAL4-BD (pGBKT7 plasmid) or GAL4-AD (pGADT7 plasmid). The constructs were transformed into the appropriate yeast strain of opposite mating type (a and α) and were grown on selection disks. After mating, both constructs were present in the diploid yeast. Yeast clones were cultivated on the control plate (**A**) and on the test plate without histidine (**B**). The latter plate was subsequently used for the β-galactosidase assay (**C**). False positives can be eliminated by addition of 3 mM 3-aminotriazol (3AT) (**D**), which is a competitive inhibitor of the *HIS3* gene product.

We further investigated which domain of CP and/or MT I is responsible for interaction. Bioinformatics analysis revealed two domains of CP: The *N*-terminal fragment consists of residues 1-78 (CP 1-78). The *C*-terminal fragment comprises residues 79-209 and harbors the vitamin B_{12} binding motif. Recent studies demonstrated that MT I can be genetically separated into two fragments, the first fragment (residues 1-87) represents the substrate recognition domain (MT I 1-87) while the second fragment (residues 88-326) contains the catalytic domain (MT I 88-326) (Studenik *et al.*, 2011). Therefore, the four aforementioned fragments of CP and MT I were used to evaluate their interactions.

The plasmids were prepared for the combination of fragments and full length proteins and were transformed to appropriate yeast strains. After mating diploid cells were used for testing the interactions (Fig. 3.16A and B). To cover all possible interactions, the fragments were fused in frame to either pGADT7 or pGBKT7 and were used for the fragment-fragment interaction test by Y2H assay (Fig. 3.16C). No interaction was found in the fragment-fragment interaction assay. In contrast, a strong auto-activation was obtained for the clones bearing the pGBKT7-MT I 88-326 fusion protein. The auto-activation can be easily identified with the combination of the blank vector pGADT7 and pGBKT7-MT I 88-326. For all combinations in which this construct was present, growth occurred on the test plates (SD-Leu-Trp-His+3AT). In the β-galactosidase assay, a color change to blue for the pair pGBKT7-MT I 88-326 and the blank vector pGADT7 was observed (data not shown). These findings indicate an auto-activation of the GAL4 reporter genes in the presence of pGBKT7-MT I 88-326.

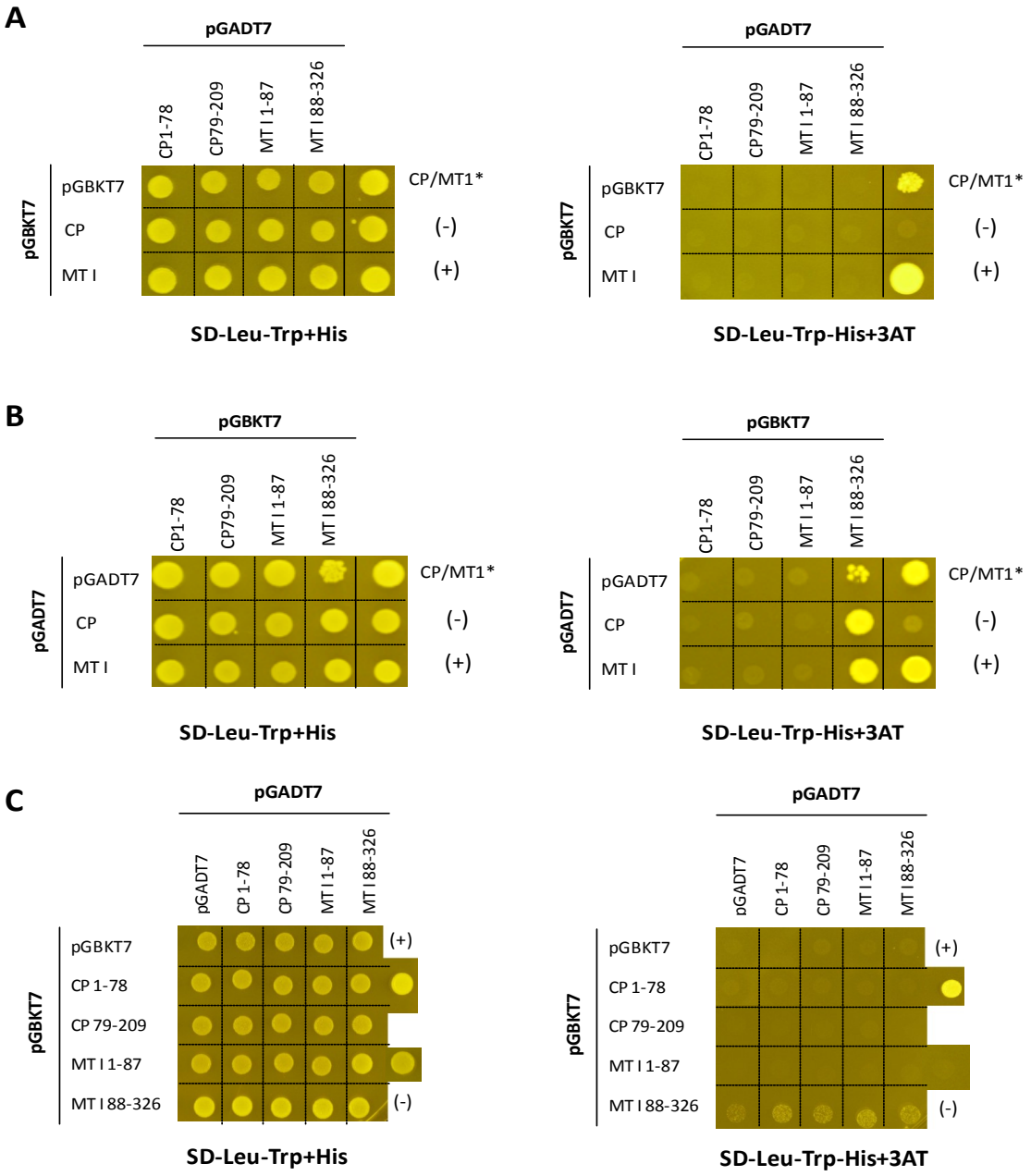

Fig. 3.16. Analysis of CP and MT I fragments possibly responsible for the CP-MT I interaction by Y2H assay. (**A**) Interaction of fragments fused to AD of GAL4 and full length proteins fused to BD of GAL4. The solid line separates the test clones on the left from the controls on the right. (**B**) Interaction of fragments fused to BD of GAL4 and full length proteins fused to AD of GAL4 (**C**) Interaction between the fragments of CP and MT I. The assays were performed on SD-Leu-Trp+His and SD-Leu-Trp-His+3AT plates. (*) The pair pGADT7-CP/pGBKT7-MT I served as an additional positive control.

3.2.3. Bacterial two-hybrid screen

In the B2H system, the proteins of interest were fused to one of the two physically separable fragments T25 and T18 of the *Bordetella pertussis* adenylate cyclase. As mentioned in the previous section, by switching the fusion to either *C*- or *N*-terminus of the T25 or T18 fragment, four possible fusion types can be achieved. This resulted in a maximum of 8 combinations for each protein-protein interaction and in 4 combinations for one protein self-interaction tests. In total, for the *O*-demethylase components 66 interaction pairs were prepared. For each pair, three randomly chosen clones were tested. Three methods were used to screen the interaction including MacConkey and LB/X-gal plates and the β-galactosidase assay in liquid cultures. The liquid culture assay shares the same mechanism of the *lacZ* gene activation as the color change of clones on LB/X-gal plates and was used for the quantiative determination of the complementation efficiency. A high β-galactosidase activity reflects the interaction between the hybrid proteins (Dove & Hochschild, 2004).

In constrast to the Y2H system, a number of interactions was detected in the B2H screen. Self interaction of proteins was observed for AE, CP, and MT I as indicated by a color change to blue (LB/X-gal) or red (MacConkey/maltose) (Fig. 3.17). For MT II, there are almost no, if any, colonies that showed a color change indicating a very low interaction potential. This was the first time in this study that MT I showed the ability to form oligomers. Beside the self-interaction of *O*-demethylase components, interactions between different protein components were also observed (Fig. 3.17). Interestingly, most of the interactions were only detected when using the fusion orientation of X-T25/ T18-Y in which X and Y are the proteins used in the test. Fusion proteins in this orientation may yield a good environment for protein folding and binding to the matching partner.

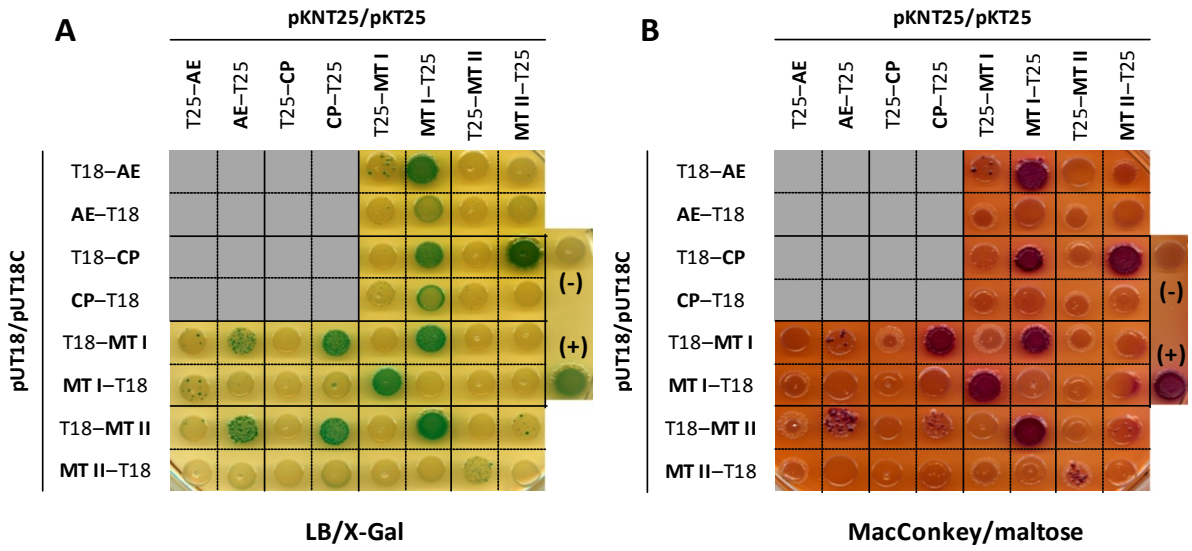

Fig. 3.17. Investigation of the interaction of the *O*-demethylase components by B2H assay. All genes were cloned into the plasmids pUT18, pUT18C, pKN25 and pKT25. Plasmids pUT18 and pUT18C allow the expression of the selected enzymes fused either to the *N*- or *C*-terminus of the T18 domain of the *B. pertussis* adenylate cyclase, respectively. Plasmids pKNT25 and pKT25 allow the expression of the selected enzymes fused either to the *N*- or *C*-terminus of the T25 domain of the adenylate cyclase, respectively. This results in 4 possible combinations for each pair which is shown in the figure as boxes framed with solid lines. (**A**) The degradation of X-Gal (color change to blue) indicates the presence of a functional adenylate cyclase due to the interaction of the two proteins of interest. (**B**) Acid production due to maltose consumption is shown as color change to red. Maltose consumption is induced by activation of the *mal* gene as a result of functional reconstitution of the T18 and T25 fragment in the case of interaction. Interactions of AE and CP were already described in Section 3.1.5 and were hidden in the grey box.

The interaction of CP-MT I which was found in the Y2H system was also observed in the B2H assay, on both LB/X-gal and MacConkey plates. Additionally, interactions between AE and MT I, CP and MT II, and MT I and MT II were detected. For AE-MT II and MT II-MT II, either weak or no signals were found. The pairs CP-MT I and CP-MT II showed reciprocal interactions (X-T25/ T18-Y and Y-T25/ T18-X) while for the pairs of AE-MT II and MT I-MT II only non-reciprocal ones were detected. This observation suggested a strong and more profound interaction between CP and the two methyltransferases than the two latter ones.

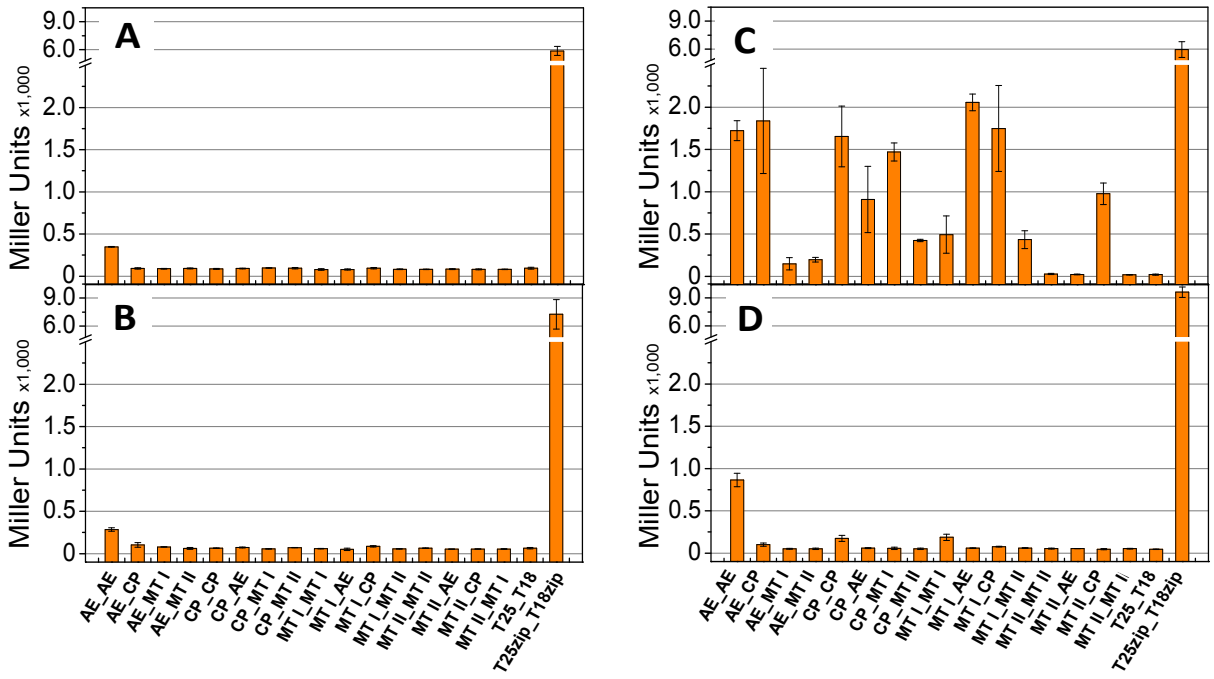

Fig. 3.18. Quantitative determination of the complementation efficiency by β-galactosidase assay. The co-transformants were grown in LB medium supplemented with appropriate antibiotics and IPTG (0.5 mM) until an OD_{600} of 0.6-1.0 was reached. The cultures were subsequently used for the ß-galactosidase activity measurement. The activities are expressed in Miller units. (**A**) Proteins fused to the *N*-termini of the T25 and T18 domains. (**B**) Proteins fused to the *C*-termini of the T25 and T18 domains. (**C**) Proteins fused to the *N*-terminus of the T25 and to the *C*-terminus of the T18 domain. (**D**) Proteins fused to the *C*-terminus of the T25 and to the *N*-terminus of the T18 domain.

The clones harboring a combination of proteins fused to either the *N*-terminal end of T25 or the *C*-terminus of T18 showed significant β-galactosidase activity (Fig. 3.18). The other fusion orientations showed low β-galactosidase activities. As depicted in Figure 3.18C, the interaction of AE-AE, AE-CP, CP-CP, CP-AE, CP-MT I, MT I-AE MT I-CP, and MT II-CP were the most significant ones among all combinations. The results of β-galactosidase assay were in good agreement with those of the test plates (Fig. 3.17).

3.2.4. Dot far-Western blot

The recombinant proteins were purified as described for the gel shift experiments. Ten pairs which represent all possible interactions were prepared for the test (Fig. 3.19). The test procedure was described in the Materials and Methods section. One protein was applied on

the membrane creating a "prey" and was incubated with its interacting partner (in solution) which served as a "bait". The negative control was included to each pair to control the unspecific binding of antibodies. The signals were detected by incubating the test membrane with the first antibody against the bait and subsequently with appropriate alkaline phosphatase-labeled secondary antibodies.

As shown in Figure 3.19, the signals for the interaction of AE-MT II appeared to be the strongest in the far-Western blot analysis. The other pairs showed either moderate or weak interactions. The interaction of CP-MT I which was shown in both two-hybrid systems appeared as weak signals on the test membrane in far-Western blot. This interaction was only detected in one direction in which MT I is on the membrane and CP in the solution. Similar results were obtained for the CP-MT II pair. The signals for the interaction were only detected when MT II was fixed on the membrane and was incubated with CP in the solution. However, the interaction of CP and MT II seems to be stronger than that of CP-MT I.

The influence of the corrinoid cofactor hydroxocobalamin on the interaction between CP and the two MTs was also investigated. The cofactor-containing form of CP was prepared as described in the Materials and Methods section. All experimental steps were carried out under anaerobic conditions. The results of the interaction of the cofactor bound CP and the two methyltransferases showed no difference to those obtained with the non-reconstituted proteins (data not shown) indicating that the presence of the cofactor does not influence the interaction of CP-MT I or CP-MT II in this experiment. In the case of the MT I and MT II pair, a moderate interaction was detected when MT I was spotted onto the strip but not when MT I is in solution. This phenomenon can be explained by the non-native conformations of the proteins, especially when spotted on the membrane. The interaction of AE-MT I was found in a reversible manner. Although good signals were observed on the test strips, the binding affinity of the two was considered to be weak because of the relatively strong intensity of the negative controls' signals which were very likely a result of non-specific binding between the prey protein and the first antibodies.

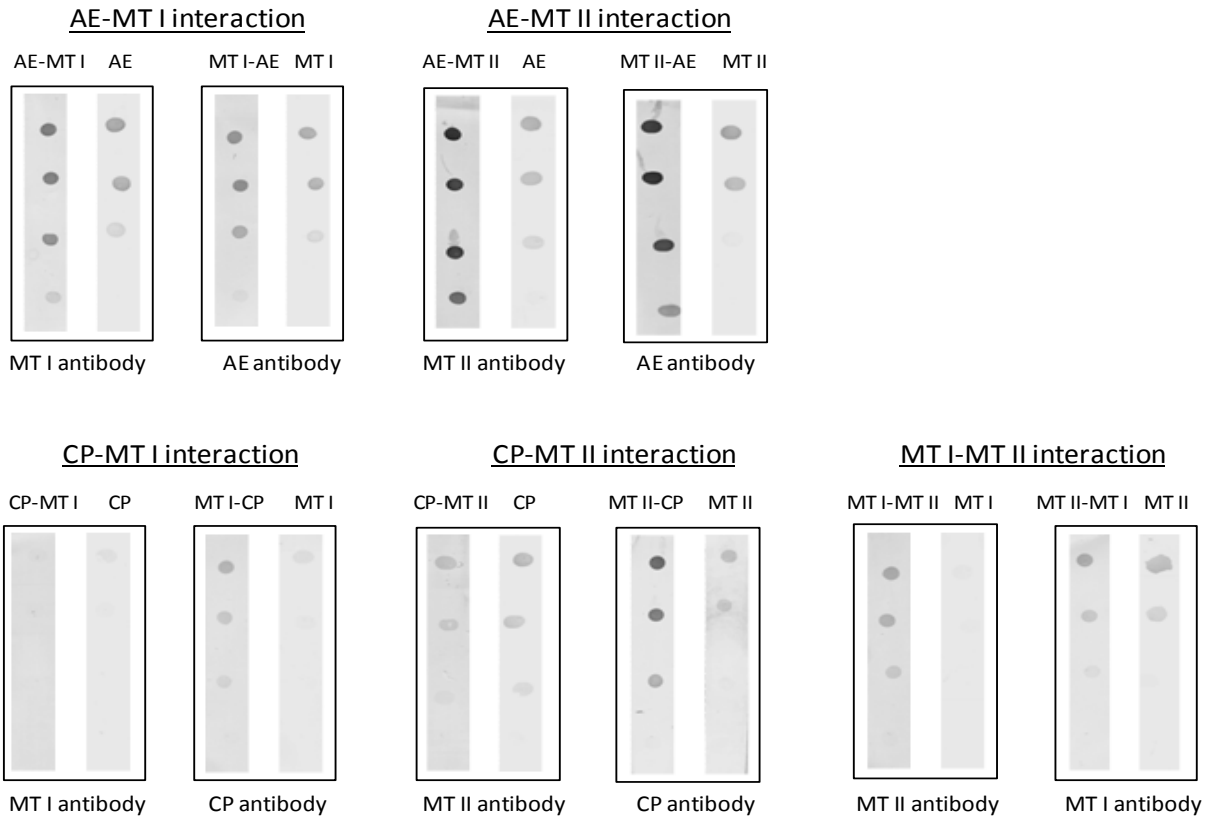

Fig. 3.19. Interaction of the *O*-demethylase components by dot far-Western blot. Each set contains the test sample (*left* strip, incubated with a bait protein) and a negative control (*right* strip, incubated with buffer alone) performed in parallel for each study. Proteins in different concentrations were spotted on a PVDF membrane as prey protein. After blocking, the membrane was incubated with the interacting partner (bait protein in solution, 0.1 mg/ml) and afterwards with the first antibody against the bait. Signals were visualized in the NBT/BCIP reaction using alkaline-phosphatase labeled secondary antibodies.

In-gel far-Western blot

Polyacrylamide gels are generally not suitable for immunoblotting because it seems to be impermeable to antibodies and large proteins. Several methods were recently developed to circumvent this obstacle (Chan *et al.*, 2008; Xiong *et al.*, 2009). One method was applied successfully by pre-treating the gel with 50% isopropyl alcohol before performing the Western blot. The sensitivity of the detection by this method was remarkable (Desai *et al.*, 2001). The in-gel far-Western blot is generally used for detection of protein but there were not many reports on using this method to study the protein-protein interaction. To allow a good accessibility of the prey and the bait proteins, an in-gel far-Western blot was performed with a

few modifications (Edmondson & Roth, 2001). The prey proteins were subjected to native PAGE. After electrophoresis, the gel was pre-treated with 50% isopropyl alcohol followed by distilled water treatment. The gel was then incubated with the bait proteins for three hours. We assumed that by performing this step, the bait proteins would have more space to move freely and bind the in-gel-prey proteins; therefore, the interaction sites would be more accessible in comparison to the far-Western blot analysis. The gel containing the bait-prey mixture was incubated with the first antibody against bait protein and then with Phototope®-HRP linked secondary antibodies (Cell Signaling, USA). Signals were developed on an x-ray film under light preventing conditions. Unfortunately, by using this method it was not possible to detect any signals (data not shown). To make sure that the test samples were on the gels, the gels were stained with Coomassie blue after immunodetection. After staining, protein bands were detected. If the native gel with the prey protein was used for Western blotting (on PVDF membrane) signals were observed on the membrane. The detection of the prey protein in the native gel failed. The results imply that the detection method used seems to be not suitable for in-gel detection. One possible explanation is that the in-gel signals could not be transferred to the film. Another possibility is that the baits did not diffuse into the gel or could not bind to the in-gel-preys so that no signal was detected.

3.3. Possible electron donors involved in the ATP-dependent corrinoid reduction catalyzed by the activating enzyme

3.3.1. Amplification of A3KS_00044 *and* A3KS_02576 *DNA fragments*

At the point we started to search for a possible electron donor *in vivo*, the genome sequence of *A. dehalogenans* was not available. Therefore, the genome sequence of the close relative *A. woodii* was analyzed (Genbank: CP002987.1). The genome of *A. woodii* consists of a single circular 4,044,785 bp chromosome with a GC content of 39.3% (Poehlein *et al.*, 2012). In total, 10 annotated ferredoxin genes were found in the genome of this species by searches using NCBI server. The database searches (BLAST) (Altschul *et al.*, 1997) were refined and the most likely candidate *Awo_c25230* was chosen for the design of degenerated primers which were used in combination with genomic DNA of *A. dehalogenans*. By using this approach, a DNA fragment of *A. dehalogenans* was amplified by PCR. The fragment was identified as a part of a gene encoding a putative ferredoxin. While these studies were

underway, the first draft version of the *A. dehalogenans* genome was released. Now, the gene fragment could be assigned to the gene *A3KS_00044* of *A. dehalogenans* and the whole gene was amplified using specific primers derived from the genome sequence of *A. dehalogenans*. In parallel, the genome sequence of *A. dehalogenans* was analyzed for the presence of other putative ferredoxin genes. At least 5 genes encoding small Fe/S cluster containing proteins are present. A3KS_02576 which shows structural similarities to a *Clostridium pasteurianum* ferredoxin (PDB database) (Berman *et al.*, 2003) was also chosen for heterologous expression in *E. coli*.

3.3.2. Sequence analysis

The evidence for the presence of [4Fe-4S] clusters of protein Fd I encoded by *A3KS_00044* was obtained by sequence alignments. Searches for sequence similarities were performed using BLASTP. The Fd I protein of *A. dehalogenans* exhibits a high degree of sequence identity to putative ferredoxins of *Clostridium ljungdahlii* and *C. carboxidivorans* (59 - 61%). The sequence identity to the annotated ferredoxin of *A. woodii* was about 93% (Fig. 3.20A). The analysis using the web-based software Myhits (Pagni *et al.*, 2004) revealed that Fd I contains four [4Fe-4S] cluster binding motifs with the consensus sequence **C**-X_2-**C**-X_2-**C**-X_3-**C**. The sixteen cysteine residues which are involved in binding of the [4Fe-4S] clusters are highly conserved (Fig. 3.20A). For the second putative ferredoxin Fd II encoded by *A3KS_02576*, the sequence identity of the protein was about 88% compared to a known ferredoxin of the methylotrophic hetero-acetogen *Butyribacterium methylotrophicum* (Saeki *et al.*, 1989). Fd II also showed high sequence homology to annotated ferredoxins of *C. pasteurianum* and *C. carboxidivorans* (64 - 66%). Two **C**-X_2-**C**-X_2-**C**-X_3-**C** motifs, probably binding the two [4Fe-4S] clusters, are highly conserved among these bacterial ferredoxins (Fig. 3.20B). Fd II consists of 55 amino acids, accounting for a molecular mass of 6 kDa which is the common size for ferredoxins found in acetogenic bacteria (Rabinowitz, 1972; Ragsdale & Ljungdahl, 1984; Reubelt *et al.*, 1991).

A. A3KS_00044

```
A. dehalogenans     MKKVVVADQA ACVKCLGCEL ACANAFYKEP VSELSCIKIT EKEDGSPKTL  50
A. woodii           MKKLVVVDQS ACVKCLGCEL ACANAFYKEP VSELACIRIT EKEDGSPKTL  50
C. ljungdahlii      MKKLVVKDKS LCMSCLSCEM ACSEAFYKTY GN--SCIKID EGKDGCVDLK  48
C. carboxidivorans  MKKLVVNDSS LCMACLSCEI ACSEAFYKTY GN--SCIKID VKKDNSPNIK  48

A. dehalogenans     VCVQCGKCAK ACEAGAITQN AKGVYMISKK LCVNCGKCVE VCPFGVLVKS  100
A. woodii           VCVQCGKCAK VCEAGAITKN AKGVYMINKK LCVNCGKCVE ACPFGVLVKS  100
C. ljungdahlii      VCNQCGVCAK KCPEEAIKQN AKGIYMIDKK ACTGCGTCVE ACPKGIIVKV  98
C. carboxidivorans  TCNQCGLCAK KCPEGAIKQN AKGIYMIDKK TCTSCFKCVE VCPKGIIVKT  98

A. dehalogenans     EDRDVPSKCI ACGICVEACP QDVLAIKES  129
A. woodii           EDRDVPSKCI ACGICVEACP QDVLAIKES  129
C. ljungdahlii      EDKPNPSKCM ACGICVKACP MGVLEIQED  127
C. carboxidivorans  EDKPNPSKCI ACGICVKACP MEVLEIQEN  127
```

B. A3KS_02576

```
A. dehalogenans     MAYKITDECI ACGSCMDECP VEAISEGD-I YVIDAATCTD CGACAEQCPV EAIVQD   55
B. methylotrophicum -AYKITDECI ACGSCADQCP VEAISEGS-I YEIDEALCTD CGACADQCPV EAIVPE   54
C. carboxidivorans  MAYKIADSCV SCGACASECP VNAISQGDSI FVIDADTCID CGNCANVCPV GAPVQE   56
C. pasteurianum     MAYKIEDSCV SCGTCASECP VNAISQGDSI FVIDESTCID CGNCANVCPV GAPVQE   56
C. botulinum        MAYKITDACV SCGACAAECP VNAISQGDSI FDIDADTCID CGNCANVCPV GAPVQD   56
```

Fig. 3.20. Sequence alignment of the putative ferredoxins Fd I (A) and Fd II (B) of *A. dehalogenans* and other closely related ferredoxins. The alignments were done using the BLAST network service (Altschul *et al.*, 1997). Conserved residues are shown in bold. The cysteine residues, predicted to bind the [4Fe-4S] clusters, are indicated in boxes. Ferredoxins of the following bacteria are compared: (**A**) *A. woodii* (Locus: AFA49280), *Clostridium ljungdahlii* (Locus: YP_003780413), *C. carboxidivorans* P7 (Locus: ZP_05391398); (**B**) *Butyribacterium methylotrophicum* (Saeki *et al.*, 1989), *C. carboxidivorans* P7 (Locus: ZP_05394166), *C. pasteurianum* (Locus: ZP_20958515), *C. botulinum* A (Locus: YP_001252608).

3.3.3. Heterologous expression of putative ferredoxin genes and reconstitution of the iron sulfur clusters

The genes encoding *A3KS_00044* and *A3KS_02576* were cloned into the pET11a vector using the *Nde*I and the *Bam*HI restriction sites of the multiple cloning region. The resulting plasmids were transformed into *E. coli* XL1-blue and then into the BL21 (DE3) strain for production of recombinant proteins. Proteins were produced in *E. coli* as *C*-terminal *Strep*-tag fusions. Cells were grown on LB medium containing ampicillin. IPTG was added after the OD of the culture reached 0.6. The cells were harvested 16 h after induction and were disrupted using a French Press. After the first French press cycle, Fd I was insoluble and only

detected in the total protein fraction (Fig. 3.21A, lane 3). The second French Press cycle of the same cell extracts yielded in a higher amount of soluble protein (Fig. 3.21A, lane 4). The protein was purified by affinity chromatography on *Strep*-tactin. The apparent molecular mass of the isolated protein was estimated to be 15 kDa by SDS-PAGE and was in good agreement with the one calculated from the amino acid sequence (14.2 kDa).

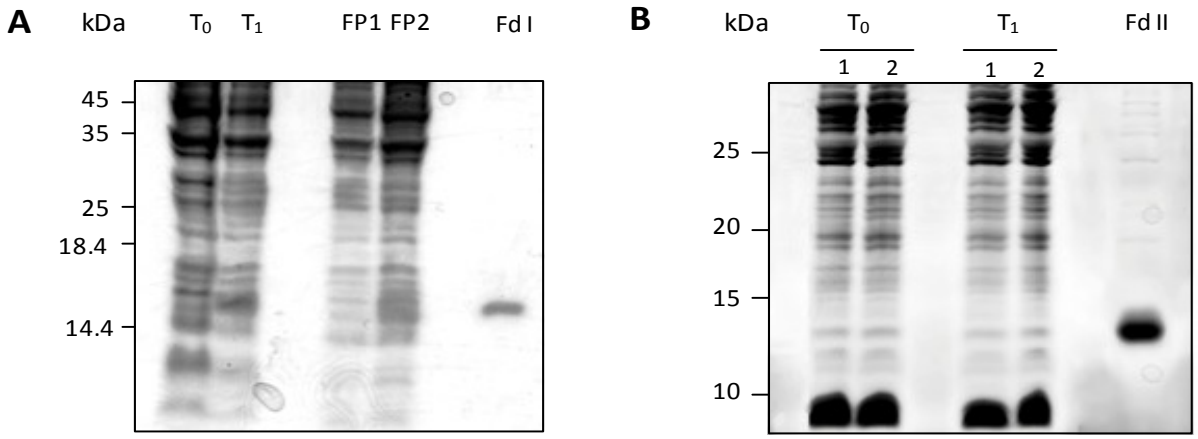

Fig. 3.21. SDS-PAGE of heterologously expressed putative ferredoxins of *A. dehalogenans*. (**A**) Production of Fd I after Coomassie stain. T_0 and T_1 are the crude extracts of Fd I before adding IPTG (lane 1) and after overnight induction (lane 2), respectively. FP1: Soluble fraction of the first French Press cycle. FP2: Soluble fraction of the second French Press cycle. Fd I: purified Fd I (1 µg). (**B**) Production of Fd II after silver stain. 1 µg of the crude extract of Fd II or purified protein were applied. Lanes 1 and 2 of T_0: crude extracts before adding IPTG; lanes 1 and 2 of T_1: crude extracts after adding IPTG. Fd II: purified Fd II.

The crude extract of the second putative ferredoxin Fd II did not show any trace amount of the recombinant protein after SDS-PAGE and Coomassie staining. Assuming that the Coomassie stain might not be suitable for detection of the protein, silver stain was used. Fd II was isolated according to the method of Fd I. The purity of isolated protein was checked by SDS-PAGE and silver stain. After silver stain of the gel containing crude extract samples and purified ferredoxin, a band of around 12 kDa was detected for purified Fd II (Fig. 3.21B, lane 5) which corresponds to the double molecular mass of Fd II compared to the calculated one. The reason for this phenomenon is unknown. A possible explanation is that the presence of multi-charged iron sulfur clusters in the protein might influence the separation by SDS-PAGE. The yield of purified protein was very low (about 0.1% of total protein) despite all attempts to optimize the production of ferredoxin. Nevertheless, sufficient protein was

obtained for the characterization of the Fds I and II. The presence of the *Strep*-tag fusion proteins were verified by Western blot using anti-*Strep* antibodies (IBA, Goettingen, Germany) (data now shown).

The isolated proteins showed a slightly brown color which was a good indication for the presence of [Fe-S] clusters. However, the iron determination revealed that the isolated proteins contain only 0.1 - 0.3 mol iron per mol protein. In addition, the UV/Vis spectrum of the two proteins showed a small peak at 390 nm (data not shown) which indicates a low amount of iron. The two proteins were subjected to a reconstitution step to recover their active form. During reconstitution, the proteins were incubated with a 5-fold molar excess of ammonium iron(III) citrate and lithium sulfide in the presence of DTT. Reconstituted proteins were obtained after passing through a desalting column. The iron determination showed that reconstituted Fd I contained approximately 20 mol of Fe per mol protein which is slightly higher than the expected value (16 mol of Fe per mol protein). Reconstituted Fd II contained 8 mol Fe per mol protein after reconstitution. This value is in excellent accordance with the presence of 2 [4Fe-4S] clusters as described above.

3.3.4. Characterization of Fd I and Fd II by UV/Vis spectroscopy

The reconstituted putative ferredoxins were dark green (Fd I) or brown (Fd II) in colour. The absorption spectrum of both proteins is depicted in Figure 3.22. A shoulder (Fd I) or peak (Fd II) at around 400 nm and a protein peak at 280 nm were visible. Both ferredoxins could be reduced by Ti(III)citrate resulting in a significant bleaching of the peak at 400 nm. The spectrum of Fd II correlated well with other 2 [4Fe-4S] ferredoxins found in the literature, including a ferredoxin of *Methanosarcina thermophila* (Clements *et al.*, 1994) or *C. acetobutylicum* (Guerrini *et al.*, 2008). The UV/Vis spectrum of Fd I was a little different from that of the Fd II, which is maybe due to the presence of a higher number of iron in the protein.

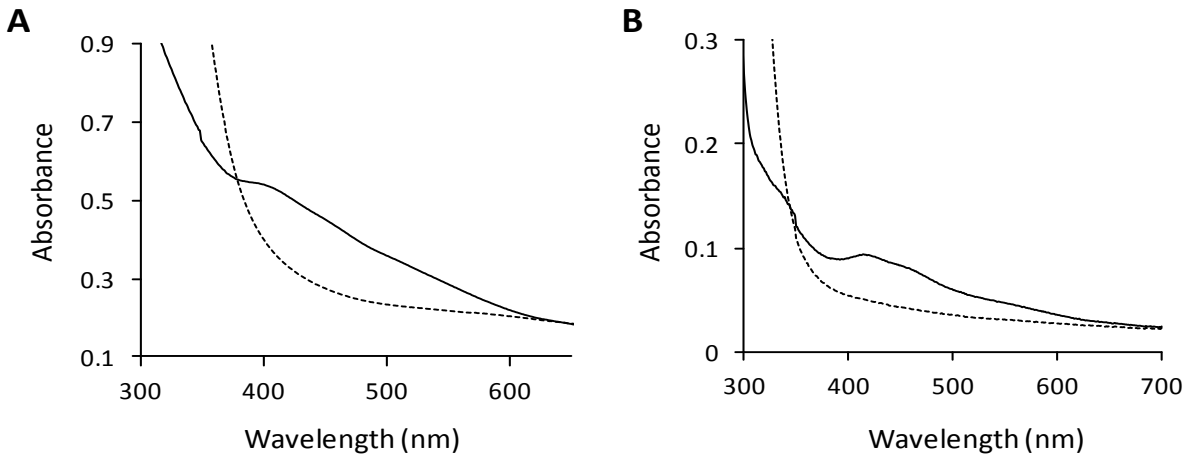

Fig. 3.22. UV/Vis spectra of Fd I (A) and Fd II (B). The spectra of samples were recorded in 50 mM Tris HCl, pH 7.5. The spectra of the oxidized proteins (solid line) and the Ti(III)citrate-reduced proteins (dotted line) are shown. The spectrum of the reduced proteins could only be recorded down to 360 nm due to the strong absorbance caused by Ti(III)citrate below this wavelength. Fd I: 0.58 mg/ml; Fd II: 0.15 mg/ml.

In order to check the ability of the purified Fds to act as electron donors for the reductive activation reaction catalyzed by AE, the functionality of these proteins had to be tested. Since ferredoxin often serves as electron acceptor for hydrogenases or formate dehydrogenases, the reduction of the purified ferredoxins by these enzymes was studied. For this purpose, crude extracts of *A. dehalogenans* were prepared and tested for hydrogenase and formate dehydrogenase activities. In the presence of formate (5 mM) or hydrogen (100%, 1 atm) with methyl viologen as artificial electron acceptor, addition of the crude extract to the enzyme assay resulted in a significant increase in absorbance at 578 nm indicating the reduction of methyl viologen (data not shown). This indicates a high hydrogenase and formate dehydrogenase activity of the crude extract. The Fds I and II were then used in an assay to check if the crude extract is able to reduce the Fds under anoxic condition. The crude extract or Ti(III)citrate as a control was step-wise added to the solution containing Fd I or Fd II saturated with hydrogen. The result showed no significant reduction of the Fds by using the crude extract while the reduction by Ti(III)citrate was observed as shown earlier. Similar results were observed when using formate as electron donor. Since the reduction of both Fds by enzymes of the crude extract of *A. dehalogenans* (e. g. hydrogenase or formate dehydrogenase) was not detected, the involvement of the purified Fds in the reductive activation seems to be unlikely. Indeed, in the presence of ATP and the purified Fd I or Fd II, AE failed to activate the oxidized CP under anaerobic conditions (data not shown).

4. Discussion

Methyl transfer catalyzed by the *O*-demethylases is a key step in the methylotrophic metabolism of acetogens. The enzyme systems catalyze the transfer of the methyl group from a phenyl methyl ether to tetrahydrofolate forming methyltetrahydrofolate which is further oxidized to CO_2. The reducing equivalents generated in this process are used for the synthesis of acetyl-CoA. In *Acetobacterium dehalogenans*, the *O*-demethylating systems were found to consist of four components, two methyltransferases (MT I and MT II), a corrinoid protein (CP) and an activating enzyme (AE). During numerous methyl transfer cycles, the cob(I)alamin form of CP may be accidentally oxidized to the inactive form cob(II)alamin due to the low redox potential of the cob(II)/cob(I)alamin couple. The reductive activation of the corrinoid cofactor of CP is required to maintain the methyltransferase reaction. This reductive activation is mediated by AE. Hence, the corrinoid protein in its Co(II)-form is a substrate for AE and should interact with this enzyme. The interaction of AE and CP_{van} was earlier demonstrated by Schilhabel *et al* (2009). The identification and expression of four different CP genes (encoding CP_{van}, CP_{ver}, CP_{syr}, CP_{gua}) of *A. dehalogenans* enabled the further investigation on the interaction of the two components. Based on the fact that the four CPs show high homology and only one AE was found, it was assumed that the *O*-demethylase system may require only one AE for the activation of different CPs. The results of gel shift experiments described in this communication provide strong evidence for this hypothesis. From the data, it is obvious that AE is able to interact with the four different CPs in the presence of the corrinoid cofactor hydroxocobalamin. For all interaction pairs, the dimeric complex was formed with a stoichiometry of 1:1 suggesting that AE interacts with the four CPs in a similar mode of action. The ability to interact and activate multiple CPs was confirmed by the corrinoid reduction assay. AE was able to reduce all four different CPs under the same assay conditions. However, the specific activities of the various CPs differ slightly. AE was most active on CP_{syr}. The reduction activity towards CP_{van} is comparable to that towards CP_{syr}. The specific activities on the other two were about 50% - 70% of the activity compared to that with CP_{syr}. No relationship between the sequence identity and the specific activity was found. We could not exclude that CP_{ver} and CP_{gua} may require different derivatives of cobalamin rather than hydroxocobalamin *in vivo* which may provide the optimal conditions for the interaction and corrinoid activation. Notably, the extraction of corrinoids resulted in only one B_{12} peak (unpublished data). Thus, it is likely that only one

cobalamin is present in the different CPs. The ability of AE to recognize different CPs is similar to the function of RamA in *Methanosarcina barkeri*, a member of RACE proteins. It functions as the activator of corrinoid-dependent methylamine methyltransferases. The enzyme is capable of reducing the corrinoid proteins of trimethylamine, dimethylamine, and monomethylamine methyltransferases (MttC, MtbC and MtmC, respectively). However, the interaction of the activator and the corrinoid proteins has not been shown (Ferguson *et al.*, 2009).

The presence or absence of the corrinoid cofactor significantly affects the native form of CP and consequently affects the interaction of AE and CP. The cofactor-free CPs did not show any defined band in the native gel while the reconstituted CPs generally showed strong bands. Moreover, in gel shift experiments the interactions between AE and the four CPs cannot be observed in the absence of the corrinoid cofactor. These observations seem to be good evidence for the influence of the corrinoid cofactor on the correct conformation of CP. Under the experimental conditions applied in the gel shift experiments, CP may require hydroxocobalamin for correct folding which is essential for the binding to its interacting partner AE. The crucial role of the cofactor in alternating the conformation of CP for methyl transfer reactions was demonstrated before for the corrinoid containing methionine synthase (Matthews *et al.*, 2008). Since the redox potential of the Cob(II)/Cob(I) couple is very low, the inactive cob(II)alamin form of CP was used in the test. The presence of the inactive cofactor may change the conformation of CP in such a way that AE is able to recognize CP and interacts. In a similar activation system, RACo of *Carboxydothermus hydrogenoformans*, the corrinoid protein (CFeSP) possesses a relatively high redox potential of the cob(II)/cob(I)alamin couple which is 50 - 100 mV more positive compared to other cobalamin containing methyltransferases (Harder *et al.*, 1989). Thus, the active cob(I)alamin form was more stable and interaction studies were performed in the presence of the CFeSP in different redox states. In this system, the activating enzyme RACo appears to have a higher affinity to the inactive [Co(II)-CFeSP] than to the active [Co(I)-CFeSP] form, which makes sense since only the Co(II)-form is the substrate of RACo. Therefore, it may be assumed that the interaction between AE and CP requires the inactive Co(II)-form of CP. Cob(I)alamin harboring CP is not a substrate of AE, therefore it is very likely that its affinity to AE is lower than to that of the inactive one.

It should be mentioned that the reductive activation of CP is ATP-dependent. The presence of Ti(III)citrate as reducing agent with a very low redox potenial is not sufficient to reduce cob(II)- to cob(I)alamin (Schilhabel *et al.*, 2009). *In vitro* experiments require the addition of ATP besides Ti(III)citrate and AE to fulfill the reductive activation of CP. The ATP hydrolysis during activation could be demonstrated (unpublished data). In gel shift experiments, the absence of ATP did not have any effect on the interaction of the two proteins. This observation suggests a direct interaction between AE and CP in the presence of the inactive Cob(II) species. Unlike corrinoid proteins of methyltransferases involved in methylation of CODH/ACS (CO dehydrogenase/acetyl-CoA synthase) (Menon & Ragsdale, 1998; Menon & Ragsdale, 1999; Svetlitchnaia, 2006), CPs of *O*-demethylases of *A. dehalogenans* do not contain any iron-sulfur cluster. The reductive activation by AE increases the midpoint redox potential of CP by more than 200 mV to -320 mV at pH 7.5 (Siebert *et al*., 2005). ATP is probably required for altering the redox potential of CP to more "positive" rather than for contributing to the interaction of the two proteins. The standard redox potential of the cob(II)/cob(I)alamin varies according to the type of the corrinoid and environment. The redox potential of a base-on corrinoid was shown to be significantly lower than that of the base-off corrinoid (-700 mV and -400 mV, respectively) (Harder *et al.*, 1989; Pratt, 1993). The presence of ATP may induce a conformational change that favors the formation of the base-off form and shifts the redox potential to more positive as reported in the case of the methyltransferase activating protein (MAP) of *M. barkeri* (Daas *et al.*, 1996a). Another possibility is that the binding of AE to ATP and/or the hydrolysis of ATP may lead to a conformational change in such a way that an unknown electron donor has access and transfers the electron to AE to facilitate the reduction of CP. Further experiments are required to confirm these hypotheses.

The activator of a 2-hydroxyisocaproyl-CoA dehydratase of *Clostridium difficile* catalyzes the reductive activation in an ATP dependent reaction. In this protein, the reduction of the dehydratase requires a very low redox potential of about -900 mV while the redox potential of the activator is ca. -350 mV (Buckel *et al.*, 2005). A hydrolysis of two ATP should overcome the redox barrier between the two proteins. Reduction of the activator and binding of ATP induce conformational changes of the activator which enables the electron transfer to the dehydratase as shown in *Acidaminococcus fermentans* (Hans *et al.*, 2002). As soon as the complex between the activator and dehydratase has been formed, ATP is hydrolysed (Kim *et*

al., 2007). In *A. dehalogenans*, AE of the *O*-demethylase in the presence of ATP and Ti(III)citrate increases the redox potential of the corrinoid cofactor to about -320 mV (Siebert *et al*., 2005). The activation mechanism of CP therefore differs from that of the dehydratase in this anaerobic bacterium.

The interaction between AE and CP was also observed by two other assay systems: the bacterial two-hybrid screen (B2H) and far-Western blot. Surprisingly, the corrinoid cofactor was not required for the interaction. In the bacterial two-hybrid system, the interaction of AE and CP was only observed when one protein was fused to the *N*-terminal part of T25 and the other protein was fused to the *C*-terminus of T18. Protein fused in this orientation may yield optimal folding so that the interaction occurs. It should be noted that cobalamin is not produced by the *E. coli* strains used for the test. This indicates that the interaction of the two fusion proteins does not necessarily require the corrinoid cofactor. However, it should be considered that the fusion of the proteins may create a folding which is different from the one of the physiologic environment. Thus, it is very likely that the interaction between the two fusion proteins may occur in this way. The interaction between AE and CP was also detected by far-Western blot analysis. The presence or absence of the corrinoid cofactor did not have any influence on the interaction of the two proteins in these experiments. This finding was in accordance with the result of the B2H assay, but contradictory to that of the gel shift experiment. One possible explanation for these results is that the folding of the proteins may be affected by the methods used in this study. In far-Western blot, one of the proteins is applied onto the membrane, which may lead to a conformational change, by which the interaction sites of either AE and/or CP are more exposed. If so, an interaction of AE and CP is more likely and takes place even in the absence of the corrinoid cofactor. The interaction between AE and CP was not detected in the yeast two-hybrid system (Y2H). In yeast, the biosynthesis of cobalamin does not take place. If the assumption for the crucial role of the corrinoid cofactor on the interaction between AE and CP is true, the interaction of the two proteins will not occur. Moreover, when the proteins are fused to either GAL4 DNA binding or activating domain, there is a possibility that the fusion domains may interfere with the protein's function or binding regions. Therefore, it is not surprising that no interaction of the two components was found in the Y2H assay.

The native gel also revealed self-association forms of the test proteins. In the presence of the cofactor, CP_{van}, CP_{syr}, and CP_{gua} exhibit the monomeric forms, whereas CP_{ver} runs as dimeric

protein. In the bacterial two-hybrid system, CP_{van} in the form of a chimeric protein also shows self-interaction which suggests the ability to form a dimer. The oligomerization of AE was not only found in the gel shift experiment but also in the Y2H and B2H assays. In the native gel, AE possesses a dimeric form under the experimental conditions provided. Under certain conditions, AE forms multimers which were detected as a ladder of bands in the native gel (data not shown). The signal for the interaction of the two proteins could only be detected when AE was in the dimeric form. When AE forms a multimer, it is difficult to differentiate between the bands of the complex AE-CP and the trimeric form of AE. In the Y2H system, the cells of the AE-AE pair grew on the test plate which indicates the formation of dimers or multimers of the activating enzyme. In addition, the interaction of the AE-AE pair is the only one which was detected for all four combinations in the B2H assay. These combinations showed a significant β-galactosidase activity as a result of a high level of adenylate cyclase complementation. Three of four combinations of AE-AE showed the highest β-galactosidase activity in comparison to the other interaction pairs. These results are strong indications for the formation of dimers and oligomers of AE.

The activator of the 2-hydroxyglutaryl dehydratase, an [4Fe-4S] enzyme catalyzing the ATP-dependent reductive activation of the dehydratase, also shows a homodimeric form in its crystal structure (Locher *et al.*, 2001). The bacterial protein RACo of *C. hydrogenoformans*, a protein which belongs to the COG3984 family as described for AE, is also a homodimer as shown by protein crystallization (Hennig *et al.*, 2012). RACo has a similar function as AE. RACo harbors a [2Fe-2S] cluster at the *N*-terminus and catalyzes the reductive activation of a corrinoid dependent methyltransferase in an ATP-dependent reaction. Unlike the dehydratase activator whose dimeric structure contains a single [4Fe-4S] cluster located at the interface between its two identical subunits (Buckel *et al.*, 2004), the homodimeric RACo harbors two [2Fe-2S] clusters which seem to act independently. The complex formation of RACo and the CFeSP was predicted as two molecules of CFeSP per one homodimer activator (Hennig *et al.*, 2012) which is in accordance with our results of the gel shift experiment, in which, according to the predicted size of the shifted band, a complex of 2 AE and 2 CP was formed.

In the Y2H system, it was possible to create stable protein fragments of the *O*-demethylase components to study a sub-molecular interaction. In order to identify the specific domain which is involved in the self-association of AE, two fragments of AE (AE1-133 and AE134-598) were prepared. The results revealed that the AE1-133 fragment interacts not only with

itself but also with the full length AE. The *C*-terminal fragment does not show any interaction. This result provides clear evidence that the *N*-terminal part of the protein is involved in the self-interaction of the AE molecule. Studies on the crystal structure of the activator RACo revealed that the region involved in the dimerization of this protein is located at the middle domain (residues 126-206). The similar fragment of AE, AE 101-176 was prepared and was tested for the self-association ability by the Y2H assay. This fragment showed no interaction in the Y2H screen. However, we could not exclude the possibility that the self-interaction of AE101-176 as well as the interaction of AE-CP was not detectable by Y2H assays.

By employing a combination of the four different methods, several interactions of the *O*-demethylase components distinct from AE and CP were found. Some interactions confirmed the ones previously reported, some others were found for the first time. However, these interactions should be carefully evaluated. For gel shift experiments, six possible combinations of the four components of the *O*-demethylase system were prepared (AE-CP, AE-MT I, AE-MT II, CP-MT I, CP-MT II, MT I-MT II). Each individual protein showed a visible band in the native gel. CP and MT I were monomers while AE forms a dimer. Since the MT II band is diffuse in the gel, its multimeric form remains to be determined. Unfortunately, no interaction was found for the combinations tested except for the positive control, the AE-CP pair, suggesting that the testing conditions of the gel shift experiment were not suitable for the detection of interactions of the other components. It is very likely that MT II has the affinity to CP containing methyl-cob(III)alamin rather than the Cob(II)-form used in the test, since methyl-cob(III)alamin bound CP is the substrate of MT II according to the reaction mechanism. Several studies demonstrated that the different redox states of the cobalamin have a significant effect on the conformation of the molecule. Specific conformational changes determine the binding of CP to either MT I or MT II and facilitate the specific methyl transfer reaction (Jarrett *et al.*, 1998; Hagemeier *et al.*, 2006; Datta *et al.*, 2008; Koutmos *et al.*, 2009). For this reason, methyl-cob(III)alamin bound CP was prepared for the test. Under light protected conditions, MT II showed no interaction with methyl-cob(III)alamin bound CP as no shifted band appeared in the native gel. It cannot be excluded that the light sensitive form methyl-cob(III)alamin bound CP may degrade during the separation which takes 4 - 5 hours including the pre-incubation of the proteins. Furthermore, the diffuse band of MT II on the native gel implies that the method may not provide optimal conditions for MT II like it does for the others.

Similar to the results obtained from gel shift experiments, only a few interactions were detected in the yeast two-hybrid screening, namely AE-AE and CP-MT I. The interaction of CP-MT I is in accordance to the reaction mechanism as CP is the substrate of MT I. The interaction of methyltransferase I and the corrinoid protein has been studied for different enzyme systems (Banerjee & Matthews, 1990; Svetlitchnaia *et al.*, 2006; Matthews *et al.*, 2008). In methanol-coenzyme M methyltransferase of *M. barkeri*, the formation of a protein complex consisting of the methanol-binding methyltransferase and the corrinoid protein (MtaBC) is essential for the catalysis. The methyltransferase MtaB binds at the *N*-terminal arm and at the corrinoid cofactor of the MtaC (Hagemeier *et al.*, 2006). In the acetogen *M. thermoacetica*, the corrinoid iron-sulfur protein methyltransferase (MeTr) catalyzes the tranfer of methyl group from methyltetrahydrofolate to the corrinoid protein (CFeSP). The crystal structure of the complex CFeSP/MeTr revealed interaction sites. The *C*-terminal α-helix of MeTr (residues 255-262) interacts with the helix (residues 191-204) of the small subunit of CFeSP. A weak hydrophobic interaction between MeTr and the large subunit ([4Fe-4S]-binding domain) of the CFeSP was also detected. The formation of the CFeSP/MeTr complex results in a conformational change of the corrinoid binding domain and this is necessary for catalysis (Kung *et al.*, 2012). It should be noted that MeTr shows structrural homology to the dihydropteroate synthases (DHPS) protein family which MT II belongs to. Although most of the residues involed in pterin binding are conserved, the cobalamin binding of region of MeTr differs from the DHPSs (Doukov *et al.*, 2000). To identify residues which are important for the interaction of CP and MT I in *A. dehalogenans*, several fragments of the two proteins including the cobalamin binding domain of CP and the substrate binding and catalytic domain of MT I were prepared. Under the assay conditions, no interaction between these fragments was observed in Y2H assay, with the exception of an auto-activation of the MT I 88-326 fragment. The fusion of MT I 88-326 to the DNA binding domain of GAL4 may possess a transcriptional activation domain that activates the expression of the reporter genes. It was estimated that up to 10% of fusions of *c*DNA inserts to the DNA binding domain lead to an auto-activation of the reporter genes (Fashena *et al.*, 2000). Therefore, all combinations in which the pGBKT7-MT I 88-326 fragment was involved were considered to be false positives.

The B2H screening revealed a high number of interactions between the components of the *O*-demethylase system. The oligomerization of AE and CP were proven as described above. The

multimerization of MT I was shown for the first time in *A. dehalogenans*. In the other systems such as *M. thermoacetica* the crystal structure of the CFeSP/MeTr complex also showed MeTr as homodimeric protein (Kung *et al.*, 2012). In the methanogen *M. barkeri*, the crystal structure of the methanol-cobalamin methyltransferase complex (MtaBC) revealed a heterotetramer composed of two methyltransferases and two corrinoid proteins (Hagemeier *et al.*, 2006). In these methyltransferase systems, the corrinoid protein appears to be a subunit of the methyltransferase rather than a separate protein as in the acetogenic enzyme systems. The interaction of CP-MT I detected by the Y2H assay was confirmed in the B2H screening. Unlike the results in the Y2H assay, the interaction between CP and MT I was detected in the reciprocal way and was one of the most significant interactions determined by the β-galactosidase assay.

Interaction between CP and MT II was also found in the B2H system. Only a few data about the interaction of these proteins are reported. The interaction of the corrinoid protein and methyltransferase II (AdoMet:Cob) of the corrinoid-dependent methinonine synthase in *E. coli* was essential for the methyl transfer of methylcobalamin to homocystein to form methionine (Matthews, 2001). In *M. barkeri*, the interaction of the methyltransferase II (MtaA) and the corrinoid protein (MtaC) was predicted based on the crystal structure of the MtaBC complex and a known structure related to MtaA. The three-component MtaABC complex was formed to catalyze the two-step methyl transfer process (Hagemeier *et al.*, 2006). The interaction in which more than two components of the *O*-demethylase systems are involved may also take place *in vivo*. A strong interaction between AE and MT I or weak interactions of the AE-MT II and the MT I-MT II pairs detected in the B2H assay might be the first clues for this assumption. The formation of the complexes such as AE-CP-MT I or MT I-CP-MT II during the catalysis should not be excluded. However, we could not rule out that the aformentioned interactions may not take place *in vivo*. The B2H assay is carried out with hybrid proteins that are possibly overproduced in comparison to the native expression level of the proteins. This may lead to the fact that some low affinity interactions can be exaggerated. Under native conditions (e. g., at lower levels of expression), such interactions may not occur (Karimova *et al.*, 2005). It is also possible that fusion forms of the proteins may result in alternation of the native folding in such a way that an interaction can occur or is disabled. Therefore, more experimental evidence is required to support the assumption of the involvement of more than two components in the complex formation. Taken together, the

B2H system revealed a number of interactions which were not observed with the methods described before. The formation of a dimer (or oligomer) of MT I was demonstrated. The interaction between CP and the two methyltransferases was shown which is in accordance to the reaction mechanism of *O*-demethylases.

The interaction between AE and MT II was shown by far-Western blot for the first time. According to the mechanism of the *O*-demethylase reaction the two enzymes seemingly have no connection with each other since AE is the activator of cob(II)alamin whereas MT II transfers the methyl group of methyl-cob(III)alamin to tetrahydrofolate. The *in vivo* interaction is therefore unlikely. In far-Western blot analysis signals for the interaction of this pair were the most intense ones among all test samples which imply a strong binding of the two. Hydropathy analysis by a web-based software (Bowen, 2008) revealed that MT II contains more hydrophobic regions than the other components. AE is also found to be a hydrophobic protein. Therefore, the interaction shown by far-Western blot is possibly based on unspecific hydrophobic interactions of the two proteins. In case of the MT I and MT II pair, the moderate interaction was detected when MT I was spotted onto the strip but not when MT I is in solution. This phenomenon can be explained by the non-native conformation of the proteins. Once protein is blotted onto the membrane, the unspecific binding of the protein with the membrane may lead to conformational changes. In a direction where the conformation of protein was not optimal. The interaction sites might be hidden. Similarly, the interaction of CP-MT I and CP-MT II can only be obtained when the two MTs are fixed onto the membranes and were incubated with CP in the solution but not *vice versa*. This observation leads to an alternative implication that the CP in its "free form" has a native folding and it can move freely to bind MT I and MT II. On the other way around, when CP was blotted onto the membrane its interaction sites might be blocked so that MT I and MT II have no access. The results of far-Western blot also indicated that the reconstituted cofactor containing CP has no influence on the association with the two MTs in the far-Western blot.

The results revealed a new evidence of functional interactions of the *O*-demethylase components of *A. dehalogenans*. Using a combination of *in vitro* and *in vivo* methods, a number of interactions were observed. Several interactions found in this study confirm the results previously reported, while some interactions were observed for the first time. The protein-protein interactions of the *O*-demethylase components are summarized in Figure 4.1.

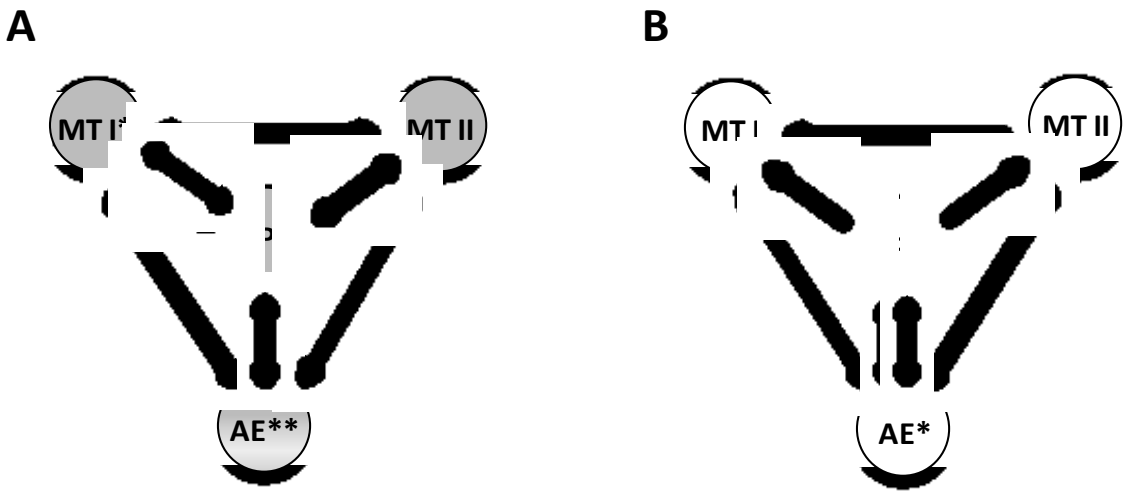

Figure 4.1. Interactions of the *O*-demethylase components deduced from the results of the different methods applied. (**A**) Interactions deduced from *in vivo* two-hybrid screens. (**B**) Interactions deduced from *in vitro* gel shift experiments and far-Western blot analysis. The thickness of the solid arrows indicates the strength of the interactions of the B2H screens (**A**) or far-Western blot experiments (**B**). The dotted arrows indicate the interactions deduced from Y2H screens (**A**) or gel shift experiments (**B**). Self-interaction of the protein detected by one (*) or two (**) methods. For details please refer to the text.

From the gel shift experiments, the interaction between AE and CP in the presence of the corrinoid cofactor was confirmed. Furthermore, the self-interactions of AE and CP which imply the oligomerization ability of these proteins were demonstrated. The gel shift experiments provided the first direct evidence for the ability of AE to recognize and interact with different CPs. An advantage of the gel shift experiment over the other methods used in this study is the ability to evaluate the stoichiometries of the interacting partners. For AE and the four different CPs a ratio of 1:1 was determined. While the gel shift experiment seems to provide suitable conditions to study the interaction between AE and CP, it appears to have some limitations when applying to the other proteins. Little information about the oligomerization and interaction in which the two methyltransferases are involved were obtained by this assay. The ability to detect the interactions by this *in vitro* method depends on many factors, one of which is that the experimental conditions may be not suitable for the interactions, or the binding of proteins indeed occurred but the complex dissociated prior to or during electrophoresis. The *in vivo* yeast two-hybrid system offered an alternative method to detect the interactions. The two-hybrid system is described to be more sensitive than many *in vitro* methods and may be suitable to detect the weak or transient interactions (Berggard *et al.*, 2007; Coates & Hall, 2003; Fields, 2001). The Y2H analysis performed here confirmed the

dimerization ability of AE and the interaction between CP and MT I which was demonstrated in some other systems. Furthermore, initial evidence for the involvement of the *N*-terminal part in the multimerization of AE was shown. However, none of the remaining combinations were found to interact. The Y2H system is prone to yield false negatives due to several reasons. The plasmid constructs may significantly affect the folding of the hybrid protein which results in a protein not interacting with its partner. The interaction surfaces of proteins can also be masked when the protein is present in the fusion form. It is also possible that the fusion protein may be toxic to the yeast cells. This problem can be controlled by employing a control plate as indicated in the experiments presented here. The Y2H screens may also generate significant number of false positives (Fields & Song, 1989). This might be due to either non-specific activation of the reporter genes or auto-activation which is a result of the activators of transcription with the binding domain as in the case of the pGBKT7-MT I 88-326 construct. The combination of this fragment and the empty vector resulted in the growth on the test plate. It is therefore essential to include the combination of test proteins and the empty vectors to control the false positives in the Y2H assay.

To uncover as many types of interactions as possible, it is important to use other two-hybrid methods such as bacterial two-hybrid system. Principally, the B2H system shows several advantages over the Y2H assay. The B2H is based on the indirect activation which may help to reduce the non-specific activation that occurred in the Y2H system. The method uses the bacterial cells which may result in faster detection because the yeast cells usually need longer time to grow. Moreover, the interaction efficiency can be quantitated by the β-galactosidase assay. Unlike the Y2H assay which has only one option of fusing proteins to the *C*-terminal end of the GAL4 domains the B2H system provides all four possibilities of fusions. This was demonstrated by the results of the B2H screens. The type of fusion appears to have an effect on the ability of *O*-demethylase members to interact with their interacting partners. Most of the interactions were found only when one protein was fused to the *N*-terminus of T25 and the other was fused to the *C*-terminus of T18. The results of B2H assay confirmed the self associations of AE and CP. Moreover, the oligomerization of MT I was detected. The B2H assay also confirmed the interaction between CP and MT I which was detected in the Y2H system and the interaction of CP and MT II which is in accordance to the reaction mechanism. Some weak interactions such as AE-MT II and MT I-MT II were also found as described above. The B2H system, however, also has some significant drawbacks. Despite our efforts to

stabilize the methods, the B2H results seem to be not reproducible. As shown in the Western blot experiment, the accumulation of the fusion proteins was difficult to obtain and does not follow any predictable rules. The results indicated that it is important to perform the control experiment which was rarely reported in other B2H studies. We suppose that these phenomena may be only specific to the *cyaA* deficient strains required for the screen. To confirm this hypothesis, some random constructs were transformed to the *E. coli* strain XL1-blue and were cultivated using the specific conditions similar to the assay. The cell extracts were used for Western blots using AE or CP antibodies. In this case, all fusion proteins of the test were detected (data not shown). This indicated that the accumulation and stability of proteins was significantly affected by the strains required for the test. Similar results were described in the literature (Chan *et al.*, 2009; Workentine *et al.*, 2009). Although the initial data appeared to be promising, the drawback of non-reproducibility and instability made B2H more difficult to apply for further investigation of protein-protein interactions.

Similar to the two-hybrid systems, the far-Western blot method seems to have an effect on the conformation of the proteins under the assay conditions. As indicated in the B2H and far-Western blot assays, the interaction between AE and CP does not require the presence of the corrinoid cofactor. This observation is contradictory to the results obtained by the gel shift experiments and may be explained by the influence of the experimental conditions, which are different for the different methods, on the folding of the protein. The hybrid chimeras generated in B2H system may provide an optimal folding of protein necessary for the interaction. In far-Western blot, once the protein is immobilized on the membrane, the conformation may have changed in such a way that the interaction site became more exposed or hidden depending on the characteristics of the membrane and the nature of the protein. This can be fully applied to the other interaction pairs used in the far-Western blot experiment beside the AE-CP pair. Therefore, unspecific binding derived from the non-native conformation of proteins should be taken into account when interpreting the results of the far-Western blot analysis.

As mentioned above, the reductive activation is essential to generate the active form of CP. *In vitro*, this reaction is catalyzed by AE in the presence of ATP and an artificial electron donor. The electron donor *in vivo* is unknown so far. The first evidence of the involvement of ferredoxins in the reactivation reaction was mentioned by Kaufmann *et al.* (1998b), where fractions containing hydrogenase showed to ability to conduct the activation of CP in the

presence of AE, ATP, H_2 and methyl viologen. Ferredoxin is widely known to play an important role in electron transfer in various metabolic reactions (Valentine, 1964). In acetogens, ferredoxin was found as an electron donor of methylene tetrahydrofolate reductase of *Clostridium formicoaceticum* (Clark & Ljungdahl, 1984). The reduced ferredoxin or carbon monoxide dehydrogenase/acetyl-CoA synthase is believed to be the electron donor for the CFeSP from *M. thermoacetica* during the reductive activation of oxidized corrinoid protein (Harder *et al.*, 1989; Menon & Ragsdale, 1998). To evaluate the possibility of ferredoxin as an *in vivo* electron donor, several attempts were made. One strategy was to isolate the ferredoxin from the crude extract of *A. delalogenans*. However, all attempts to purify the ferredoxin failed (data not shown). Alternatively, there was an option to search for the putative ferredoxin genes in the genome of *A. dehalogenans* and heterologously express them in *E. coli*. Here, we cloned and heterologously expressed two different putative ferredoxins genes of the genomic DNA of *A. dehalogenans*. The two putative ferredoxins Fd I and Fd II contain sets of conserved Fe-S binding motifs (**C**-X_2-**C**-X_2-**C**-X_3-**C**) characteristic for ferredoxins containing 4 [4Fe-4S] and 2 [4Fe-4S] clusters, respectively. The putative ferredoxin Fd I exhibits the highest amino acid sequence identity with the annotated ferredoxin Awo_c25230 of the closely related acetogen *A. woodii*. The soluble protein could only be obtained after the second cycle of French Press. The reconstituted Fd I showed an UV/Vis spectrum slightly different from other isolated ferredoxins of anaerobic bacteria which might be a result of the high number of iron in the protein. Fd II shows the highest similarity to a known 2 [4Fe-4S] ferredoxin of the anaerobe *Butyribacterium methylotrophicum* (83%). Unlike Fd I, Fd II can only be detected by silver stain but not by Coomassie stain after SDS PAGE. The protein showed a double size in the gel as compared to the calculated one from the amino acid sequence which is possibly a result of the presence of multi-charged iron sulfur clusters. The UV/Vis spectrum of Fd II showed a high similarity to other isolated ferredoxins from anaerobes (Bruschi & Guerlesquin, 1988). Although these proteins showed similar characteristics to ferredoxins of other anaerobic bacteria, they failed to show any involvement in the CP reactivation process. The crude extract of *A. dehalogenans* did not show any ability to reduce both Fds I and II with H_2 or formate under the conditions applied. Therefore, it is not clear if the ferredoxins were functional. Hence, the *in vivo* electron donor for the reductive activation of CP is still under investigation.

5. References

Altschul, S. F., Madden, T. L., Schaffer, A. A., Zhang, J., Zhang, Z., Miller, W. & Lipman, D. J. (1997). Gapped BLAST and PSI-BLAST: a new generation of protein database search programs. *Nucleic Acids Res* **25**, 3389-3402.

Anderson, I., Held, B., Lapidus, A. & other authors (2012). Genome sequence of the homoacetogenic bacterium *Holophaga foetida* type strain (TMBS4 T). *Stand Genomic Sci* **6**, 174-184.

Bache, R. & Pfennig, N. (1981). Selective isolation of *Acetobacterium woodii* on methoxylated aromatic acids and determination of growth yields. *Arch Microbiol* **130**, 255-261.

Bandarian, V. & Matthews, R. G. (2004). Measurement of energetics of conformational change in cobalamin-dependent methionine synthase. *Methods Enzymol* **380**, 152-169.

Banerjee, R. & Ragsdale, S. W. (2003). The many faces of vitamin B12: catalysis by cobalamin-dependent enzymes. *Annu Rev Biochem* **72**, 209-247.

Banerjee, R. V., Johnston, N. L., Sobeski, J. K., Datta, P. & Matthews, R. G. (1989). Cloning and sequence analysis of the *Escherichia coli* metH gene encoding cobalamin-dependent methionine synthase and isolation of a tryptic fragment containing the cobalamin-binding domain. *J Biol Chem* **264**, 13888-13895.

Banerjee, R. V. & Matthews, R. G. (1990). Cobalamin-dependent methionine synthase. *FASEB J* **4**, 1450-1459.

Berggard, T., Linse, S. & James, P. (2007). Methods for the detection and analysis of protein-protein interactions. *Proteomics* **7**, 2833-2842.

Berman, H., Henrick, K. & Nakamura, H. (2003). Announcing the worldwide Protein Data Bank. *Nat Struct Biol* **10**, 980.

Birnboim, H. C. & Doly, J. (1979). A rapid alkaline extraction procedure for screening recombinant plasmid DNA. *Nucleic Acids Res* **7**, 1513-1523.

Blondel, A. & Bedouelle, H. (1991). Engineering the quaternary structure of an exported protein with a leucine zipper. *Protein Eng* **4**, 457-461.

Bowen, R. V. (2008). Protein Hydrophobicity Plots. http://www.vivo.colostate.edu/molkit/hydropathy/.

Bradford, M. M. (1976). A rapid and sensitive method for the quantitation of microgram quantities of protein utilizing the principle of protein-dye binding. *Anal Biochem* **72**, 248-254.

Bruschi, M. & Guerlesquin, F. (1988). Structure, function and evolution of bacterial ferredoxins. *FEMS Microbiol Rev* **4**, 155-175.

Buckel, W., Hetzel, M. & Kim, J. (2004). ATP-driven electron transfer in enzymatic radical reactions. *Curr Opin Chem Biol* **8**, 462-467.

Buckel, W., Martins, B. M., Messerschmidt, A. & Golding, B. T. (2005). Radical-mediated dehydration reactions in anaerobic bacteria. *Biol Chem* **386**, 951-959.

Bugg, T. D., Ahmad, M., Hardiman, E. M. & Rahmanpour, R. (2011a). Pathways for degradation of lignin in bacteria and fungi. *Nat Prod Rep* **28**, 1883-1896.

Bugg, T. D. H., Ahmad, M., Hardiman, E. M. & Singh, R. (2011b). The emerging role for bacteria in lignin degradation and bio-product formation. *Curr Opin Biotech* **22**, 394-400.

Burke, S. A., Lo, S. L. & Krzycki, J. A. (1998). Clustered genes encoding the methyltransferases of methanogenesis from monomethylamine. *J Bacteriol* **180**, 3432-3440.

Causier, B. & Davies, B. (2002). Analysing protein-protein interactions with the yeast two-hybrid system. *Plant Mol Biol* **50**, 855-870.

Chan, C., Winstone, T. L. & Turner, R. (2008). Investigating protein–protein interactions by far-Westerns. In *Protein – Protein Interaction*, pp. 195-214. Edited by M. Werther & H. Seitz: Springer Berlin Heidelberg.

Chan, C. S., Chang, L., Rommens, K. L. & Turner, R. J. (2009). Differential interactions between Tat-specific redox enzyme peptides and their chaperones. *J Bacteriol* **191**, 2091-2101.

Clark, J. E. & Ljungdahl, L. G. (1984). Purification and properties of 5,10-methylenetetrahydrofolate reductase, an iron-sulfur flavoprotein from *Clostridium formicoaceticum*. *J Biol Chem* **259**, 10845-10849.

Clements, A. P., Kilpatrick, L., Lu, W. P., Ragsdale, S. W. & Ferry, J. G. (1994). Characterization of the iron-sulfur clusters in ferredoxin from acetate-grown *Methanosarcina thermophila*. *J Bacteriol* **176**, 2689-2693.

Coates, P. J. & Hall, P. A. (2003). The yeast two-hybrid system for identifying protein–protein interactions. *J Pathol* **199**, 4-7.

Daas, P. J. H., Hagen, W. R., Keltjens, J. T., vanderDrift, C. & Vogels, G. D. (1996a). Activation mechanism of methanol:5-hydroxybenzimidazolylcobamide methyltransferase from *Methanosarcina barkeri*. *J Biol Chem* **271**, 22346-22351.

Daas, P. J. H., Wassenaar, R. W., Willemsen, P., Theunissen, R. J., Keltjens, J. T., vanderDrift, C. & Vogels, G. D. (1996b). Purification and properties of an enzyme involved in the ATP-dependent activation of the methanol:2-mercaptoethanesulfonic acid methyltransferase reaction in *Methanosarcina barkeri*. *J Biol Chem* **271**, 22339-22345.

Daniel, S. L., Wu, Z. G. & Drake, H. L. (1988). Growth of thermophilic acetogenic bacteria on methoxylated aromatic-acids. *FEMS Microbiol Lett* **52**, 25-28.

Daniel, S. L., Keith, E. S., Yang, H. C., Lin, Y. S. & Drake, H. L. (1991). Utilization of methoxylated aromatic compounds by the acetogen *Clostridium thermoaceticum* - expression and specificity of the Co-dependent *O*-demethylating activity. *Biochem Bioph Res Comm* **180**, 416-422.

Datta, S., Koutmos, M., Pattridge, K. A., Ludwig, M. L. & Matthews, R. G. (2008). A disulfide-stabilized conformer of methionine synthase reveals an unexpected role for the histidine ligand of the cobalamin cofactor. *Proc Nat Acad Sci* **105**, 4115-4120.

Desai, S., Dworecki, B. & Cichon, E. (2001). Direct immunodetection of antigens within the precast polyacrylamide gel. *Anal Biochem* **297**, 94-98.

Diekert, G. & Wohlfarth, G. (1994). Metabolism of homoacetogens. *Anton Leeuw Int J G* **66**, 209-221.

Doukov, T., Seravalli, J., Stezowski, J. J. & Ragsdale, S. W. (2000). Crystal structure of a methyltetrahydrofolate- and corrinoid-dependent methyltransferase. *Structure* **8**, 817-830.

Dove, S. & Hochschild, A. (2004). A bacterial two-hybrid system based on transcription activation. In *Protein-Protein Interactions*, pp. 231-246. Edited by H. Fu: Humana Press.

Drennan, C. L., Huang, S., Drummond, J. T., Matthews, R. G. & Lidwig, M. L. (1994). How a protein binds B_{12}: A 3.0 A X-ray structure of B_{12}-binding domains of methionine synthase. *Science* **266**, 1669-1674.

Edmondson, D. G. & Roth, S. Y. (2001). Identification of protein interactions by far Western analysis. *Curr Protoc Mol Biol* **55**, 20.6.1–20.6.10.

Engelmann, T., Kaufmann, F. & Diekert, G. (2001). Isolation and characterization of a veratrol:corrinoid protein methyl transferase from *Acetobacterium dehalogenans*. *Arch Microbiol* **175**, 376-383.

Evans, J. C., Huddler, D. P., Hilgers, M. T., Romanchuk, G., Matthews, R. G. & Ludwig, M. L. (2004). Structures of the N-terminal modules imply large domain motions during catalysis by methionine synthase. *Proc Natl Acad Sci* **101**, 3729-3736.

Fashena, S. J., Serebriiskii, I. & Golemis, E. A. (2000). The continued evolution of two-hybrid screening approaches in yeast: how to outwit different preys with different baits. *Gene* **250**, 1-14.

Ferguson, T., Soares, J. A., Lienard, T., Gottschalk, G. & Krzycki, J. A. (2009). RamA, a protein required for reductive activation of corrinoid-dependent methylamine methyltransferase reactions in methanogenic archaea. *J Biol Chem* **284**, 2285-2295.

Fields, S. & Song, O. (1989). A novel genetic system to detect protein-protein interactions. *Nature* **340**, 245-246.

Fields, S. (2001). Two-hybrid and related systems. In *eLS*: John Wiley & Sons, Ltd.

Fish, W. W. (1988). Rapid colorimetric micromethod for the quantitation of complexed iron in biological samples. In *Methods in Enzymol*, pp. 357-364. Edited by Bert L. Valee & James F. Riordan: Academic Press.

Frazer, A. (1995). *O*-Demethylation and other transformations of aromatic compounds by acetogenic bacteria. In *Acetogenesis*, pp. 445-483. Edited by H. Drake: Springer US.

Frenkel, J. (2010). Untersuchungen zu Ether-spaltenden Methyltransferasen in *Acetobacterium dehalogenans*. Diploma Thesis. Friedrich Schiller University Jena.

Gietz, R. D. & Schiestl, R. H. (2007a). High-efficiency yeast transformation using the LiAc/SS carrier DNA/PEG method. *Nat Protoc* **2**, 31-34.

Gietz, R. D. & Schiestl, R. H. (2007b). Quick and easy yeast transformation using the LiAc/SS carrier DNA/PEG method. *Nat Protoc* **2**, 35-37.

Guerrini, O., Burlat, B., Leger, C., Guigliarelli, B., Soucaille, P. & Girbal, L. (2008). Characterization of two 2[4Fe-4S] ferredoxins from *Clostridium acetobutylicum*. *Curr Microbiol* **56**, 261-267.

Hagemeier, C. H., Krer, M., Thauer, R. K., Warkentin, E. & Ermler, U. (2006). Insight into the mechanism of biological methanol activation based on the crystal structure of the methanol-cobalamin methyltransferase complex. *Proc Natl Acad Sci* **103**, 18917-18922.

Hans, M., Bill, E., Cirpus, I., Pierik, A. J., Hetzel, M., Alber, D. & Buckel, W. (2002). Adenosine triphosphate-induced electron transfer in 2-hydroxyglutaryl-CoA dehydratase from *Acidaminococcus fermentans*. *Biochem* **41**, 5873-5882.

Harder, S. R., Lu, W. P., Feinberg, B. A. & Ragsdale, S. W. (1989). Spectroelectrochemical studies of the corrinoid/iron-sulfur protein involved in acetyl coenzyme A synthesis by *Clostridium thermoaceticum*. *Biochem* **28**, 9080-9087.

Härter, A. (2011). Evolution der Interaktion floraler Proteine. Dissertation. Friedrich Schiller University Jena.

Heldt, H.-W. & Heldt, F. (2005). Phenylpropanoids comprise a multitude of plant secondary metabolites and cell wall components. In *Plant Biochemistry (Third Edition)*, pp. 435-454. Burlington: Academic Press.

Hennig, S. E., Jeoung, J. H., Goetzl, S. & Dobbek, H. (2012). Redox-dependent complex formation by an ATP-dependent activator of the corrinoid/iron-sulfur protein. *Proc Natl Acad Sci* **109**, 5235-5240.

Jarrett, J. T., Huang, S. & Matthews, R. G. (1998). Methionine synthase exists in two distinct conformations that differ in reactivity toward methyltetrahydrofolate, adenosylmethionine, and flavodoxin. *Biochem* **37**, 5372-5382.

Karimova, G., Pidoux, J., Ullmann, A. & Ladant, D. (1998). A bacterial two-hybrid system based on a reconstituted signal transduction pathway. *Proc Natl Acad Sci* **95**, 5752-5756.

Karimova, G., Ullmann, A. & Ladant, D. (2000a). *Bordetella pertussis* adenylate cyclase toxin as a tool to analyze molecular interactions in a bacterial two-hybrid system. *Int J Med Microbiol* **290**, 441-445.

Karimova, G., Ullmann, A. & Ladant, D. (2000b). A bacterial two-hybrid system that exploits a cAMP signaling cascade in *Escherichia coli*. *Methods Enzymol* **328**, 59-73.

Karimova, G., Dautin, N. & Ladant, D. (2005). Interaction network among *Escherichia coli* membrane proteins involved in cell division as revealed by bacterial two-hybrid analysis. *J Bacteriol* **187**, 2233-2243.

Kaufmann, F., Wohlfarth, G. & Diekert, G. (1997). Isolation of *O*-demethylase, an ether-cleaving enzyme system of the homoacetogenic strain MC. *Arch Microbiol* **168**, 136-142.

Kaufmann, F., Wohlfarth, G. & Diekert, G. (1998a). *O*-demethylase from *Acetobacterium dehalogenans* - Substrate specificity and function of the participating proteins. *Eur J Biochem* **253**, 706-711.

Kaufmann, F., Wohlfarth, G. & Diekert, G. (1998b). *O*-demethylase from *Acetobacterium dehalogenans* - Cloning, sequencing, and active expression of the gene encoding the corrinoid protein. *Eur J Biochem* **257**, 515-521.

Kim, J., Lu, Y. & Buckel, W. (2007). ATP- and redox-induced conformational changes in the activator of the radical enzyme 2-hydroxyisocaproyl-CoA dehydratase. *Comptes Rendus Chimie* **10**, 742-747.

Koutmos, M., Datta, S., Pattridge, K. A., Smith, J. L. & Matthews, R. G. (2009). Insights into the reactivation of cobalamin-dependent methionine synthase. *Proc Natl Acad Sci* **106**, 18527-18532.

Kreft, J. U. & Schink, B. (1994). *O*-demethylation by the homoacetogenic anaerobe *Holophaga foetida* studied by a new photometric methylation assay using electrochemically produced cob(I)alamin. *Eur J Biochem* **226**, 945-951.

Kreft, J. U. & Schink, B. (1997). Specificity of *O*-demethylation in extracts of the homoacetogenic *Holophaga foetida* and demethylation kinetics measured by a coupled photometric assay. *Arch Microbiol* **167**, 363-368.

Kreher, S., Studenik, S. & Diekert, G. (2010). Ether cleaving methyltransferases of the strict anaerobe *Acetobacterium dehalogenans*: controlling the substrate spectrum by genetic engineering of the N-terminus. *Mol Microbiol* **78**, 230-237.

Kung, Y., Ando, N., Doukov, T. I., Blasiak, L. C., Bender, G., Seravalli, J., Ragsdale, S. W. & Drennan, C. L. (2012). Visualizing molecular juggling within a B_{12}-dependent methyltransferase complex. *Nature* **484**, 265-269.

Laemmli, U. K. (1970). Cleavage of structural proteins during assembly of head of bacteriophage T4. *Nature* **227**, 680-685.

Lange, A. (2009). *O*-Demethylasen in *Acetobacterium dehalogenans*: Bildung verschiedener Methyltransferasen I in Abhängigkeit vom Wachstumssubstrat. Diploma Thesis. Friedrich Schiller University Jena.

Leclerc, D., Wilson, A., Dumas, R. & other authors (1998). Cloning and mapping of a cDNA for methionine synthase reductase, a flavoprotein defective in patients with homocystinuria. *Proc Natl Acad Sci* **95**, 3059-3064.

Liesack, W., Bak, F., Kreft, J. U. & Stackebrandt, E. (1994). *Holophaga foetida* gen. nov., sp. nov., a new homoacetogenic bacterium degrading methoxylated aromatic compounds. *Arch Microbiol* **162**, 85-90.

Locher, K. P., Hans, M., Yeh, A. P., Schmid, B., Buckel, W. & Rees, D. C. (2001). Crystal structure of the *Acidaminococcus fermentans* 2-hydroxyglutaryl-CoA dehydratase component A. *J Mol Biol* **307**, 297-308.

Louvet, O., F. Doignon, et al. (1997). Stable DNA-binding yeast vector allowing high-bait expression for use in the two-hybrid system. *Biotechniques* **23**, 816-820.

Masai, E., Katayama, Y. & Fukuda, M. (2007). Genetic and biochemical investigations on bacterial catabolic pathways for lignin-derived aromatic compounds. *Biosci Biotech Biochem* **71**, 1-15.

Matthews, R. G. & Goulding, C. W. (1997). Enzyme-catalyzed methyl transfers to thiols: the role of zinc. *Curr Opin Chem Biol* **1**, 332-339.

Matthews, R. G. (2001). Cobalamin-dependent methyltransferases. *Acc Chem Res* **34**, 681-689.

Matthews, R. G., Koutmos, M. & Datta, S. (2008). Cobalamin-dependent and cobamide-dependent methyltransferases. *Curr Opin Struct Biol* **18**, 658-666.

Matthews, R. G. (2009). Cobalamin- and corrinoid-dependent enzymes. *Met Ions Life Sci* **6**, 53-114.

Meister, W., Hennig, S. E., Jeoung, J.-H., Lendzian, F., Dobbek, H. & Hildebrandt, P. (2012). Complex formation with the activator RACo affects the corrinoid structure of CFeSP. *Biochem* **51**, 7040-7042.

Menon, S. & Ragsdale, S. W. (1998). Role of the [4Fe-4S] cluster in reductive activation of the cobalt center of the corrinoid iron-sulfur protein from *Clostridium thermoaceticum* during acetate biosynthesis. *Biochem* **37**, 5689-5698.

Menon, S. & Ragsdale, S. W. (1999). The role of an iron-sulfur cluster in an enzymatic methylation reaction - Methylation of CO dehydrogenase/acetyl-CoA synthase by the methylated corrinoid iron-sulfur protein. *J Biol Chem* **274**, 11513-11518.

Messmer, M., Wohlfarth, G. & Diekert, G. (1993). Methyl-chloride metabolism of the strictly anaerobic, methyl chloride-utilizing homoacetogen strain MC. *Arch Microbiol* **160**, 383-387.

Miller, J. & Stagljar, I. (2004). Using the yeast two-hybrid system to identify interacting proteins. *Methods Mol Biol* **261**, 247-262.

Miller, J. H. (1972). *Experiments in molecular genetics*. Cold Spring Harbor, N.Y.

Müller, V. (2003). Energy conservation in acetogenic bacteria. *Appl Environ Microbiol* **69**, 6345-6353.

Mullis, K. B. (1994). PCR and scientific invention: The trial of DuPont vs. Cetus. In *The Polymerase Chain Reaction*. pp. 427-441. Edited by K. B. Mullis, F. Ferré & R. A. Gibbs: Birkhäuser Boston.

Naidu, D. & Ragsdale, S. W. (2001). Characterization of a three-component vanillate *O*-demethylase from M*oorella thermoacetica*. *J Bacteriol* **183**, 3276-3281.

Pagni, M., Ioannidis, V., Cerutti, L., Zahn-Zabal, M., Jongeneel, C. V. & Falquet, L. (2004). MyHits: a new interactive resource for protein annotation and domain identification. *Nucleic Acids Res* **32**, 332-335.

Phizicky, E. M. & Fields, S. (1995). Protein-protein interactions: methods for detection and analysis. *Microbiol Rev* **59**, 94-123.

Poehlein, A., Schmidt, S., Kaster, A. K. & other authors (2012). An ancient pathway combining carbon dioxide fixation with the generation and utilization of a sodium ion gradient for ATP synthesis. *PloS one* **7**, e33439.

Pratt, J. M. (1993). Making and breaking the Co-alkyl bond in B_{12} derivatives. *Met Ions Biol Syst* **29**, 229-286.

Rabinowitz, J. (1972). Preparation and properties of clostridial ferredoxins. *Methods Enzymol* **24**, 431-446.

Ragsdale, S. W. & Ljungdahl, L. G. (1984). Characterization of ferredoxin, flavodoxin, and rubredoxin from *Clostridium formicoaceticum* grown in media with high and low iron contents. *J Bacteriol* **157**, 1-6.

Ragsdale, S. W. (2008). Enzymology of the Wood-Ljungdahl pathway of acetogenesis. *Ann N Y Acad Sci* **1125**, 129-136.

Reubelt U., Wohlfarth, G., Schmid, R., Diekert, G. (1991). Purification and characterization of ferredoxin from *Peptostreptococcus productus* (strain Marburg). *Arch Microbiol* **156**, 422-426.

Saeki, K., Yao, Y., Wakabayashi, S., Shen, G.-J., Zeikus, J. G. & Matsubara, H. (1989). Ferredoxin and rubredoxin from *Butyribacterium methylotrophicum*: complete primary structures and construction of phylogenetic trees. *J Biochem* **106**, 656-662.

Sambrook, J., Russell, D. W. & Sambrook, J. (2006). *The condensed protocols from Molecular cloning : A laboratory manual*. Cold Spring Harbor, N.Y.

Sauer, K. & Thauer, R. K. (1997). Methanol:coenzyme M methyltransferase from *Methanosarcina barkeri*. Zinc dependence and thermodynamics of the methanol:cob(I)alamin methyltransferase reaction. *Eur J Biochem* **249**, 280-285.

Sauer, K. & Thauer, R. K. (1999). Methanol:coenzyme M methyltransferase from *Methanosarcina barkeri* - substitution of the corrinoid harbouring subunit MtaC by free cob(I)alamin. *Eur J Biochem* **261**, 674-681.

Schägger, H. (2006). Tricine-SDS-PAGE. *Nat Protoc* **1**, 16-22.

Schilhabel, A., Studenik, S., Vodisch, M., Kreher, S., Schlott, B., Pierik, A. J. & Diekert, G. (2009). The ether-cleaving methyltransferase system of the strict anaerobe *Acetobacterium dehalogenans*: analysis and expression of the encoding genes. *J Bacteriol* **191**, 588-599.

Schrauzer, G. N. & Deutsch, E. (1969). Reactions of cobalt(I) supernucleophiles. The alkylation of vitamin B_{12}s cobaloximes(I), and related compounds. *J Am Chem Soc* **91**, 3341-3350.

Sperfeld, M. (2012). Reductive activation of protein bound vitamin B_{12} - Characterization of a new metallo-ATPase by site directed mutagenesis. Master Thesis. Friedrich Schiller University Jena.

Studenik, S., Kreher, S. & Diekert, G. (2011). The ether-cleaving methyltransferase of the strict anaerobe *Acetobacterium dehalogenans*: analysis of the zinc-binding site. *FEMS Microbiol Lett* **318**, 131-136.

Studenik, S., Vogel, M. & Diekert, G. (2012). Characterization of an *O*-demethylase of *Desulfitobacterium hafniense* DCB-2. *J Bacteriol* **194**, 3317-3326.

Stupperich, E. & Konle, R. (1993). Corrinoid-dependent methyl transfer reactions are involved in methanol and 3,4-dimethoxybenzoate metabolism by *Sporomusa ovata. Appl Environ Microbiol* **59**, 3110-3116.

Svetlitchnaia, T., Svetlitchnyi, V., Meyer, O. & Dobbek, H. (2006). Structural insights into methyltransfer reactions of a corrinoid iron-sulfur protein involved in acetyl-CoA synthesis. *P Natl Acad Sci* **103**, 14331-14336.

Switzer, R. C., 3rd, Merril, C. R. & Shifrin, S. (1979). A highly sensitive silver stain for detecting proteins and peptides in polyacrylamide gels. *Anal Biochem* **98**, 231-237.

Towbin, H., Staehelin, T. & Gordon, J. (1979). Electrophoretic transfer of proteins from polyacrylamide gels to nitrocellulose sheets - procedure and some applications. *Proc Natl Acad Sci* **76**, 4350-4354.

Traunecker, J., Preuß, A. & Diekert, G. (1991). Isolation and characterization of a methyl chloride utilizing, strictly anaerobic bacterium. *Arch Microbiol* **156**, 416-421.

Valentine, R. C. (1964). Bacterial ferredoxin. *Bacteriol Rev* **28**, 497-517.

Wood, H. G. (1991). Life with CO or CO_2 and H_2 as a source of carbon and energy. *FASEB J* **5**, 156-163.

Workentine, M. L., Chang, L., Ceri, H. & Turner, R. J. (2009). The GacS-GacA two-component regulatory system of *Pseudomonas fluorescens*: a bacterial two-hybrid analysis. *FEMS Microbiol Lett* **292**, 50-56.

Xiong, X., Ouyang, J., Xiong, X., Zhai, S. & Baeyens, W. R. G. (2009). Chemiluminescence-based detection technologies for biomolecules, mainly in gel electrophoresis. *TrAC Trends Anal Chem* **28**, 961-972.

Zimmermann, W. (1990). Degradation of lignin by bacteria. *J Biotech* **13**, 119-130

Acknowledgments

I would like to express my deep gratitude to my thesis advisors, Prof. Gabriele Diekert and Dr. Sandra Studenik. Without their support and active participation in every step of the process, this thesis may never have been completed. Prof. Diekert introduced me to the fields of microbiology and biochemistry. She provided excellent, very dedicated and knowledgeable guidance and good atmosphere for doing research. I have been lucky enough to have the second advisor, Dr. Studenik. She cared so much about my work, she responded to my questions and queries very promptly. She read every chapter of this thesis a number of times, which eventually transformed it to a readable thesis. I would like to thanks my third thesis advisor, Prof. Kristen Küsel, for her support and helpful suggestions for my PhD thesis.

I would also like to offer my special thanks to all the staffs and colleagues in the Institute of Microbiology, Department of Applied and Ecological Microbiology. I thank Dr. Schubert, Greisher, Sperfeld, Reinhold, MacNelly and many others for being with me all the time and for their important comments and scientific helps which contributed significantly to improve this thesis. I acknowledge the financial support and great assistance from Jena School for Microbial Communications during three years of my graduate study in Jena.

I am very thankful to my friends here in Jena for sharing friendship and supports. Especially thanks to Tung, Tam, Son, Duc, Phong-My and other Vietnamese friends in Germany, you guys have all been truly amazing friends. I will remember every moment we had together. I thank many other Vietnamese friends in my country, Canada or elsewhere in the world who always cheered me up in time and helped me whenever I need them.

Finally, I thank my wife for her constant love and support. She was always there to stand by me through the good times and bad. I would thank my parents and my sister for their faith in me. They have been the enormous sources of strength and motivation for me throughout this journey.

Eigenständigkeitserklärung

Entsprechend der geltenden, mir bekannten Promotionsordnung der Biologisch-Pharmazeutischen Fakultät der Friedrich-Schiller-Universität Jena erkläre ich, Hai Dang Nguyen, geboren am 22.09.1980, dass ich die vorliegende Dissertation eigenständig angefertigt und alle von mir benutzten Hilfsmittel und Quellen angegeben habe. Es wurde weder die Hilfe eines Promotionsberaters in Anspruch genommen, noch haben Dritte für Arbeiten, welche im Zusammenhang mit dem Inhalt der vorliegenden Dissertation stehen, geldwerte Leistungen erhalten. Die vorgelegte Dissertation wurde außerdem weder als Prüfungsarbeit für eine staatliche oder andere wissenschaftliche Prüfung noch als Dissertation an einer anderen Hochschule eingereicht. Diese Arbeit ist weder identisch noch teilidentisch mit einer Arbeit, welche an der Friedrich-Schiller-Universität Jena oder einer anderen Hochschule zur Erlangung eines akademischen Grades oder als Prüfungsleistung vorgelegt worden ist.

_____

Hai Dang Nguyen

Jena, den……

CURRICULUM VITAE

Name: Nguyen Hai Dang
Date of birth: Sep 22nd, 1980
Gender: Male
Nationality: Vietnamese

EDUCATION:

- **Master of Pharmaceutical Chemistry** **03/03/2003 - 02/25/2005**
  Major: Natural Product Chemistry
  Chungnam National University, 305-764 GungDong, Daejon, Korea

- **Bachelor of Science in Engineer of Biotechnology** **09/05/1998 - 08/19/2002**
  Major: Biotechnology
  Hanoi Open University, Bach Khoa, Hai Ba Trung, Hanoi, Vietnam

PROFESSIONAL EXPERIENCES:

- **PhD Student – JSMC Fellow** **Since Mar, 2010**
  Institute of Microbiology, Department of Applied and Ecological Microbiology, Friedrich Schiller University Jena, Jena, Germany.

- **Researcher** **Jan, 2008 – Mar, 2010**
  Institut Armand Frappier, Institut National de la Recherque Scientifice (INRS), Quebec, Canada.

- **Researcher** **Feb, 2005 – Jan, 2008**
  Institute of Natural Products Chemistry, Vietnam Academy of Science and Technology, Hanoi, Vietnam.

- **Researcher** **Apr, 2006 – Jun, 2006**
  3 month study visit at International Center for Chemical Science, University of Karachi, Karachi, Pakistan.

- **Researcher** **Feb, 2003 – Feb, 2005**
  Laboratory of Pharmacognosy, College of Pharmacy, Chungnam National University, Daejon, Korea.

- **Researcher** **Jan, 2002 – Oct, 2002**
  Center for Cellular Biotechnology and Molecular Biology, Hanoi National University, Hanoi, Vietnam.

LIST OF PUBLICATIONS

1. **Hai Dang Nguyen**, Sandra Studenik, Gabriele Diekert**.** Corrinoid activation by a RACE protein: Studies on the interaction of the proteins involved. *FEMS Microbiol Lett,* 345(1), 31-38, 2013.
2. Tran Manh Hung, **Nguyen Hai Dang**, Jin Cheol Kim, Han-Su Jang, Sung-Woo Ryoo, Jeong Hyung Lee, Jae Sue Choi, KiHwan Bae, Byung Sun Min. Alkaloids from roots of *Stephania rotunda* and their cholinesterase inhibitory activity. *Planta Med*, 76, 1762-1764, 2010.
3. Tran Manh Hung, **Nguyen Hai Dang**, Jin Cheol Kim, Jae Sue Choi, Hyeong Kyu Lee, Byung Sun Min. Phenolic glycosides from *Alangium salviifolium* leaves with inhibitory activity on LPS-induced NO, PGE_2, and TNF-α production. *Bioorg Med Chem Lett*, 19, 4389-4393, 2009.
4. **Nguyen Hai Dang**, Nguyen Van Thanh, Phan Van Kiem, Le Mai Huong, Chau Van Minh, and Young Ho Kim. Two new triterpene glycosides from the Vietnamese sea cucumber *Holothuria scabra*. *Arch Pharm Res,* 30(11), 1387-1391, 2007.
5. Phan Van Kiem, **Nguyen Hai Dang**, Ha Viet Bao, Hoang Thanh Huong, Chau Van Minh, Le Mai Huong , Jung Joon Lee, and Young Ho Kim. New cytotoxic benzopyrans from the leaves of *Mallotus apelta*. *Arch Pharm Res*. 28(10), 1131-1134, 2005.
6. **Nguyen Hai Dang**, XinFeng Zhang, MingShan Zheng, Kun Ho Son, Hyeun Wook Chang, Hyun Pyo Kim, KiHwan Bae, and Sam Sik Kang. Inhibitory constituents against cyclooxygenase from *Aralia cordata* Thunb. *Arch Pharm Res*, 28(1), 28-33, 2005.

Conferences:

1. **Hai Dang Nguyen**, Sandra Studenik, Gabriele Diekert. Studies on the interaction of the *O*-demethylase components of the anaerobe *Acetobacterium dehalogenans* - Interactions of the activating enzyme and the corrinoid protein. 3rd International Conference on Microbial Communication, Jena, November, 5 – 8, 2012. (*Talk*).
2. **Hai Dang Nguyen**, Sandra Studenik, Gabriele Diekert. Studies on the interaction of the *O*-demethylase components of the anaerobe *Acetobacterium dehalogenans* using two-hybrid systems. VAAM conference, Tübingen, 18–21 March 2012. (*Poster*).
3. **Hai Dang Nguyen**, Sandra Studenik, Gabriele Diekert. Studies on the interaction of the *O*-demethylase components of the anaerobe *Acetobacterium dehalogenans* using two-hybrid systems. 2nd International Conference on Microbial Communication, Jena, September 13 – 16, 2011. (*Poster*).
4. **Hai Dang Nguyen**, Sandra Studenik, Gabriele Diekert. Studies on the interaction of the *O*-demethylase components of the anaerobe *Acetobacterium dehalogenans*. VAAM conference, Karlsruhe, April 3 – 6, 2011. (*Poster*).

5. **Hai Dang Nguyen**, Sandra Studenik, Gabriele Diekert. Studies on the interaction of the *O*-demethylase components of the anaerobe *Acetobacterium dehalogenans*. 1st International Conference on Microbial Communication, Jena, September 28 – October 1st, 2010. (*Poster*).

Monographs:

1. **Nguyen Hai Dang**, Phan Van Kiem, Chau Van Minh. "Status of Natural Products, Drugs, Pharmaceuticals and Nutraceuticals in Vietnam" in *Advances in Natural Products – Importance in Health and Economy*. Ed. Zaheer Ahmeed and Ahsana Dar. Daya Publishing House, Delhi, 2008 (ISBN 978-81-7035-530-4).
2. Chau Van Minh, Phan Van Kiem, **Nguyen Hai Dang**. *Bioactive Constituents from Marine Organisms*. Science and Technology Publishing House, Hanoi, 2007 (*in Vietnamese*).

Patents:

1. Chau Van Minh, Phan Van Kiem, **Nguyen Hai Dang**, Nguyen Van Thanh, Le Mai Huong, Do Cong Thung, Tran Thu Huong, Nguyen Xuan Cuong. Holothurin A_3 with antitumor activity and the method to extract it from *Holothuria scabra*. *National Office of Intellectual Property of Vietnam,* 2008. (No: 1-0006852-000).
2. Chu Nhat Huy, Chau Van Minh, **Nguyen Hai Dang**, Nguyen Thi Minh Thu, Phan Van Kiem, Tran Thu Huong. Dracagenin B and the method to extract it from *Dracaena cambodiana*. *National Office of Intellectual Property of Vietnam,* 2008. (No: 17143).